

THE DEVELOPMENT OF A RIGID POLYURETHANE FOAM-REINFORCED
RESILIENT MASONRY WALL SYSTEM

THE DEVELOPMENT OF A RIGID
POLYURETHANE-REINFORCED
RESILIENT MASONRY WALL SYSTEM

By

CARLY M. A. FORSYTHE, B.ENG.

A Thesis

Submitted to the School of Graduate Studies

in Partial Fulfilment of the Requirements

for the Degree

Masters of Applied Science

McMaster University

© Copyright by Carly M.A. Forsythe, January 2012

MASTER OF APPLIED SCIENCE (2012)
(Civil Engineering)

McMaster University
Hamilton, Ontario

TITLE: The Development of a Rigid Polyurethane Foam-Reinforced Reinforced
Masonry Wall System

AUTHOUR: Carly M. A. Forsythe, B.Eng. (McMaster University)

SUPERVISOR: Associate Professor W. El-Dakhakhni

NUMBER OF PAGES: xii, 146

ABSTRACT

Unreinforced masonry (URM) constitutes a large part of current building inventory worldwide, and this type of construction also represents a major seismic risk, especially in developing countries where URM is widely used. During an earthquake, URM walls are unable to dissipate seismic forces without experiencing considerable damage or collapse. Due to their lack of ductility, URM walls fail in a brittle manner, which can lead to damaged face shells becoming falling debris and a major source of hazard. The aim of this study is to investigate the applicability of using polyurethane foams as an inexpensive reinforcement technique for both retrofitting existing and new URM construction.

Experimental testing of the reinforced masonry walls showed a large increase in the resiliency of the wall, with an increase in the out-of-plane capacity of up to 34 times over the URM specimen, and with the addition of rope reinforcement an increase in the out-of-plane capacity of up to 90 times the URM specimen was achieved. This system allows walls to experience a considerable amount of deflection before ultimate failure is reached. Within certain limits, the polyurethane foam is able to demonstrate elastic characteristics. By developing foam with higher densities, higher compressive, tensile, flexural and shear strengths can be reached. This type of reinforcement allows for less damage during low seismic events, and through the greater resiliency of the system, walls are able to remain stable and exhibit post-peak strength during a stronger seismic event. In its ultimate limit state, the wall will fail, however collapse is typically prevented – reducing the amount of hazardous debris and saving the lives of the buildings occupants.

ACKNOWLEDGEMENTS

The author wishes to express her sincere gratitude to Dr. El-Dakhakhni, research supervisor, for his guidance and support throughout the course of her work. I am grateful for having the opportunity to work under his supervision and for him expanding his research horizons to include some unconventional new research.

The experimental part of this investigation was made possible thanks to the efforts of Mr. Wheeler and Mr. Perrett, the technicians at the Applied Dynamics Laboratory who spent countless hours helping the author and making this project come to fruition.

A significant part of the materials needed for this research was kindly donated by BASF, POLY-MOR Canada, Boehmer's and Keppler Masonry. The author is indebted for these generous contributions.

Table of Contents

ABSTRACT	iii
ACKNOWLEDGEMENTS	iv
List of Figures	ix
List of Tables	xii
1 Introduction.....	1
1.1 Problem Definition	1
1.2 Scope and Objectives	2
1.3 Thesis Outline	2
2 Literature Review	3
2.1 Introduction	4
2.2 Types of Non-Engineered URM Buildings in Developing Countries	4
2.2.1 Adobe Buildings	4
2.3 Current Retrofitting Techniques for Non-Engineered URM	6
2.3.1 Mesh Reinforcement	6
2.3.2 Bamboo Reinforcement	12
2.3.3 Use of Rubber Tires for Reinforcement.....	14
2.3.4 Confined Masonry	20
2.4 Polyurethane Foam.....	21
2.5 Investigations into the use of Polyurethane Foam in Improving Shear Strength in URM	24
3 Preliminary Investigation into the use of Polyurethane Foam as Reinforcement in Masonry	29
3.1 Introduction	29

3.2	Materials.....	30
3.2.1	Concrete Blocks	30
3.2.2	Hand-mixed Polyurethane Foam Products Supplied by Company A.....	30
3.2.3	Industrial Polyurethane Foam Products	32
3.3	Out-of-Plane Testing of Materials in Third-Scale Masonry Wallettes	37
3.3.1	Test Configuration and Procedure	37
3.3.2	Test Observations.....	38
3.4	Conclusion.....	46
4	Experimental Compression of Full-Scale Masonry Assemblages Reinforced with Expanding Polyurethane Foam	48
4.1	Introduction	48
4.2	Materials.....	48
4.2.1	Concrete Blocks	48
4.2.2	Mortar	48
4.3	Specimen Selection and Construction.....	49
4.4	Polyurethane Foam Injection	50
4.5	Test Configuration and Procedure.....	51
4.6	Test Results	52
4.6.1	Mortar Cubes	52
4.6.2	Compression Test Observations and Discussion	53
4.7	Conclusions	58
5	Main Experimental Program—Full Scale Walls	60
5.1	Introduction	60
5.2	Materials.....	60

5.2.1	Concrete Blocks	60
5.2.2	Masonry Mortar	60
5.2.3	Urethane Polymer	61
5.2.4	Polypropylene, Nylon and Polyester Ropes.....	61
5.3	Specimen Selection and Construction.....	66
5.4	Urethane Polymer Injection	67
5.4.1	Polymer Injection Methods.....	67
5.5	Test Set-up and Instrumentation	74
5.6	Experimental Results of Full Scale Walls.....	77
5.6.1	Preliminary Full-Scale Out-of-Plane Wall Tests Using Company B Polyurethane Foam	78
5.6.2	Full Scale Out-of-Plane 3m Wall Test Analysis.....	80
5.6.3	Full Scale Out-of-Plane 3m Wall Analysis of Rope I Reinforced Walls.....	89
5.7	Categorization of Out-of-Plane Wall Behaviour.....	93
5.8	Conclusions	99
6	Conclusions	100
	REFERENCES	103
	APPENDIX A: TESTING SCHEME FOR WALLETTE SPECIMENS.....	106
	APPENDIX B: Full Experimental Results of Full Scale Walls	107
	B-1 Polyurethane Foam Reinforced 2.2 m Test Wall	107
	B-2 Polyurethane Foam Reinforced 2.2 m Test Wall	112
	Unreinforced Test Wall.....	116
	B-2 Polyurethane Foam Reinforced 3m Test Wall	120
	C-1 Low Density Polyurethane Foam Reinforced 3 m Test Wall	124

C-2 Medium Density Polyurethane Foam Reinforced 3 m Test Wall	128
C-3 High Density Polyurethane Foam Reinforced 3 m Test Wall.....	132
B-2 Polyurethane Foam and Rope I Reinforcement—Three Roped Cells	136
B-2 Polyurethane Foam and Rope I Reinforcement—Fully Reinforced	142

List of Figures

Figure 2-1: Industrial Geo-grid (Redman and Smith, 2009).....	7
Figure 2-2: Geomesh that is tied to adobe wall (Blondet et al., 2010)	8
Figure 2-3: Comparison of Parallel and Angled Polypropylene Mesh (Guragain et al., 2005).....	9
Figure 2-4: Failure of Retrofitted Specimen Under Compressive Loading (Guragain et al., 2005)	10
Figure 2-5: Out-of-Plane Load Variation With and Without Polypropylene Mesh Retrofitting (Guragain et al., 2005)	11
Figure 2-6: Adobe Wall Under Construction with Bamboo Reinforcement (Redman and Smith, 2009)	13
Figure 2-7: Externally Reinforced Bamboo Wall with Ring Beam (Redman and Smith, 2009).....	13
Figure 2-8: Scrap-Tire Tests (a) side view (b) front view (c) hybrid wall (Gölalmiş and Turer, 2007).....	14
Figure 2-9: Post-Cracking Strength Improvement Mechanism of STR (Gölalmiş and Turer, 2007).....	16
Figure 2-10: Reinforcing in an Adobe House with Tire Straps (Charleson, 2009)	17
Figure 2-11: Nailed Joint (Charleson, 2009)	17
Figure 2-12: Adobe House Used to Analyse System Level Earthquake Response (Charleson, 2009).....	19
Figure 2-13: Damage to Rear Wall of Structure After Severe Shaking (Charleson, 2009).....	19
Figure 2-14: Placement of New Tie-Columns in a Brick Masonry Wall (Badoux et al., 2004).....	20
Figure 2-15: Stress-Strain Curve for Polyurethane Foam (Dupont, 1998)	23
Figure 2-16: Wall Test Set-up (Ing, 2010)	25
Figure 2-17: Reinforcement of Wall Into Header and Footer Beams (Ing, 2010).....	26
Figure 2-18: Comparison Between Polymer Reinforced and Plain URM Wall Response (Ing, 2010).....	27
Figure 3-1: Compressive Strength vs. Density for Company B Polyurethane Foams (Company B, 2011) .	33
Figure 3-2: Tensile Strength vs. Density for Company B Polyurethane Foams (Company B, 2011)	34
Figure 3-3: Flexural Strength vs. Density for Company B Polyurethane Foams (Company B, 2011).....	34
Figure 3-4: Shear Strength vs. Density for Company B Polyurethane Foams (Company B, 2011).....	35
Figure 3-5: Walette Test Set-up for Our-of-Plane Loading.....	38
Figure 3-6: Load vs. Mid-Height Displacement for A-2 Wall 2A	40
Figure 3-7: Load vs. Average Mid-Height Displacement for B-1 Polyruethane Foam.....	42
Figure 3-8: Load vs. Average Mid-Height Displacement for B-2 Polyurethane Foam.....	43
Figure 3-9: Energy Absorption of Polyurethane Foam Wallettes	45
Figure 3-10: Comparison of Load vs. Mid-Height Deflection of all Wallettes.....	46
Figure 4-1: Compression Assemblage – Stack Pattern and Running Bond Designs	49
Figure 4-2: Poyurethane Foam Injection into Compression Assemblage.....	50
Figure 4-3: Compression Test Set-up.....	52
Figure 4-4: Fast Poly-mor Compression Assemblage Post Failure	55
Figure 4-5: Increase in Compression Strength, Normalized to the Unreinforced Specimen.....	57

Figure 5-1: Clove Hitch Knot.....	63
Figure 5-2: Rope Test Set-up	64
Figure 5-3: Stress vs. Strain of Rope I.....	66
Figure 5-4: Top-Down Injection.....	69
Figure 5-5: Injection Apparatus and Set-up.....	70
Figure 5-6: Multiple Injection Points with Scattered and Two Row Layout.....	72
Figure 5-7: Injection Preparation For Walls With Company B Polyurethane Foam.....	73
Figure 5-8: Out-of-Plane Full Scale Test Set-up	76
Figure 5-9: Comparison of Lateral Force vs. Average Lateral Mid-Height Displacement of B-1 and B-2 Walls.....	80
Figure 5-10: Lateral Load vs. Average Mid-Height Displacement Curve for the Unreinforced Control Wall	81
Figure 5-11: Comparison of Lateral Load vs. Average Lateral Mid-Height Deflection for Different Types and Densities of Polyurethane Walls	83
Figure 5-12: Comparison of Energy Absorption of 3m Walls, Normalized to Unreinforced Specimen.....	85
Figure 5-13: Work vs. Displacement for 3m Polyurethane Foam Reinforced Walls	86
Figure 5-14: Comparison of Lateral Load vs. Average Lateral Mid-Height Deflection of B-2 2m and 3m Walls.....	87
Figure 5-15: Comparison of Energy Absorption of B-2 Walls, Normalized to Unreinforced Specimen.....	89
Figure 5-16: Comparison of Lateral Load vs. Average Mid-Height Displacement for B-2 Reinforced Walls	90
Figure 5-17: Comparison of Energy Absorption of All B-2 3m Walls, Normalized to Unreinforced Specimen.....	92
Figure B-0-1: Lateral Load vs. Average Lateral Mid-Height Deflection of B-1 2.2m Wall.....	109
Figure B-0-2: Inside of Failure Plane of B-1 2.2m Wall	109
Figure B-0-3: Close-up of Initial Crack Pattern at a Deflection of 2.5mm of B-1 2.2m Wall.....	110
Figure B-0-4: Cracking Pattern of B-1 2.2m Wall	111
Figure B-0-5: Close-up of Crack Pattern of B-1 2.2m Wall.....	112
Figure B-0-6: Lateral Load vs. Average Lateral Mid-Height Deflection of B-2 2.2m Wall.....	113
Figure B-0-7: Cracking Pattern of B-2 2.2m Wall	115
Figure B-0-8: Close-up of Crack Pattern of B-2 2.2m Wall.....	116
Figure B-0-9: Lateral Load vs. Average Mid-Height Displacement Curve for the Unreinforced Control Wall.....	117
Figure B-0-10: Cracking Pattern of Unreinforced 3 m Control Wall.....	118
Figure B-0-11: Cracking Pattern of Unreinforced 3m Control Wall.....	119

Figure B-0-12: Close-up of Crack Pattern of Unreinforced 3m Control Wall	120
Figure B-0-13: Lateral Load vs. Average Lateral Mid-Height Deflection of B-2 3m Wall	121
Figure B-0-14: Cracking Pattern of B-2 3m Wall	123
Figure B-0-15: Close-up of Crack Pattern of B-2 3m Wall.....	124
Figure B-0-16: Lateral Load vs. Average Lateral Mid-Height Displacement for C-1 3m Wall.....	125
Figure B-0-17: Cracking Pattern C-1 3m Wall.....	127
Figure B-0-18: Close-up of Crack Pattern of C-1 3m Wall.....	128
Figure B-0-19: Lateral Load vs. Average Lateral Mid-Height Displacement of C-2 3m Wall	129
Figure B-0-20: Cracking Pattern of Medium Density C-2 3m Wall.....	130
Figure B-0-21: Cracking Pattern of Medium Density C-2 3m Wall.....	131
Figure B-0-22: Close-up of Crack Pattern of Medium Density C-2 3m Wall	132
Figure B-0-23: Lateral Load vs. Average Lateral Mid-Height Deflection of C-3 3m Wall	133
Figure B-0-24: Sudden Widening of Main Crack in High Density C-3 3m Wall	134
Figure B-0-25: Crack Pattern of C-3 3m Wall	135
Figure B-0-26: Close-up of Crack Pattern of C-3 3m Wall.....	136
Figure B-0-27: Lateral Load vs. Average Lateral Mid-Height Deflection of B-2 3m Wall with Three Roped Cells	137
Figure B-0-28: Pre-mature Failure of B-2 Wall With Three Roped Cells Due to Expansive Force of the Foam	138
Figure B-0-29: Cracking Pattern of B-2 3m Wall with Three Roped Cells	140
Figure B-0-30: Close-up of Crack Pattern of B-2 3m Wall with Three Roped Cells	141
Figure B-0-31: Lateral Load vs. Average Lateral Mid-Height Deflection of B-2 3m Wall with Rope in All Cells	143
Figure B-0-32: Cracking Pattern of B-2 3m Wall with Rope in All Cells.....	145
Figure B-0-33: Close-up of Crack Pattern of B-2 3m Wall with Rope in All Cells	146

List of Tables

Table 2-1: Comparison of Wall Test Capacities (Ing, 2010).....	26
Table 3-1: Reactivity of Polyurethane Foam A-2 at 21C (Polyurethane Foam A-2, Company A)	31
Table 3-2: Reactivity of Polyurethane Foam A-3 at 21°C (Polyurethane Foam A-3, Company A).....	32
Table 3-3: Performance Data of Company C Polyurethane Foams (Polyurethane foam C-1, Company C)(Polyurethane foam C-2, Company C)(Polyurethane foam C-3, Company C).....	36
Table 4-1: Summary of Compression Results	53
Table 5-1: Rope Test Results	65
Table 5-2: Comparison of Out-of-Plane Behaviour of Wall B-1 and Wall B-2	79
Table 5-3: Comparison of Different Types and Densities of Polyurethane Reinforced Walls	84
Table 5-4: Comparison of B-2 Reinforced Walls	92
Table 5-5: Component Damage Classification (ATC, 1998)	95
Table 5-6: Out-of-Plane Flexural Response Classification Guide for Polyurethane Foam Reinforced Masonry (ATC, 1998).....	97
Table A-1: Ratios of Blowing Agent and Accelerant Used in A-2 Mixes.....	106
Table A-2: Ratios of Blowing Agent and Accelerant Used in A-3 Mixes.....	106
Table B-1: Colour Scheme of Crack Pattern Figures	107

1 Introduction

1.1 Problem Definition

Although unreinforced masonry (URM) buildings perform well under service gravity loads and low lateral loads, the large amount of damage to these buildings from recent and past earthquakes shows that they are particularly vulnerable to high seismic loading. URM is weakest in the out-of-plane direction, relying only on the self-weight of the wall and the tensile strength of the mortar, which is generally very weak. This results in brittle and unstable failure during a large earthquake, often in the form of flexural cracks and collapse of the wall, which can then lead to failure of other elements within the building such as roof collapse. In addition to the full collapse of buildings, brittle masonry failure can result in a large amount of flying debris that poses a considerable threat to life safety for occupants. Mitigating this threat to life safety through inexpensive means is the motivation for this research.

Many techniques have been proposed to strengthen existing and new URM structures to withstand high seismic loads. However, most of the proposed techniques are too costly for practical application in developing countries. Most modern masonry reinforcement consists of steel rebar or fibre-reinforced plastic materials, which are very costly, and need to be applied and implemented precisely, with detailed placement and connections. Owing to the high cost of these conventional reinforcements and the lack of adherence to proper building techniques with little inspection, there is a need for a simple to use reinforcement system that is inexpensive and requires little engineering knowledge to implement. Polyurethane foam has the potential advantage to be used in this application, as it is readily available across the globe, it is easy to mix and use, and it can reinforce both a new or existing building very quickly – with foam expanding and hardening within seconds. In addition, although not within the scope of this research, polyurethane foams have superior thermal insulation properties.

1.2 Scope and Objectives

The purpose of the proposed study is to investigate methods of enhancing the out-of-plane seismic resistance of URM walls using polyurethane foam reinforcement. Although this reinforcement may also enhance both in-plane bending and in-plane shear performances, these directions of loading are beyond the scope of this study. The proposed investigation could have a significant impact on building practices in developing countries, both economically and from a life-safety perspective. This study is intended to develop and test innovative reinforcing techniques that are cost-effective and that can be applicable to both new construction and existing URM structures.

The aim of this research is to select, develop and test a system of polyurethane foam reinforced masonry so as to determine optimum foam reinforcement as well as a system for its application. Wallettes and full size wall panels consisting of standard hollow concrete block will be reinforced with different types and densities of polyurethane foam. The investigation also involves the use of common ropes to be used as additional reinforcement in combination with the polyurethane foam.

1.3 Thesis Outline

In this introductory chapter, the nature of the problem and the potential role of polyurethane foam in providing an effective out-of-plane reinforcement will be discussed. The scope of the research was laid out and the specific objectives of the investigation were set. Chapter 2 provides information on previous research carried out to provide inexpensive reinforcement solutions to adobe and URM buildings in developing countries. Previous preliminary research into the use of polyurethane foam in URM is also discussed, looking at the systems behaviour in the in-plane direction. In Chapter 3, the first phase of the experimental program conducted on simply-supported third-scale wallettes is described. Appendix A details the mixing scheme for the wallette specimens. In Chapter 4 the compressive strength of polyurethane foam reinforced assemblages is presented. In Chapter 5, the details and results of the full-size wall testing

phase of the experimental investigation are presented. The full size walls were reinforced with polyurethane foam and also a polyurethane foam and rope combination and tested under two-point loading. The details of the individual wall test results are discussed in Appendix B.

2 Literature Review

2.1 Introduction

When analyzing the destructive earthquakes of past decades, it is evident that the structural damage of such seismic activity is felt most in developing countries. This devastation is often attributed to the use of non-engineered unreinforced masonry (URM) that is not constructed to be able to resist seismic forces during an earthquake. As a result, when areas dominated by non-engineered URM experience a moderate earthquake, a catastrophic collapse of these buildings may occur.

From this reality, it is clear that more needs to be done to investigate the measures that could be taken to improve the susceptibility of these buildings to earthquake damage. A proper solution must be inexpensive and simple to implement, preferably using materials that would be locally available or easily accessible in a developing community.

This chapter aims to introduce current methods being developed and used in practice in developing countries to improve the performance of URM buildings. First it will discuss other researcher's endeavours, with a focus on improving adobe buildings. This section will then be followed by an introduction into the use of polyurethane foam as a reinforcement material. The characteristics of polyurethane foam will be explained, along with initial research into the use of this material as reinforcement in masonry construction.

2.2 Types of Non-Engineered URM Buildings in Developing Countries

2.2.1 Adobe Buildings

Adobe buildings make up a large percentage of the current housing in Africa, Asia, India, Latin America and the Middle East, with 30% of the global population living in such housing. Unfortunately, adobe structures are highly susceptible to devastating failures and collapse during earthquakes, resulting in a high level of damage and loss of life (Redman and Smith, 2009). This type of housing is particularly vulnerable during an earthquake, as it is most often unreinforced and heavy, thereby attracting greater seismic forces. In addition, the adobe mud blocks are weak and brittle, and most adobe buildings are constructed with little or no technical assistance (Blondet et al., 2010).

In developing countries, such as Peru, roughly 70% of the countries rural population live in adobe homes. Adobe buildings are popular in these regions due to the low cost and ease of construction of adobe blocks, as untrained people may create their own blocks, normally out of earthen materials already available on their property, or within their local community. Adobe homes are durable and have excellent thermal and acoustic properties, and are one of the most ecologically sustainable types of buildings that can be made (Garcia et al., 2010). However, the creation of these buildings is labour intensive and often takes a long time to complete. This is often because only a few people are working together to create a home for themselves using the minimal tools at their disposal. Unfortunately, in addition to their vulnerability during seismic activity, adobe homes are also susceptible to water damage and suffer from having an image of being the housing of the “poor”.

In 2001, El Salvador suffered an earthquake which cost the lives of 1,100 people. This devastating earthquake led to the damage or collapse of 150,000 adobe homes, effecting 1.6 million people in the country. Iran suffered even more devastating consequences of their weak housing in 2003 when the country experienced an earthquake that resulted in the destruction of 85% of their homes, killing 26,000 people and leaving 100,000 people homeless (Redman and Smith, 2009). Most recently in August of 2007 the city of Pisco, Peru suffered a substantial hit to their housing inventory. Over 80% of

the adobe houses in the region collapsed or suffered extensive damage, as the city was close to the epicentre of an earthquake that shook the country (Charleson, 2009).

In China, an earthquake in 1976 proved the susceptibility of brick masonry buildings to devastating collapse under seismic loading. The earthquake claimed the lives of 240,000 people, mainly due to the collapse of brick masonry structures (Redman and Smith, 2009).

Stone masonry buildings are typically poorly constructed, and normally built by the owners and occupants of the buildings themselves instead of by local tradesmen. The use of low strength stone and mortar in addition to inadequate wall connections leads to a very low seismic performance of stone masonry (Redman and Smith, 2009).

2.3 Current Retrofitting Techniques for Non-Engineered URM

2.3.1 Mesh Reinforcement

2.3.1.1 Polymer Mesh

Two types of polymer mesh that have been used to retrofit unreinforced masonry structures are an industrial geo-grid as seen in Figure 2-1 and a weaker mesh which is typically used as fencing on construction sites. The polymer mesh is wrapped around the wall with varying levels of coverage and then coated with a mud plaster.

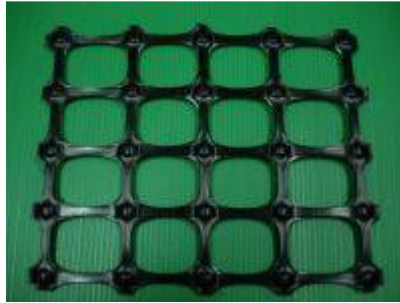


Figure 2-1: Industrial Geo-grid (Redman and Smith, 2009)

When the walls of a structure are fully covered with geo-grid mesh, the system behaves as a rigid body, and only small cracks develop. The failure of this system is that a wall can slide off of its foundation when subjected to deflections greater than 100 mm, even though there is no significant damage to the building. When subjected to deflections of 120 mm or larger, the walls can exhibit torsion which may lead to further cracking and sliding at the base of the structure (Redman and Smith, 2009).

When only 75% of the structure is covered in geo-grid mesh, vertical cracks may develop at wall corners in addition to diagonal cracks along the longitudinal walls when the building is subjected to deflections greater than 80 mm. However, the walls will be able to stay together, as the mesh is able to hold the wall together, as it provides control of the walls displacement and provides a way to redistribute stresses within the system (Redman and Smith, 2009).

When the geo-grid mesh covers only 50% of a wall area, it provides an insufficient amount of reinforcement. Large cracks may develop at deflections greater than 80mm and at larger deflections there will be a large amount of severe structural damage (Redman and Smith, 2009).

When using a weaker construction fencing mesh, covering 80% of the wall area, an adobe wall can exhibit similar behaviour to the case of the geo-mesh when it was only covering 50% of the wall area. Large cracks will develop and wall sections will

eventually break into pieces, being held together only by the mesh itself. This extra force on the mesh will lead it to fail and snap in some places, showing that more reinforcement would be required in order for this solution to work (Redman & Smith, 2009).

In order for the geogrid mesh system to work, it must be tied to both sides of the adobe wall using a plastic string as shown in Figure 2-2, and then anchored to the foundation. At the top of the wall, the mesh must be attached to a wooden ring beam. This setup allows the geomesh to increase the stiffness, strength and deformation capacity of the walls it is reinforcing by absorbing the tensile stresses that the adobe masonry is unable to resist on its own. In addition to its tensile system capabilities, the geomesh is able to contain the large broken pieces that can come off a wall during an earthquake, thus keeping the form of the walls together, still supporting the roof and thus avoiding collapse of the structure. At a cost of only \$1.50 U.S. per m², this is a material that shows great promise.



Figure 2-2: Geomesh that is tied to adobe wall (Blondet et al., 2010)

2.3.1.2 Polypropylene Packaging Strips

Polypropylene strapping is used as packaging material the world over and is both inexpensive and readily available. These bands are used to form a mesh which is then used to encase masonry walls, preventing both collapse and the escape of debris during earthquakes.

The efficiency of different mesh orientations was analyzed at the University of Tokyo, looking at mesh oriented parallel to the adobe masonry blocks, as well as mesh inclined at a 45° angle. As can be seen in Figure 2-3, the mesh oriented at a 45° angle provided more strength than the horizontal and vertical mesh. This orientation is stronger, as the angled mesh produces a high confining effect, and as the vertical deformation increases as the cracks become wider, the angled reinforcement is working at its optimum level. However, even though the angled mesh provides greater strength, the parallel mesh provides a maintained high level of strength which can be considered to improve the behaviour of the structure significantly. The parallel mesh is also much easier to manufacture and install and therefore would be the optimum solution of mesh orientation (Guragain et al., 2005).

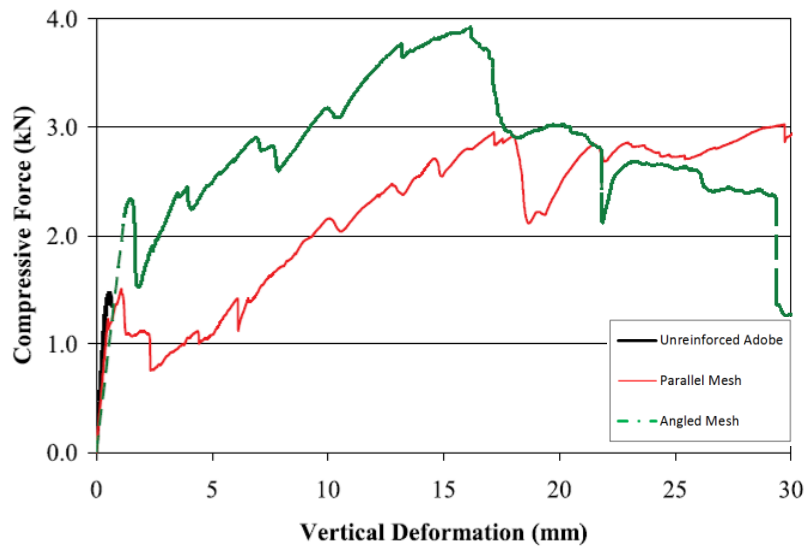


Figure 2-3: Comparison of Parallel and Angled Polypropylene Mesh (Guragain et al., 2005)

When compressive force is applied, a non-retrofitted specimen immediately splits into two pieces at the presence of the first diagonal crack, leaving no residual strength left in the specimen. However, in the retrofitted case as in Figure 2-4, cracks develop at a much slower rate, followed by a drop in strength. The reinforcement has no effect until cracking occurs; however after cracks develop the polypropylene mesh acts to regain the strength that was lost by the formation of cracks, and also acts to maintain stability of a completely cracked specimen. It can be seen in Figure 2-3 that although the reinforced specimen exhibits a drop in strength after initial cracking, it is able to retain 60% of its peak strength. Further drops in strength occurred with the formation of new cracks but were regained by the readjusting and packing of the polypropylene mesh. At a strength of approximately 2.9 kN the bands begin to fail, however as the other bands are able to take over the additional stresses, there is not a significant or drastic reduction in the strength of the specimen, and any lost strength is easily recovered. The final strength of the retrofitted specimen reached 3.0 kN which is double the initial specimen strength of 1.5 kN, while sustaining deformations 45 times larger than the non-retrofitted specimen (Guragain et al., 2005).

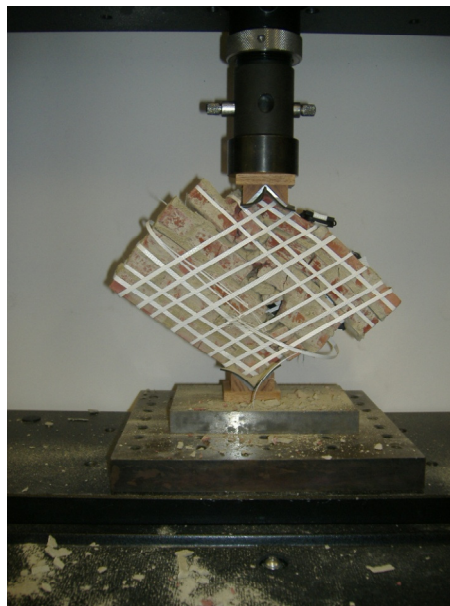


Figure 2-4: Failure of Retrofitted Specimen Under Compressive Loading (Guragain et al., 2005)

When considering out-of-plane loading of the non-retrofitted masonry, the specimen exhibits immediate failure after the first crack develops at mid-span, as can be seen in Figure 2-5. The only remaining residual strength left in the specimen is due to the interlocking of bricks and the application of load under the displacement control method. However, it can be seen that this behaviour can be significantly improved with the presence of the polypropylene meshing. In the retrofitted case, after initial cracking the specimen was able to retain 45% of its peak strength and was able to gradually regain its strength due to the effects of the mesh, reaching a final strength of double the initial peak specimen strength. It can also be seen that the retrofitted specimen was able to sustain mid-span deflections 60 times larger than the non-retrofitted specimen under out-of-plane loading (Guragain et al., 2005).

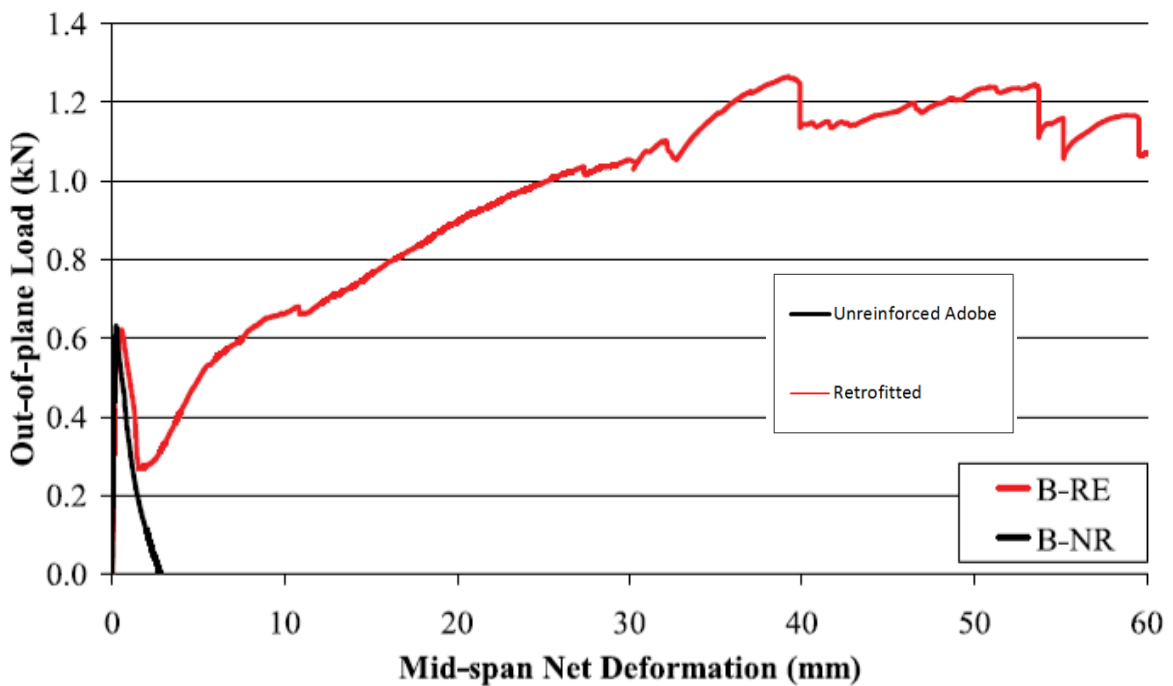


Figure 2-5: Out-of-Plane Load Variation With and Without Polypropylene Mesh Retrofitting (Guragain et al., 2005)

2.3.1.3 Plastic Carrier Bag Mesh

A polymer mesh may be developed in similar sense to the polypropylene packaging mesh, only instead of using the packing strips; plastic carrier bags are woven together. The plastic bags may be cut into strips 20 mm wide and then braided together to form a 50 mm by 50 mm mesh which can be fixed to the wall surface using tacks. Plaster should then be applied over the mesh. The testing of this mesh demonstrated that it was able to exhibit a greatly increased ductility capacity and tensile strength, with the wall failing in-plane at a force double that of the control test wall (Redman and Smith, 2009).

2.3.2 Bamboo Reinforcement

Bamboo reinforcement has the potential of increasing the amount of seismic activity that a building can handle before it reaches ultimate collapse. The bamboo system uses many components acting together such as buttresses, a ring beam, and both internal horizontal and vertical reinforcement out of bamboo. The application of bamboo used internally in the masonry as reinforcement is shown in Figure 2-6. This same system may also be applied as a retrofitting method by applying the vertical bamboo reinforcement on the external sides of the structure. This method may actually be simpler, as it avoids construction problems such as the alignment of the reinforcement and the trimming of the bricks. The retrofit arrangement may be seen in Figure 2-7 (Redman and Smith, 2009).



Figure 2-6: Adobe Wall Under Construction with Bamboo Reinforcement (Redman and Smith, 2009)

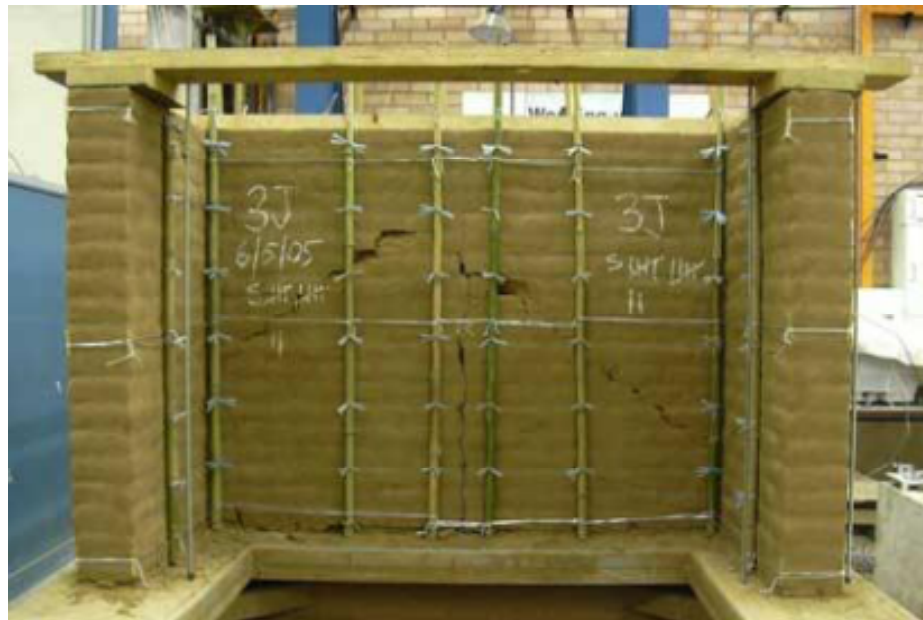


Figure 2-7: Externally Reinforced Bamboo Wall with Ring Beam (Redman and Smith, 2009)

2.3.3 Use of Rubber Tires for Reinforcement

2.3.3.1 Post-Tensioning Using Rubber Tires

Post-tensioning can greatly increase the out-of-plane bending capacity of an unreinforced masonry system while also preventing corner separation. Used tires contain a steel-mesh and wires that have been vulcanized with a rubber coating and these materials can be re-used as a structural strengthening material in post-tensioning. The use of scrap tires as reinforcement is environmentally friendly and reduces both land and air pollution. This retrofitting method is extremely viable for developing countries, as scrap tires are free and in abundance, thereby substantially reducing reinforcing costs (Gölälmış and Turer, 2007).

The scrap tire reinforcement forms a chain system around the wall, wrapping it in the vertical direction as can be seen in Figure 2-8. At the top and bottom of the wall, the reinforcement is placed over two cylindrical logs which act to distribute the forces on the wall and prevent stress concentrations. A hybrid system may also be used, using only two scrap tire reinforcements at the top and bottom of the wall, connecting them with vertical rebar, thereby simplifying the system and reducing cost and application time (Gölälmış and Turer, 2007).

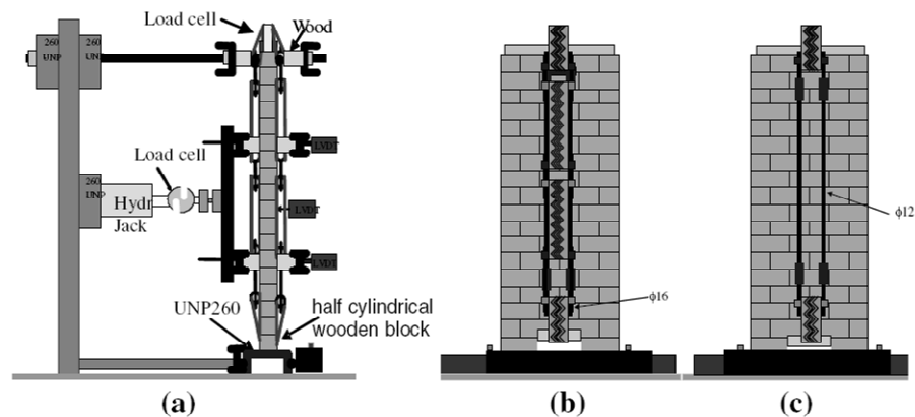


Figure 2-8: Scrap-Tire Tests (a) side view (b) front view (c) hybrid wall (Gölälmış and Turer, 2007)

Testing of the system showed that post-tensioning with scrap tire reinforcement resulted in a 500% increase in both strength and out-of-plane bending capacity of the wall compared to an unreinforced adobe specimen, along with a 15 times increase in energy dissipation capacity (Gökalmiş and Turer, 2007).

Both the hybrid and scrap tire reinforcement chain perform equally, apart from a minor difference in the amount of drift they can experience. This can be expected, as the chain system has three times more tires than the hybrid system, therefore the overall stiffness of the hybrid wall was three times that of the more ductile chain system (Gökalmiş and Turer, 2007).

Figure 2-9 demonstrates how scrap tire reinforcement works to improve the post-cracking strength of URM. When tire-reinforced wall specimens begin to act in the non-linear range, their increase in strength is governed by the compressive strength of the wall, and hence both the normal and hybrid system act in a similar manner. The drift ratio and energy dissipation capabilities of the system are governed by the stiffness of the scrap tire reinforcement. As the wall is loaded, the reinforcement becomes more flexible, and the drift capacity and energy dissipation capabilities of the system increase, making it an effective post-tensioning mechanism. Note that due to the elastic nature of the scrap tire reinforcement, the deformations in the nonlinear range has fully recovered (Gökalmiş and Turer, 2007).

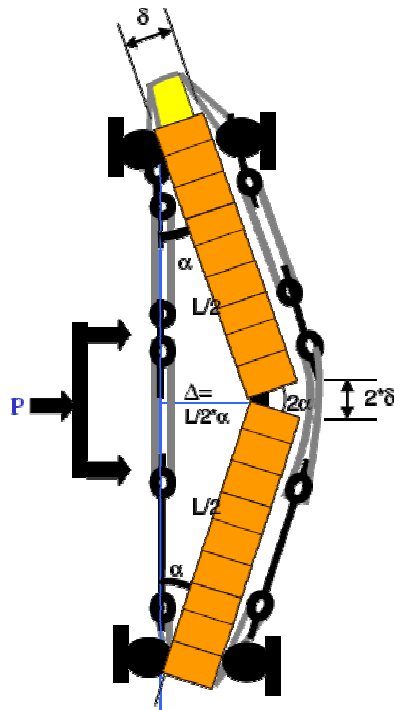


Figure 2-9: Post-Cracking Strength Improvement Mechanism of STR (Gölalmiş and Turer, 2007)

2.3.3.2 Rubber Tire Mesh Reinforcement

This reinforcement method cuts tires into thin straps approximately 5m long, and uses them as reinforcement, joining the straps using a simple nailed joint. As in the post-tensioning tire reinforcement case, the tires pass over and under the wall; however there is no post-tensioning applied. Instead, the tires are applied to the wall both vertically and horizontally to act as a large dual system as see in Figure 2-10 (Charleson, 2009).

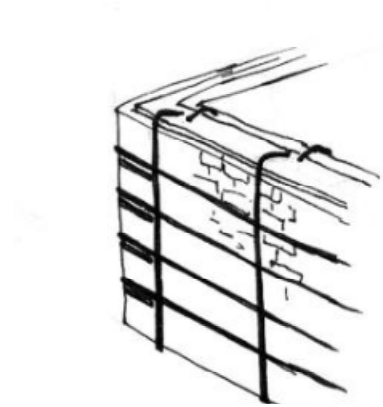


Figure 2-10: Reinforcing in an Adobe House with Tire Straps (Charleson, 2009)

Straps are connected together by overlapping the straps to form a butt joint as can be seen below in Figure 2-11. Nails on either side of the joint are bent around the overlapped tire so as to prevent any premature failure of the rubber and nail (Charleson, 2009).



Figure 2-11: Nailed Joint (Charleson, 2009)

To create the mesh, tire straps are wrapped horizontally around the wall at 600 mm intervals. This composite system works together to develop a system in which the tension forces developed due to out-of-plane bending are equilibrated by the horizontal compression strut of the tire reinforcement. Vertical tire strapping reinforcement is placed at 1.2 m intervals along the length of the walls. This acts to provide out-of-plane resistance, especially around doors and other wall openings. The vertical reinforcement also acts as a proper mechanism of tying the walls to the roof, which prevents the roof from being separated from the wall during an earthquake, which would normally lead to

collapse of the entire roof structure. The vertical tire strapping also improves the sliding shear resistance of the wall due to their clamping effect on the wall and the increased tensile strains when the wall undergoes substantial deflection. The vertical reinforcement also helps to develop in-plane diagonal compression struts in the walls. One disadvantage of this system is that it provides so much ductility that upon earthquake action, P- Δ effects need to be taken into consideration (Charleson, 2009).

This system of reinforcement was tested on a full-scale adobe house at the Catholic University of Peru in Lima, where they subjected the house to a mild, moderate and severe earthquake in order to assess the system and the damage that would result, as depicted in Figure 2-12. When subjected to mild shaking, no damage was observed. As intensity built to simulate a moderate earthquake, vertical cracks began to form at the corners of the large rear wall, which would have normally collapsed if the building had not been horizontally reinforced and restrained. The rear walls also exhibited cracking due to out-of-plane failure; however no cracking developed in the in-plane direction. When subjected to a severe earthquake, the structure did experience significant damage, but was not in any danger of collapse. Out-of-plane failure had a significant effect on the building, with the walls suffering large cracks while the piers experienced moderate cracking. However, only one block was dislodged from the system at the location of significant out-of-plane failure. As can be seen in Figure 2-13, there was substantial damage to the wall, but the system acted together to keep the wall together and prevent collapse (Charleson, 2009).



Figure 2-12: Adobe House Used to Analyse System Level Earthquake Response (Charleson, 2009)



Figure 2-13: Damage to Rear Wall of Structure After Severe Shaking (Charleson, 2009)

2.3.4 Confined Masonry

Unreinforced masonry may be confined by the introduction of vertical reinforced concrete or reinforced masonry tie columns, shown in Figure 2-14. These columns act to confine the walls at all corners and intersections, as well as at door and window openings. In order for the tie columns to be effective, they must intersect with an equivalent tie beam at floor levels. Confinement acts to prevent disintegration and to improve energy dissipation; however confinement has minimal effect on the ultimate load resistance of the structure (Badoux et al., 2004).

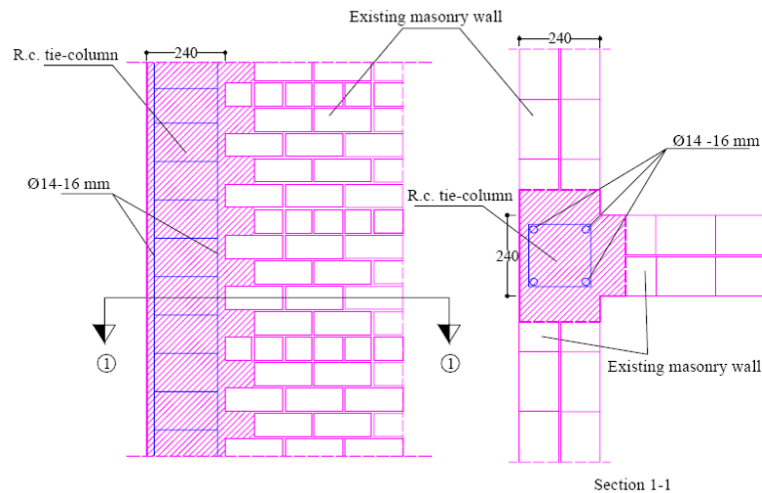


Figure 2-14: Placement of New Tie-Columns in a Brick Masonry Wall (Badoux et al., 2004)

This system is widely used in Asia, Latin America and Europe. This technique is cost-effective for implementation in a new building; however as a retrofit method it involves the demolition and reconstruction of wall sections, and hence is not economical in most cases (Badoux et al., 2004).

2.4 Polyurethane Foam

Polyurethanes in its different forms can be used to create a wide variety of products, from wheels of inline skates to cushions for furniture. By altering its components, polyurethane foams can be strong enough to be used as structural members or can be made soft enough to be used for cosmetic applicator sponges (Thomson, 2005). The main chemical make-up of polyurethane foam is a base polyol and isocyanate, formed in 1:1 by volume reaction with the help of a catalyst and blowing agent.

Blowing agents are chemicals that must be compatible with the base resin, produce a void-free compact outer skin when mixed with the resin, and must give the best blowing efficiency for the minimum amount of chemical concentration for the lowest price. A blowing agent can significantly affect the physical properties of foam, such as its density, foam structure, shrinkage quality and its cooling time. Increasing the concentration of a blowing agent generally reduces the density, reduces shrinkage, improves surface quality, and increases the needed cooling time of the polyurethane foam product. Examples of common blowing agents are freons, carbon dioxide (formed by the reaction of isocyanate and water), nitrogen, or compressed air (Shutov, 1986).

Rigid polyurethane foams possess a number of characteristics which make it a desirable material to use in structural applications. Rigid polyurethane foams can be mixed at room temperature without requiring any additional heat, they adhere to many kinds of materials such as steel and wood, the density can be varied over a wide range, they are resistant to petroleum, oils, and other non-polar solvents, they have great insulating properties, and they can be made with on-site foaming techniques such as spray foaming and pour-in-place foaming (Shutov, 1986).

The strength of rigid urethane foams may be altered by using different catalysts, foaming agents, types of mixing, types of foaming systems, as well as different base polyols and isocyanates, which all can alter the cell structure of the foam. By changing

these various ingredients, the foam can be made to be brittle with a high modulus and low elongation, or to be more flexible with a low modulus (Dupont, 1998).

The properties of rigid polyurethane foams can be altered by using various methods, such as by changing the foaming composition, using different techniques for handling the foaming composition, and by using different moulds that may be subjected to different environments. However, changes that do not affect the density of the foam typically do not affect the overall strength of the foam. In order to obtain any noticeable change in strength properties, a change in density is required, which can be obtained by varying the amount of blowing agent used to make the foam (Dupont, 1998).

Polyurethane foams can be affected by extreme temperatures. The foam can soften at high temperatures, leading to a loss in strength and a change in the foams dimensions. Low temperatures have less effect on the foam, making them only slightly harder and more brittle. However, between the general temperature range of -73°C to 121°C , the product is stable, with the yield point in compression remaining unaffected. Considering this stable temperature range is within the temperature limits that most countries experience, this product is clearly suitable for both northern and tropical climates (Dupont, 1998).

A benefit of using this material is its very fast cure time. High density polyurethane foams are able to reach 90% of their full compressive strength within 15 minutes of injection, with lower density foams reaching this state even quicker. Studies have shown that properties of the foam such as compressive, tensile, flexural and shear strength as well as elastic properties are greatly controlled by the density of the specimen, with higher densities of foam resulting in higher strength properties (Dupont, 1998).

The stress-strain curve for rigid polyurethane foams contains an elastic region in which stress is nearly proportional to strain. This elastic region can vary from 5-10% of total strain, and is only limited by the yield point of the material. This stress-strain relationship can be found in Figure 2-15 for a low-density polyurethane. Beyond this

yield point, the foam has little elastic recovery, as the cell structure of the foam is crushed and permanently deformed. At this point on the curve, a plateau forms and deflection continues to increase with little to no increase in stress. For low-density foams, this plateau can extend up to 70% strain in compression. As foam density increases, the extent of this plateau decreases proportional to the increase in density. The stress-strain curve is also sensitive to the loading rate, with a higher loading rate resulting in a decreased plateau length. Beyond this plateau region, the polymer increased in both strength and stiffness and it becomes denser (Dupont, 1998).

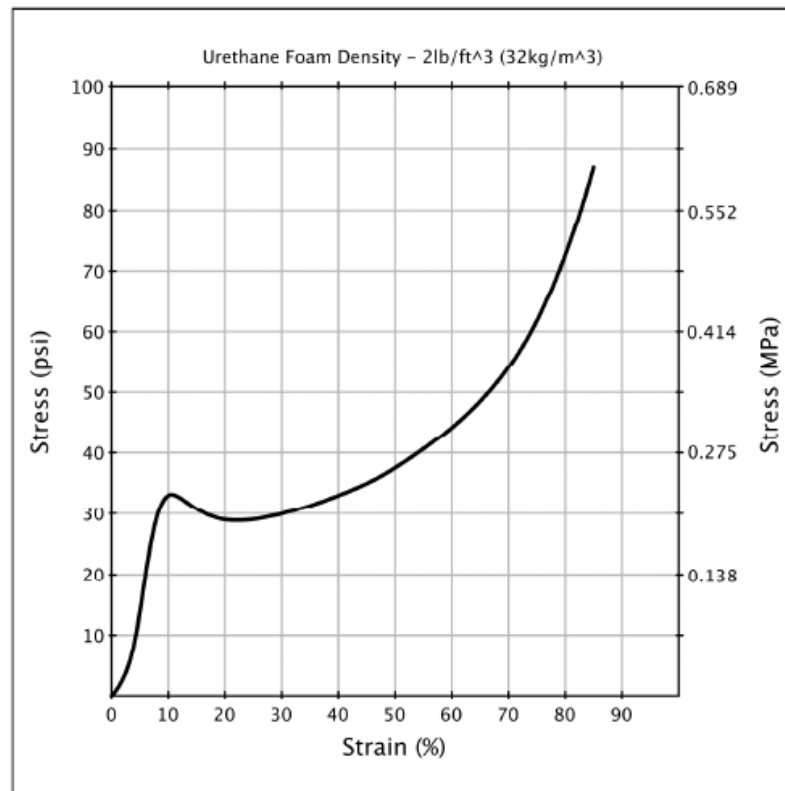


Figure 2-15: Stress-Strain Curve for Polyurethane Foam (Dupont, 1998)

The majority of low density rigid polyurethane foams have an oblong cell structure which results in anisotropic behaviour. Most rigid polyurethane foams are typically up to twice as strong in the direction of foam expansion, with this behaviour

even more pronounced where the foam is allowed to expand through a long vertical distance. The amount of anisotropy in the foam can be reduced by injecting it into a confined space, thereby making the product denser. When injecting polyurethane foam into confined spaces, the outer perimeter layers of the injection surface start to cure while the centre is still very fluid and continuing to expand. This continuing expansion further densifies the outer layers and increases the products overall strength (Dupont, 1998).

2.5 Investigations into the use of Polyurethane Foam in Improving Shear Strength in URM

A study investigating a new method of retrofitting URM, involving the injection of expanding urethane polymers to fill the cores of URM walls to increase their strength and ductility was undertaken at the University of Western Ontario. The focus of this study was to analyze the effects of urethane polymers on their ability to improve the capacity and behaviour of URM walls subjected to in-plane cyclic lateral loads.

A wall can fail in tension, shear or compression depending on its aspect ratio and the amount of axial load acting on the specimen. A tension failure is characterized by rocking behaviour, a shear failure constitutes blocks slide along a bed joint, and a compression failure results in vertical cracks throughout the wall. A diagonal crack may form due to a combination of in-plane lateral and compressive loads, which is most commonly seen in load bearing shear wall structures. At high axial loads, compressive forces increase joint friction which enhances shear strength and reduces tensile force at the heel of the wall. A double-diagonal X pattern crack can form across the face of the wall using multiple load reversals under high axial load. At a low axial load, toe crushing and wall rocking may occur (Ing, 2010).

In the testing at the University of Western Ontario, a 9 course high wall was selected for testing, having an aspect ratio of 1.0 so as not to favour any failure method.

The walls were constructed using standard materials and practices, with overall wall dimensions of 1810 mm tall by 1790 mm wide. The test set-up for the shear wall tests is shown in Figure 2-16. Bolted to the strong floor, this reaction frame provided adequate strength and stiffness to test the walls (Ing, 2010).

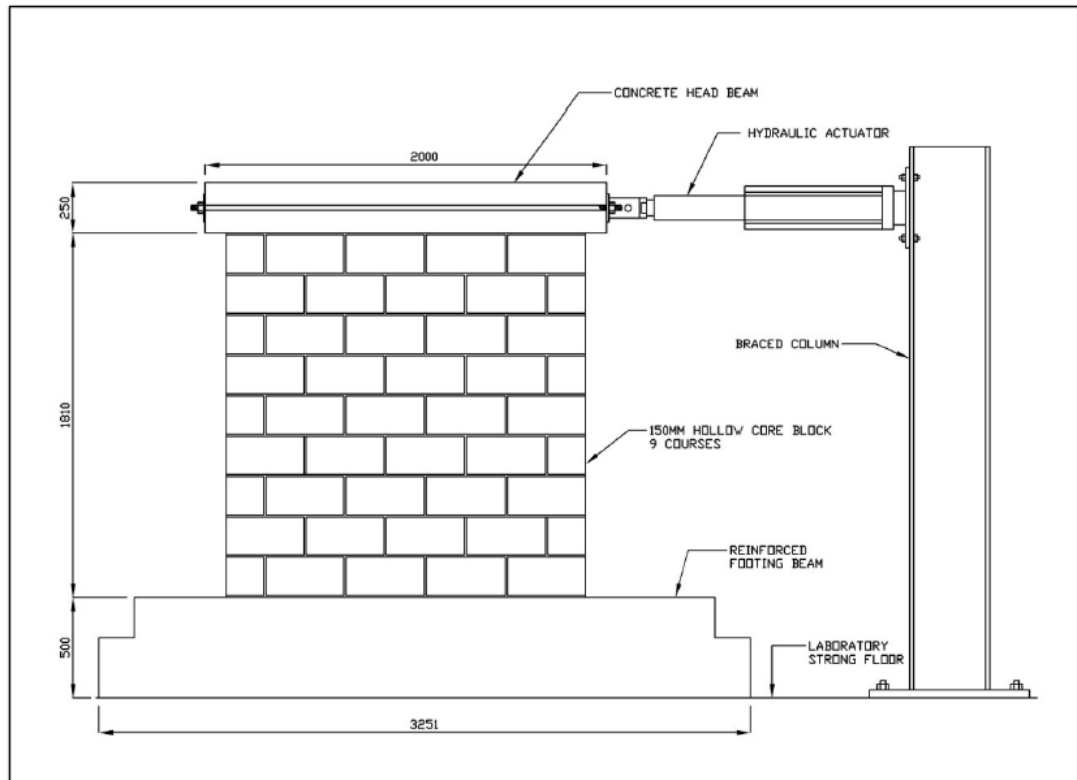


Figure 2-16: Wall Test Set-up (Ing, 2010)

With the weakest and more critical failure planes being located along the top and base mortar joints, it was necessary to upgrade these joints to ensure a failure plane within the wall and not along these critical joints. Steel angles were bolted through the wall at the top and base courses and anchored into the head and base beams using threaded not, as shown in Figure 2-17 (Ing, 2010).

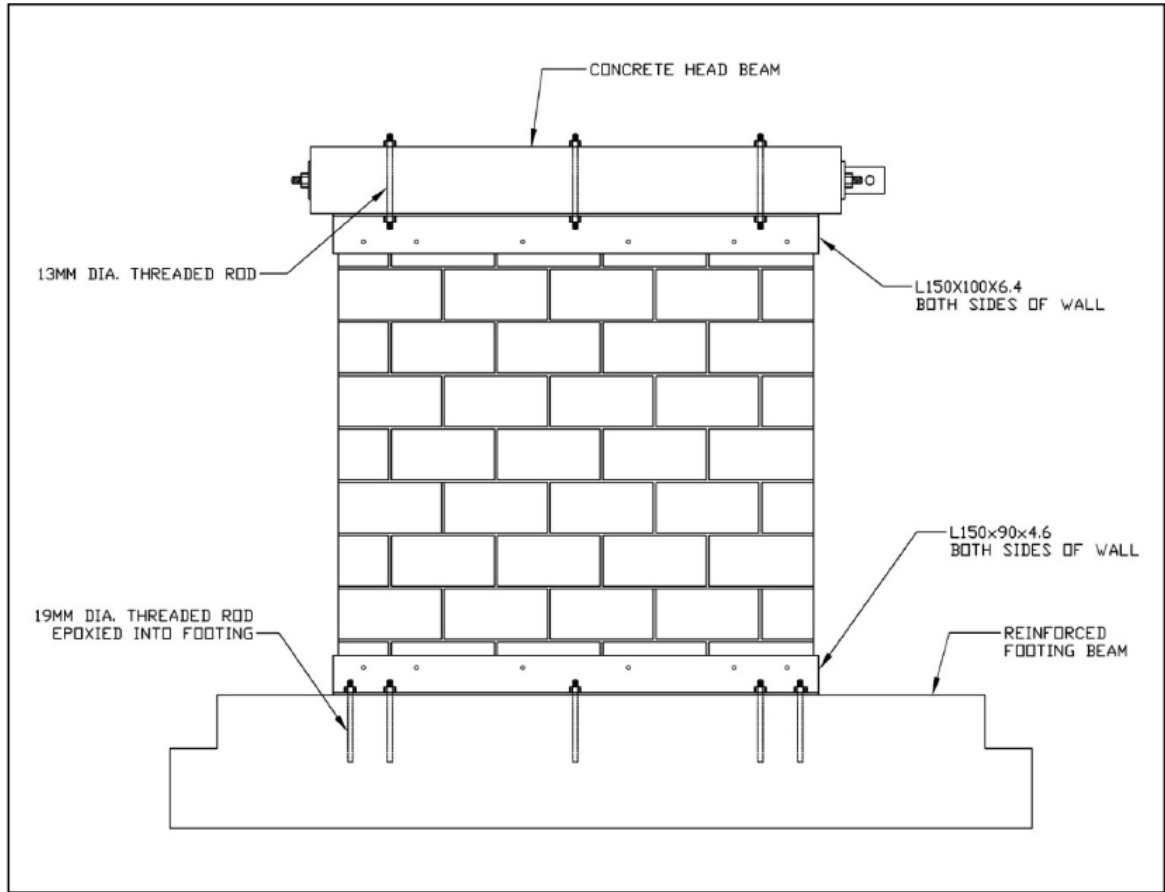


Figure 2-17: Reinforcement of Wall Into Header and Footer Beams (Ing, 2010)

When the four walls were tested, both unreinforced and reinforced specimens exhibited rocking, with sliding and toe crushing. When a tensile crack developed and began to spread, the walls showed a loss in strength and began to rock. As can be seen in Table 2-1, the polyurethane foam reinforcement increased the capacity of the wall by 2.5 times (Ing, 2010).

Table 2-1: Comparison of Wall Test Capacities (Ing, 2010)

Wall Type	Average Peak Load (kN)	% Increase
Unreinforced	5.9	248.5
Polymer Reinforced	14.5	

A comparison of an unreinforced and polymer reinforced wall specimen is shown in Figure 2-18. The polymer core of the polyurethane foam reinforced wall was able to increase the tensile and shear capacities of the specimen, providing the wall with higher initial strength as compared to the URM specimen. The foam reinforced specimen exhibited greater energy dissipation capacity, as after peak load was reached and initial failure occurred, each polymer core had to be progressively overloaded, allowing the system to maintain close to peak loads over a range of displacements. As polymer cores ruptured and cracks widened, the wall capacity gradually diminished to the point that it exhibited similar behaviour to the URM specimen. At this time when the polymer cores had ruptured and the wall was not able to maintain any residual strength, the wall exhibited sliding behaviour. The polyurethane foam reinforcement was able to increase energy absorption of the URM wall by 167% (Ing, 2010).

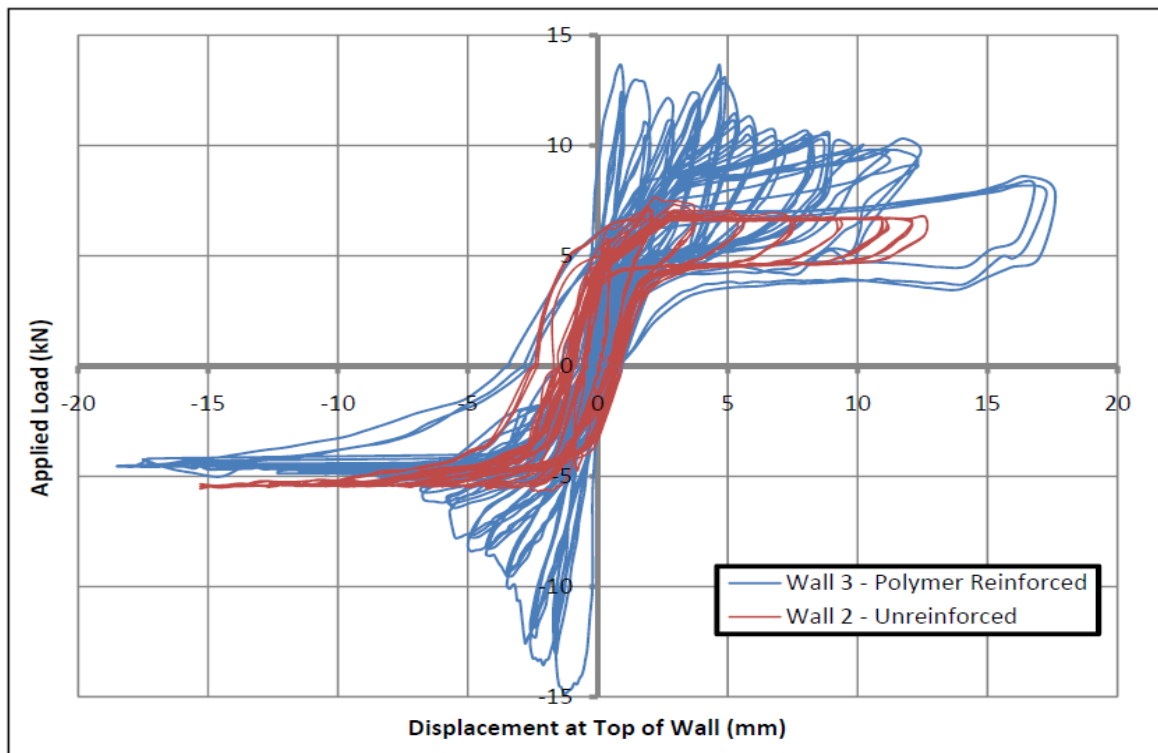


Figure 2-18: Comparison Between Polymer Reinforced and Plain URM Wall Response (Ing, 2010)

Under low seismic loading, representing a serviceability state, the wall showed high elastic peak strength and was able to withstand ground motions without any appreciable damage. Under a stronger earthquake, the retrofitted wall began to crack, but showed great stability and demonstrated post peak strength, providing increased ductility to the system when compared to the URM case. Under strong seismic loading, representing an ultimate limit state, the polyurethane foam-reinforced wall did fail, but did not collapse, thereby reducing the amount of debris.

3 Preliminary Investigation into the use of Polyurethane Foam as Reinforcement in Masonry

3.1 Introduction

In this chapter, the details of new polyurethane foam reinforcement materials as well as the investigation carried out to examine their effectiveness in enhancing the out-of-plane load resistance of masonry walls is described. The experimental program was divided into three separate phases: wallette testing, compression testing of masonry assemblages, and full scale wall tests. This chapter covers the investigation into the applicability of these new materials as reinforcement in masonry, as well as wallette testing to select the appropriate materials to be used in the next phase of testing. The details of the compression testing of masonry assemblages is presented in Chapter 4, while the details of the full scale wall tests are described in Chapter 5.

Prior to using these new polyurethane foam materials in full size walls, it was deemed reasonable to test them on wallettes made of third-scale concrete block to examine parameters such as bonding, strength of material, increase in energy absorption, and the overall enhancement in the out-of-plane response. Simply supported wallettes were tested under monotonic two-point loading. The details of the wallette specimens, test set-up and test results are reported in Section 3.3. The new proposed reinforcement materials are described in the next section. Polyurethane foam materials supplied by three different companies were used for this testing, and these companies will hereby be referred to as Company A, Company B and Company C. Conclusions drawn from the behaviour of each material under out-of-plane loading are discussed and compared at the end of this chapter.

3.2 Materials

3.2.1 Concrete Blocks

The concrete masonry blocks used for this preliminary walette stage of testing were third-scale blocks made in-house at the university. As the strength of the blocks themselves was not a factor in this testing, a collection of scrap blocks were used, of varying compressive strength.

3.2.2 Hand-mixed Polyurethane Foam Products Supplied by Company A

3.2.2.1 Polyurethane Foam A-1

Polyurethane foam A-1 is a one component low-viscosity, 100% solids hydrophilic polyurethane injection resin. When this resin reacts with water, it produces a closed-cell foam with a high tensile strength and excellent flexibility and adhesion characteristics. This product is able to withstand thermal expansion and contraction, as well as wet/dry and freeze/thaw cycles. Polyurethane foam A-1 exhibits excellent resistance to fungi, gasses and chemicals (Polyurethane Foam A-1, Company A).

This type of polyurethane foam is normally used to seal leaking hairline as well as large leaking cracks and joints in concrete and masonry in tunnels, manholes, culverts, dams and water-treatment plants. This polyurethane foam forms in a reaction time of 75-90 seconds and develops a cured tensile strength of 1.03-2.76 MPa (Polyurethane Foam A-1, Company A).

3.2.2.2 Polyurethane Foam A-2

Polyurethane foam A-2 is a one-component polyurethane hydrophobic injection resin that has an optional accelerator which controls the setting time of the polyurethane foam. The resin reacts with water to form resilient and flexible foam which plugs and seals leaks in concrete structures. To control the rate of expansion and the reaction with water, the temperature of the resin and the amount of accelerant used can be changed.

Accelerator can be added to the resin to control reaction or gel time, in the ratios shown in Table 3-1. Water can then be added to the system at 5-10% by weight in order to produce the desired amount of foam expansion (Polyurethane Foam A-2, Company A).

Table 3-1: Reactivity of Polyurethane Foam A-2 at 21C (Polyurethane Foam A-2, Company A)

% Accelerator Used (relative to resin)	Reaction Time (sec)
1	100
2	70
3	40
6	35
10	29

When the polyurethane foam is in its cured state, it repels water, possesses high tensile strength and has excellent adhesion and flexibility. This product is able to withstand thermal expansion and contraction, as well as wet/dry and freeze/thaw cycles. Polyurethane foam A-2 exhibits excellent resistance to fungi, gasses and chemicals. This type of polyurethane foam is normally used to seal leaking hairline as well as large leaking cracks and joints in concrete and masonry. It also is used to seal rock pockets and joints. The cured tensile strength of the product is 0.55MPa (Polyurethane Foam A-2, Company A).

3.2.2.3 Polyurethane Foam A-3

Polyurethane foam A-3 is a one-component polyurethane hydrophobic injection resin, that when paired with an optional accelerant can control the reaction and gel time. The resin reacts with water to form rigid closed-cell foam that is capable of sealing high-pressure and high-volume water leaks from large voids and openings in concrete or granite structures. In order to reach the desired rate of expansion and the reaction of the resin to water, the temperature and the amount of accelerant can be altered. Accelerator can be added to the resin to adjust reaction and gel time in the ratios shown in Table 3-2.

Water can then be added to the system at 5-20% water content by weight in order to achieve the desired amount of polyurethane foam expansion. Depending on the outside temperature and the amount of accelerant used, the average reaction time of the foam can range from 20 seconds to 6 minutes (Polyurethane Foam A-3, Company A).

Table 3-2: Reactivity of Polyurethane Foam A-3 at 21°C (Polyurethane Foam A-3, Company A)

% Accelerator Used (relative to resin)	Reaction Time (sec)
4	43
8	25
12	15
16	12

In its cured state this polyurethane foam has the ability to repel water and is semi-rigid. This product is used to seal large leaking cracks and joints in concrete and masonry in utility vaults, tunnels, manholes, culverts, dams and water-treatment plants. Polyurethane foam A-3 has a tensile strength of 1.9MPa (Polyurethane Foam A-3, Company A).

3.2.3 Industrial Polyurethane Foam Products

3.2.3.1 Company B Polyurethane Foam

Company B offers efficient and effective solutions to settled structures and unstable soil conditions. The company works with expanding rigid polyurethane foams, which are formed from a mix of a base polyol, isocyanate, and the addition of a blowing agent. The information presented in this section has been obtained from Company B product manuals and from studies undertaken by the company (Company B, 2011).

The effect of density on the compressive, tensile, flexural, and shear strength properties can be seen in Figure 3-1-Figure 3-4. Typical free blown densities range from

32-48 kg/m³ (2-3 lb/ft³) and increase under confinement to 80 kg/m³ (5 lb/ft³) when injected under flooring, and can reach even higher values of 320 kg/m³ (20 lb/ft³) in deep injection levels (Company B, 2011).

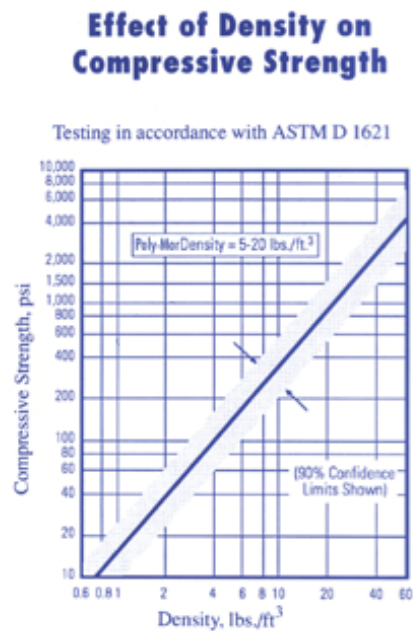


Figure 3-1: Compressive Strength vs. Density for Company B Polyurethane Foams (Company B, 2011)

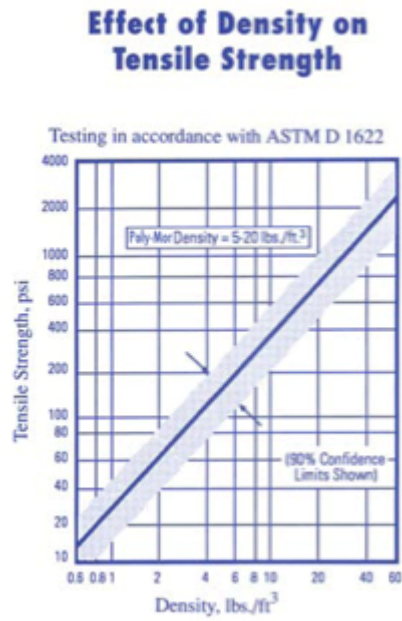


Figure 3-2: Tensile Strength vs. Density for Company B Polyurethane Foams (Company B, 2011)

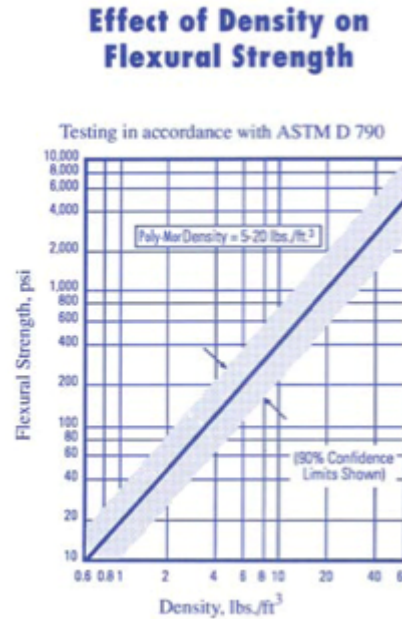


Figure 3-3: Flexural Strength vs. Density for Company B Polyurethane Foams (Company B, 2011)

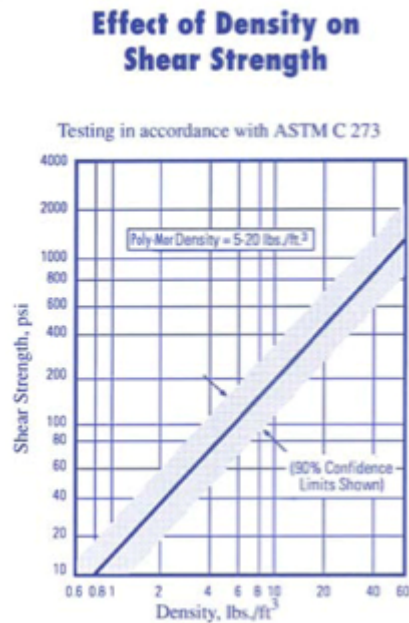


Figure 3-4: Shear Strength vs. Density for Company B Polyurethane Foams (Company B, 2011)

Company B polyurethane foams are designed for subterranean void fill applications. Each foam has a free rise density of 40.05kg/m^3 when processed unrestrained in the open environment. However, this density will increase depending on the amount of foam pumped into the confined void space (Company B, 2011).

Polyurethane foam B-1 is a two-component water-blown low density spray polyurethane foam system that is designed for soil stabilization, road bed construction, deep hole injection and void filling. This type of foam is tolerant to variations in mixing conditions, becomes inert after curing, and is able to maintain a constant volume with no shrinkage. When the foam is machine mixed at a temperature of 60°C , it has a rise time of 5 seconds, will be tack free within 11 seconds and will be firm within 90 seconds. Physically, the fast foam will have greater than 85% closed cell content, and have an excellent resistance to solvents, mold and mildew (Polyurethane foam B-1, Company B).

Polyurethane foam B-2 is a two-component polyurethane foam system designed for use as a void fill and a trench-break material. When the trench foam is mixed by hand

at 10°C, it has a cream time of 1 second, a tack free time of 8 seconds and a rise time of 10 seconds. The trench foam has a compressive strength at maximum loading of 219kPa and closed cell content greater than 95%. Like the B-1 foam, the B-2 foam also has an excellent resistance to solvents (Polyurethane foam B-2, Company B).

3.2.3.2 *Company C Polyurethane Foam*

Each of the polyurethane foams supplied by Company C are made of a two component urethane foam system, which is specially formulated for pour-in-place applications. This system displays good flow characteristics and can be mixed using either a high or low-pressure machine. The polyurethane foams are environmentally friendly, and are manufactured using recycled plastic material, soya oil material, and use zero ozone depletion substances (ODS) blowing agents. Each of the polyurethane foams are created by mixing isocyanate with a formulated resin at a mixing ratio of 1:1 by volume (Polyurethane foam C-1, Company C), (Polyurethane foam C-2, Company C), (Polyurethane foam C-3, Company C). Below are the important data about the low, medium and high density foams used, which were mixed using a high-pressure machine.

Table 3-3: Performance Data of Company C Polyurethane Foams (Polyurethane foam C-1, Company C)(Polyurethane foam C-2, Company C)(Polyurethane foam C-3, Company C)

	Low Density	Medium Density	High Density
Applications	- Flotation - Insulating panels - Wall cavities	- Plastic totes insulation - Thermal insulation for residential doors - Thermal insulation for garage doors - Insulating panels	- Thermal insulation for pipe lines - Thermal insulation for refrigerator units - Insulating panels
Cream Time (sec)	10-14	11-15	10-14
Gel Time (sec)	75-90	50-60	55-70
Free-Rise Density (kg/m³)	30.44-32.84	32.84-36.84	36.84-40.05
Compressive Strength (kPa)	162	181	194

3.3 Out-of-Plane Testing of Materials in Third-Scale Masonry Wallettes

3.3.1 Test Configuration and Procedure

The wallettes were built in a single wythe running bond. The wallettes with polyurethane foams were 3 units wide by 9 courses high. No mortar was used with Company A wallettes so as to examine the out-of-plane strength of the polyurethane foam by itself without the contributing effect of mortar. Another reason that no mortar was initially used in the construction of the wallettes, is that eventually the intent is to use this polyurethane foam system with interlocking masonry block in which no mortar is used. Mortar was used with Company B wallettes, so as to simulate the actual wall that was to be tested in the full scale tests.

The wallette specimens were tested under simply supported 2 point monotonic out-of-plane loading. The span between supports for all specimens was kept the same at 560mm and the spacing between the central load lines was 150mm for the polyurethane-reinforced wallettes. The two point loading beam allows the failure path to be either toothed or straight within the constant moment region. In order to transfer the main load to these smaller load beams, a spreader plate was used. Linear variable differential transducers (LVDT's) with 30mm stroke were used to measure the midspan deflection of each specimen. Figure 3-5 shows the test set-up and instrumentation of a typical wallette specimen.



Figure 3-5: Wallette Test Set-up for Out-of-Plane Loading

3.3.2 Test Observations

3.3.2.1 Company A Polyurethane Foams

Polyurethane foam A-1 was not used to reinforce any wallettes, as it proved to be too viscous of a foam, with a rather slow reaction time, making the product unsuitable for use. Both of the other Company A polyurethane foams proved to be suitable, and nine different walls reinforced with each type of foam were produced, varying the blowing agent and amount of accelerant in each, using a low, medium and high amount of both blowing agent and accelerant. 300 mL of A-2 polyurethane resin was mixed with the ratios of blowing agents and accelerant shown in Appendix A in Table A-1. 300mL of A-3 polyurethane resin was mixed with the ratios of blowing agents and accelerant shown in Table A-2 of Appendix A, with the typical results of changing the amount of blowing agent shown when using a small amount of accelerant.

The first Company A wallette that was tested was wall 2A, made with A-2 resin, a medium amount of accelerant (5% by volume) and a small amount of blowing agent (5% by volume). When the wallette was first put into the set-up and the loading beam was resting on the wallette, it was visually clear that the loading beam itself was causing the wall to deflect. The loading apparatus applied at the center of the wallette weighs a total of 35.4kg, which is roughly the same weight as the wallette itself and results in a force of 347N being applied to the wall. The out-of-plane loading test was run under these conditions and it was suspected that this brand of polyurethane foam would not prove to be a viable reinforcement for masonry. As the weight of the loading beam relative to the wallette was so significant, the load from the loading beam was added to the applied loading.

The load versus mid-height deflection diagram is shown below in Figure 3-6 and clearly shows the quick failure of this foam during testing. The maximum load capacity that the wallette was able to withstand was just under 450N, and with such a small area under the load-deflection curve, it can be seen that the wallette was able to absorb just a small amount of energy before it reached ultimate failure. As the majority of the specimen's load capacity came from the superimposed load from the loading apparatus and not from applied loading, this shows how much of an influence the loading from the loading beam had on the testing.

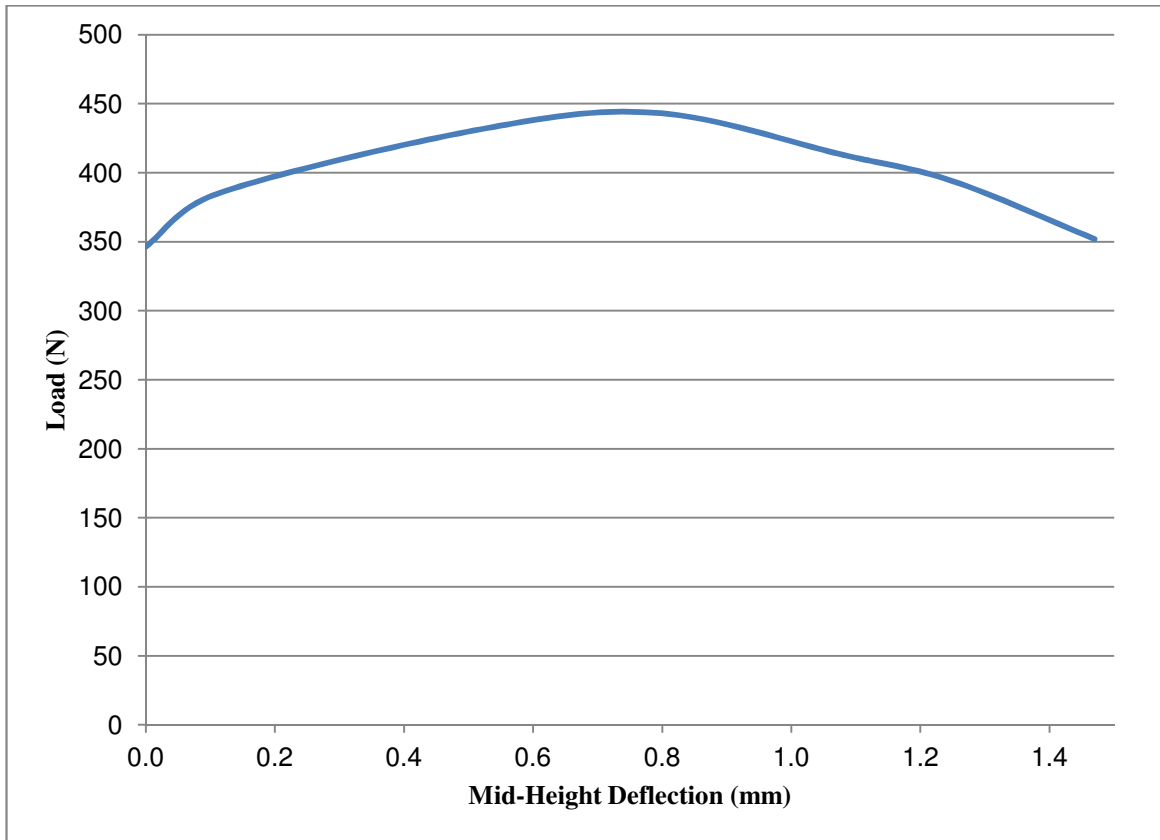


Figure 3-6: Load vs. Mid-Height Displacement for A-2 Wall 2A

This test set-up with the heavy loading beam could not be changed, as appropriate lighter materials that would be able to perform the same loading functions could not be found at the time. An attempt was made to test wallette 5C, however similar problems were encountered. Under only its own weight, the wallette experienced significant deflection and began to crack which led to the failure of the specimen before testing could occur. The remaining Company A wallettes were chosen not to be tested at this time.

3.3.2.2 *Company B Polyurethane Foams*

Company B wallettes contained mortar between the blocks, and they first experienced a crack along the mortar joints before the the foam was able to take on the loading, providing extra load resistance to the system. The initial problems experienced with the Company A tests, that resulted from using very heavy load beams were not corrected in these tests, but instead the increase in deflection due to the application of this loading beam was measured to as to establish the initial effects of this extra load on the specimen. The extra load from the loading beam was again accounted for in the load calculations.

When the loading beam was initially applied to the B-1 wallette, the wallette experienced an average deflection of 1.1mm at the mid-height of the specimen. When the main loading was applied, a crack opened up near the fixed load and continued to propagate until it developed along the entire width of the specimen. This crack eventually opened up slightly and then gave out suddenly when the specimen reached ultimate failure. In Figure 3-7, the load versus deflection diagram shows a load-deflection response more typical of the behaviour expected for a full-size wall. The B-1 wallette was able to withstand a force of 850N for the extent of its loading time, pre-cracking. After the first crack opened up, releasing most of its 2,937Nmm of built-up energy, the specimen was quick to fail as can be seen in the figure by the consecutive drops in load over a period of only 1mm of deflection. After testing was complete, it was verified that the B-1 foam did in fact fill every cell of the specimen.

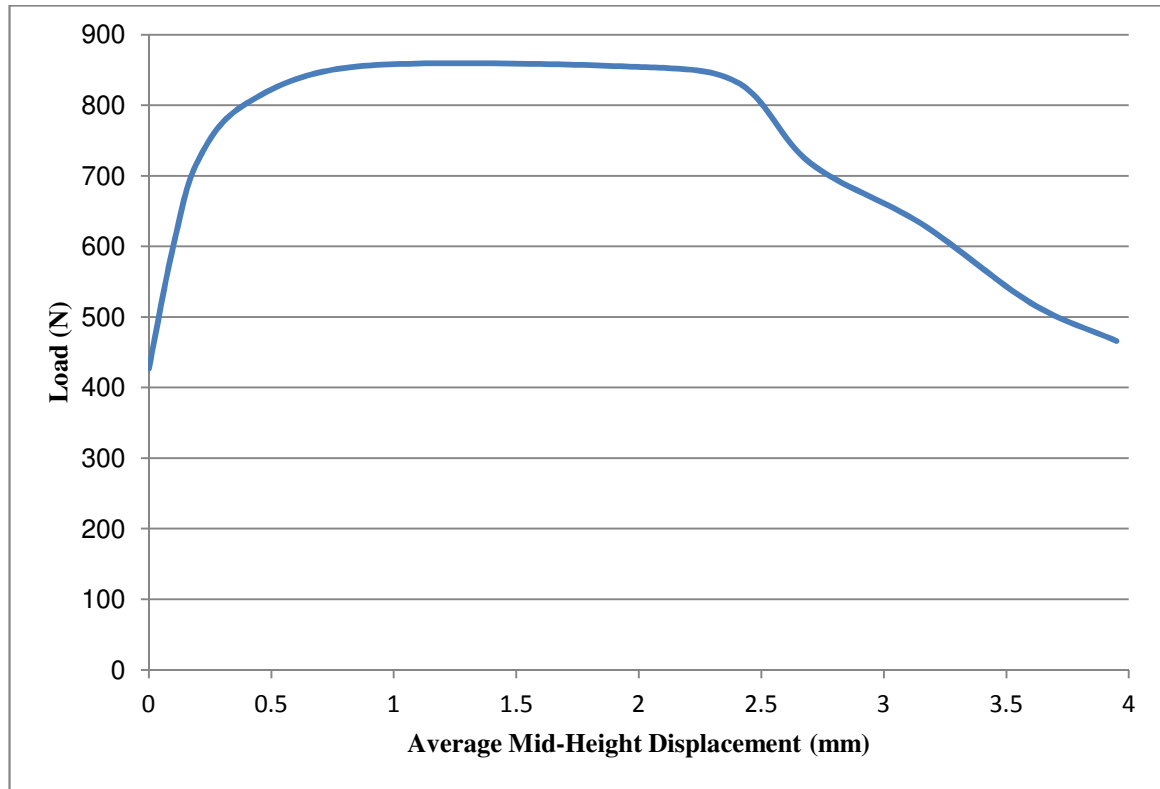


Figure 3-7: Load vs. Average Mid-Height Displacement for B-1 Polyurethane Foam

The B-2 polyurethane foam wallette was tested under the same conditions as the B-1 foam, and the additional weight of the heavy loading beam was again accounted for. The application of the loading beam caused an initial deflection of only .046mm, which is very small compared to the initial deflections of the previously tested polyurethane foams. This superior performance of the B-2 polyurethane foam can again be seen in the load versus deflection diagram shown in Figure 3-8. The B-2 foam wallette was able to carry loads up to 1.575kN and reach deflections over 7mm before ultimate failure was reached. This specimen was able to absorb 8,743Nmm of energy, far and above the energy dissipating capabilities of the other foam wallettes. The trench foam wallette cracked along the exact same mortar joint near the fixed load as the B-1 foam wallette, however the extent that this crack pattern was able to widen and open up before reaching ultimate failure was significantly greater than the B-1 foam specimen.

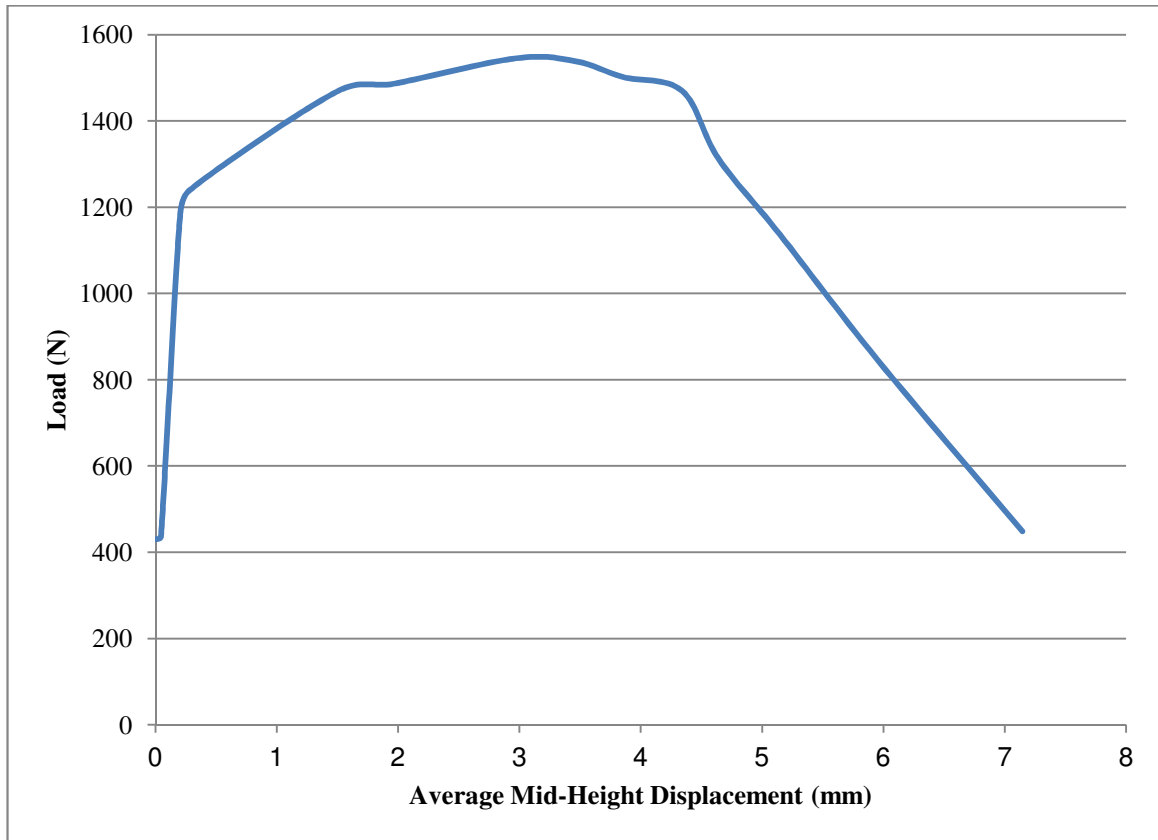


Figure 3-8: Load vs. Average Mid-Height Displacement for B-2 Polyurethane Foam

3.3.2.3 Comparison of Polyurethane Foams Based on Out-of-Plane Wallette Testing

In the out-of-plane testing of wallettes reinforced with different polyurethane foams, there were a few inconsistent variables which may have led to a negative impact on the wallette testing of the Company A polyurethane foam products. The wallettes made from Company A foams were made by hand while using no mortar, while the Company B polyurethane foam wallettes were mixed by professionals using specifically designed equipment and used mortar to hold the blocks of the wallettes together. The Company A wallettes could not be constructed with mortar, as the hand-mixed foam could only fill 3-5 courses high at a time. This meant that the Company A wallettes had

to be built while they were simultaneously being filled with foam, thus making the use of mortar impractical.

A good comparison of the strength of the polyurethane foams themselves can be seen by analyzing the behaviour that each wall exhibited after the same loading beam was added to each specimen prior to testing. The hand-mixed Company A wallettes crumbled from the heavy load of the loading beam, and in some cases were not able to sustain their own self-weight even prior to the application of the loading beam. However, the Company B wallettes were able to carry the weight of the loading beams, experiencing only small deflections of 1.1mm in the B-1 foam wallette and 0.05mm in the B-2 foam wallette. As the B-2 foam wallette showed very little deflection under such high load application, it showed that it had superior strength properties when compared to the B-1 foam wall—as all the other variables between these two wallettes were constant besides the type of foam used.

In a direct comparison of the energy absorption capabilities of each of the three foams in Figure 3-9, the B-2 foam clearly outperforms the other two specimens; with an energy absorption capability almost double that of the Company A 5A wallette, and almost three times that of the B-1 polyurethane foam.

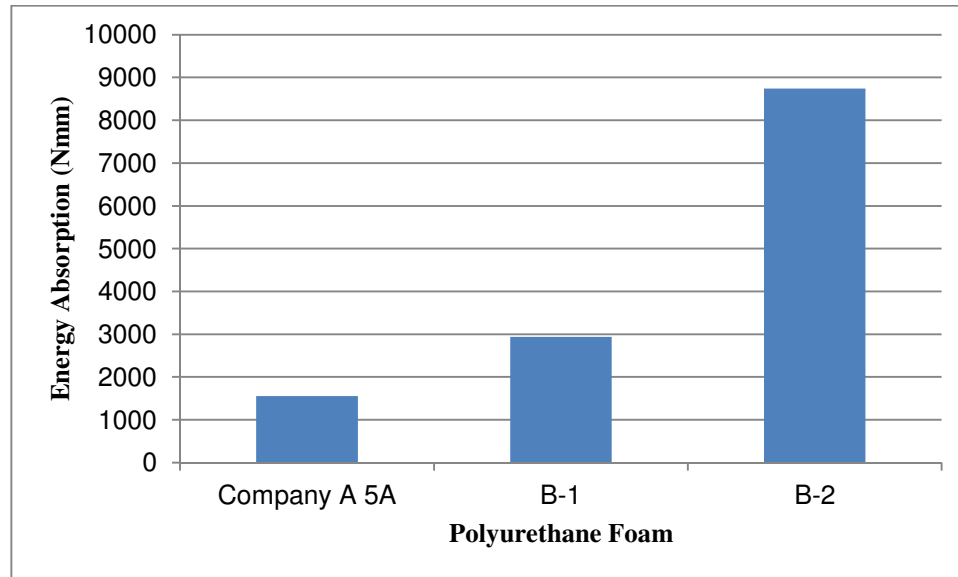


Figure 3-9: Energy Absorption of Polyurethane Foam Wallettes

In Figure 3-10, the load versus deflection diagram shows that the Company B polyurethane foams each followed a similar load-deflection path, with the B-2 foam being capable of sustaining almost twice as much load and twice as much deflection as the B-1 foam specimen. Each of the two Company B wallettes experienced two large losses in strength, as the specimen first cracked, and as these cracks widened prior to ultimate failure. At the point of failure, each of the wallettes failed at roughly the same load, between 440-460N, suggesting that the ultimate load capacity of the polyurethane foams would be in this range, and would be a function of the testing set-up and wallette configuration and potentially not dependent on the strength of the foam itself. However, as each of the foams experienced significantly different amounts of deflection at this same level of ultimate loading, it would suggest that the amount of deflection that the wallette can expect to experience at ultimate failure would be directly related to the strength and density properties of the chosen foam. The Company A-5A wall exhibited very different behaviour, as the wallette cracked as soon as testing began. This crack gradually widened over the course of testing until ultimate failure was reached. This

specimen could not exhibit any further losses in load, as the remaining load on the specimen was solely from the loading beam apparatus.

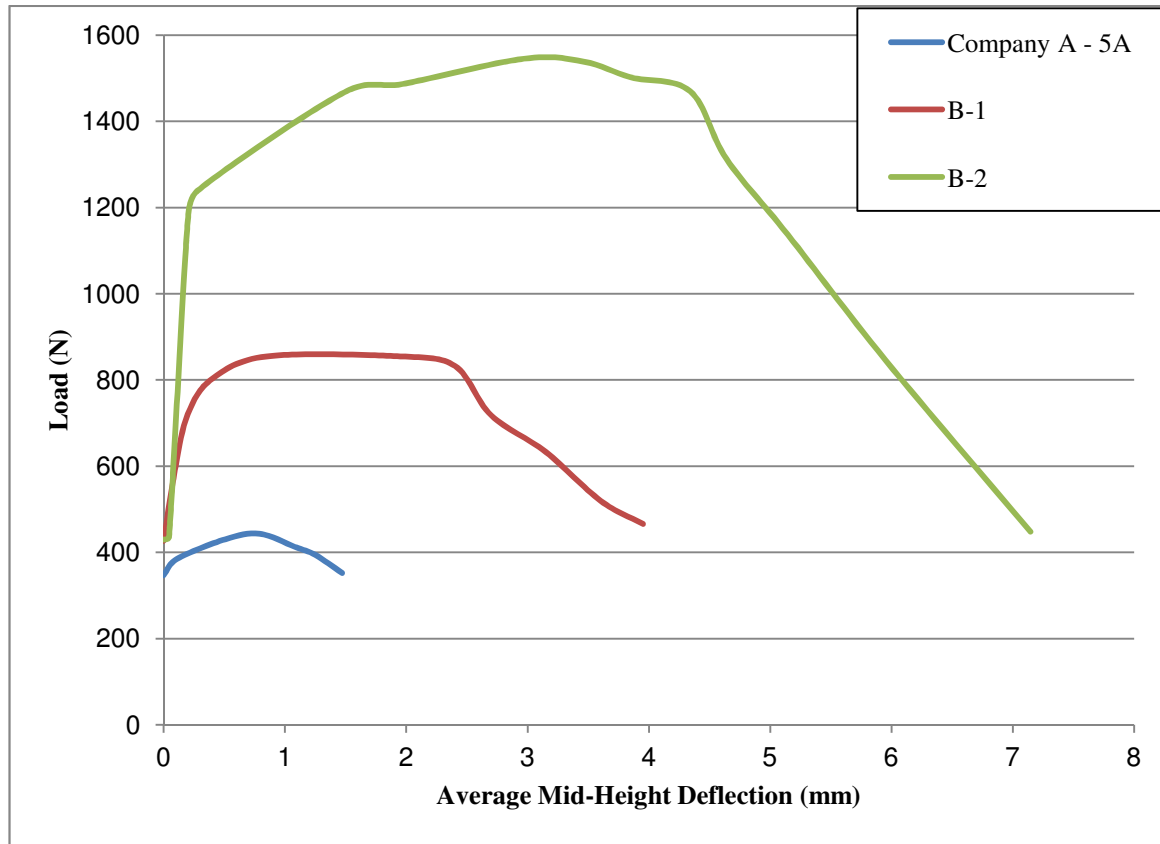


Figure 3-10: Comparison of Load vs. Mid-Height Deflection of all Wallettes

3.4 Conclusion

Through the investigation into the use of different polyurethane foams to be used as reinforcement in masonry a lot was discovered about not only the type of polyurethane foams that should be used, but also about how the foams work to enhance the out-of-plane behaviour of masonry in general. It was clear that as the strength and density of the foams increased, the resulting out-of-plane strength of the wallettes reinforced with these foams increased likewise. From this wallette testing, it was determined that a professionally mixed product should be used for the full-size testing as it provides a

consistent product that can be relied upon, along with its simple injection system into already made unreinforced masonry walls. In the case of Company A foams that are hand-mixed, there will be inconsistency from one mix to the next, and no simple reliable way of getting a large quantity of foam within the wall while it is being built. It was decided that the Company B polyurethane foams deserved further investigation in full-scale testing, along with the Company C foams.

4 Experimental Compression of Full-Scale Masonry Assemblages Reinforced with Expanding Polyurethane Foam

4.1 Introduction

In this chapter, the effectiveness of polyurethane foams at increasing the compressive capacity of masonry is studied. This study was undertaken concurrently with the previously discussed wallette testing, in order to better understand different polyurethane foams and their behaviour when used as reinforcement in masonry. As masonry already tends to have a high compressive strength when acting alone within URM, it is necessary to look at any additional benefits that polyurethane foam could bring to the masonry system.

4.2 Materials

The range of material parameters was restricted to using one size of full-size block, two types of mortar, two types of Company B polyurethane foams and three types of Company C polyurethane foams. Each group of foam assemblages were built using the same type of block and same mortar, so as to reduce variability within test groups. All materials were of standard construction so as to best represent current industry practice.

4.2.1 Concrete Blocks

Standard hollow concrete block units with frogged ends were used in the construction of the masonry assemblages. The full-size blocks had dimensions of 190mmx190mmx390mm with a gross area of 75,250mm², a normal weight block density and a minimum specified gross concrete compressive strength of 15MPa, meeting Canadian CSA A165.1 standards.

4.2.2 Mortar

Type S mortar (for structural application) was used in the fabrication of all assemblages. The mortar for Company B assemblages was mixed from base ingredients,

while the mortar for the remaining assemblages was made from a factory produced pre-mix. Each type of mortar was mixed and prepared by experienced masons who then constructed the assemblages. Seven 50mm cubes were sampled to determine the compressive strength properties of each mortar.

4.3 Specimen Selection and Construction

In the making of the four course assemblages, two different block configurations were used, which are both detailed in Figure 4-1 below. The first design consisted of four blocks stacked on top of each other. The assemblages with this type of design were previously constructed by another student. The blocks and mortar used in this simply-stacked four course assemblage are the same as those used to build the 2.2m Company B walls. The second type of assemblage was constructed by alternating full blocks with two half-blocks so as to simulate a running bond configuration. This assemblage design better represents the behaviour of an actual section of wall, and was used for the unreinforced assemblage as well as those assemblages containing Company C polyurethane foams.

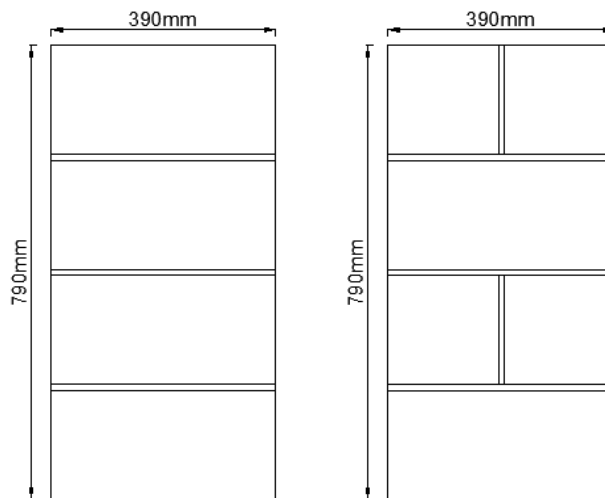


Figure 4-1: Compression Assemblage – Stack Pattern and Running Bond Designs

4.4 Polyurethane Foam Injection

As the masonry assemblages were quite short in height, the polyurethane foam was able to be injected by inserting a rod down the length of the masonry core, and raising the rod accordingly as the foam rose. This process, which can be seen below in Figure 4-2 was repeated for each core. The mortar in the masonry assemblages was allowed to cure for at least 28 days before the polyurethane foam injection process.



Figure 4-2: Polyurethane Foam Injection into Compression Assemblage

Polyurethane foams have great expansive capabilities, which allow the liquid material to expand at a significantly high rate as the chemicals react and the foam is formed. This high rate of expansion can put a great deal of pressure on the blocks, and if the expanding foam becomes confined in some way, the force of the expanding foam can force a separation between the mortar joint and the blocks, causing the assemblage to fail and come apart during the injection process. In the case of the B-1 compression assemblage, the outward pressure of the foam as it expanded was too much for the central mortar joint to take and the top and bottom half of the assemblage broke apart. Thus, only a two block high assemblage was tested using the B-2 polyurethane foam.

The masonry assemblages built in a stack pattern were built with openings on the ends of the cells, where the blocks did not line up perfectly, leaving an end area not filled in with mortar. When the polyurethane foam is injected into the cells of these assemblages, the foam is then allowed to seep out of these openings as it rises. As polyurethane foam becomes denser and hence stronger under confinement, as compared to when it is allowed to freely expand in all directions, measures were taken to close these openings on the masonry assemblages. A mixture of foam tubing and duct tape was used on the stack pattern assemblages. On all assemblages built with the running bond, these holes were filled with mortar while they were being built.

4.5 Test Configuration and Procedure

The compression test set-up is shown in Figure 4-3 and illustrates the configuration of the masonry assemblage within a compression test machine. The load applied was monitored by a load cell within the floor of the machine, and was connected to a data acquisition system which recorded the readings. LVDT's were affixed to the masonry on each side of the assemblage to monitor deflections over the whole height of the specimen. The LVDT's were located so as to span every mortar joint where most of the assemblage's deflection was likely to occur.



Figure 4-3: Compression Test Set-up

4.6 Test Results

4.6.1 Mortar Cubes

The mortar cubes were tested to determine the compressive strength of the mortar, according to ASTM C109 (2011). It was determined that the mortar strength varied significantly, with the compressive strength of the mortar for the unreinforced assemblage being 12.4MPa, while the mortar for the Company C assemblages had a compressive strength of 16.3MPa, and the Company B assemblages had a mortar compressive strength of 31.6MPa, almost double the compressive mortar strength of the Company B

specimens. The large variation in compressive strength values for the same type of mortar is not uncommon, as there could be fluctuations in the water/cement ratio, which can be caused by evaporation according to the mason's pace, and also by the amount of water used to make the appropriate mortar consistency, which when using pre-mix mortar can vary significantly

4.6.2 Compression Test Observations and Discussion

In general, failure of all compression assemblages initiated in a similar manner. As the loading of the sample increased, a small crack would form in the web of the masonry block, in the direction parallel to the loading of the specimen, and would continue to grow and widen along the length of the specimen until failure occurred. In both the unreinforced assemblage and those assemblages filled with foam, the first visible crack in the specimen occurred at approximately the same load level, as can be inferred from Table 4-1. However, although the specimens' failure initiated in a similar manner, the unreinforced assemblage, and those assemblages filled with foam behaved very differently following initial web-splitting.

Table 4-1: Summary of Compression Results

Compression Assemblage	First Visible Crack (kN)	Ultimate Load (kN)
URM	460	574
Polyurethane Foam B-1	635	754
Polyurethane Foam B-2	450	911
Polyurethane Foam C-1	450	783
Polyurethane Foam C-2	460	800
Polyurethane Foam C-3	N/A	819
Average for Polyurethane Foams		813

When the vertical crack developed and expanded in the URM assemblage, the failure mode was very brittle and immediate, and the failure resulted in the complete disintegration of the sample and many pieces of flying debris. In contrast, those

assemblages filled with foam were able to significantly increase their load capacity after these initial side cracks developed, and far surpass the load carrying capacity of the unreinforced assemblage, increasing their load carrying capacity on average by 42%. This significant increase in failure load may be attributed to the increased cross-sectional area of the specimens and the strong tensile strength of the polyurethane foam. The benefit of the polyurethane foam reinforcement is that it is able to stabilize the face shell after web splitting, thus enabling the prism to carry more load as the face shell is still standing as one assemblage with no collapse. Even at ultimate failure, none of the foam-reinforced specimens suffered disintegration and all were capable of supporting their own self-weight as can be seen in Figure 4-4. The bond strength between the polyurethane foam and the inner masonry block surface held all of the failed pieces of the assemblage together, preventing them from collapsing. This is particularly important as such bonding effect (acting as a structural integrity reinforcement) can significantly prevent catastrophic URM collapse.



Figure 4-4: Fast Poly-mor Compression Assemblage Post Failure

Of significance is that each of the foam-reinforced specimens demonstrated residual strength after peak loading. This behaviour could be beneficial during an earthquake, when a building could be subjected to peak loading conditions only for a brief period of time. In this situation, the walls would still remain standing and be able to carry some gravity load.

The ability of a foam-filled masonry wall to stay intact while experiencing extreme failure has huge implications for performance-based engineering. As these assemblages were able to carry a significant amount of compression post-failure, this may suggest that masonry walls of a single story dwelling reinforced with these polyurethane foams would potentially be able to support the loading from the roof, even when the walls

are completely damaged. Reinforcing URM buildings with this material may prevent them from total collapse and the loss of lives, and possibly resulting in placing affected buildings into the *Life Safety* instead of the *Collapse Prevention* seismic performance category.

Also of note, is that as the density of the specimen provided by each company increased from low- to high-density, the ultimate load that the masonry assemblage was able to carry increased likewise. The increase in compressive capacity as polyurethane foam density increased can be seen more clearly in Figure 4-5. As the medium-density foam provided by Company B was the highest performing foam overall, this testing also shows that although an increase in density does increase polyurethane foam's compressive strength, there are other factors within the make-up of the foam that contribute to the making of a stronger foam. The strain profiles of each assemblage are shown in Figure 4-6.

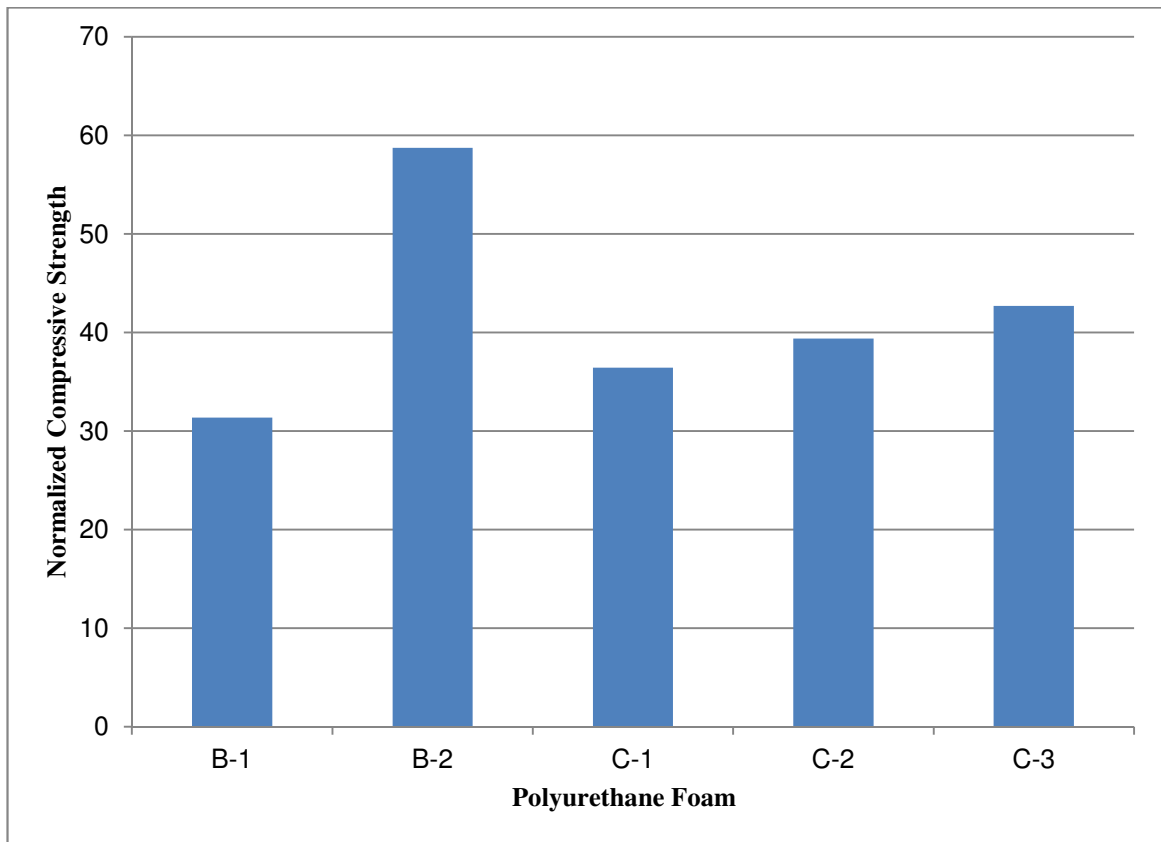


Figure 4-5: Increase in Compression Strength, Normalized to the Unreinforced Specimen

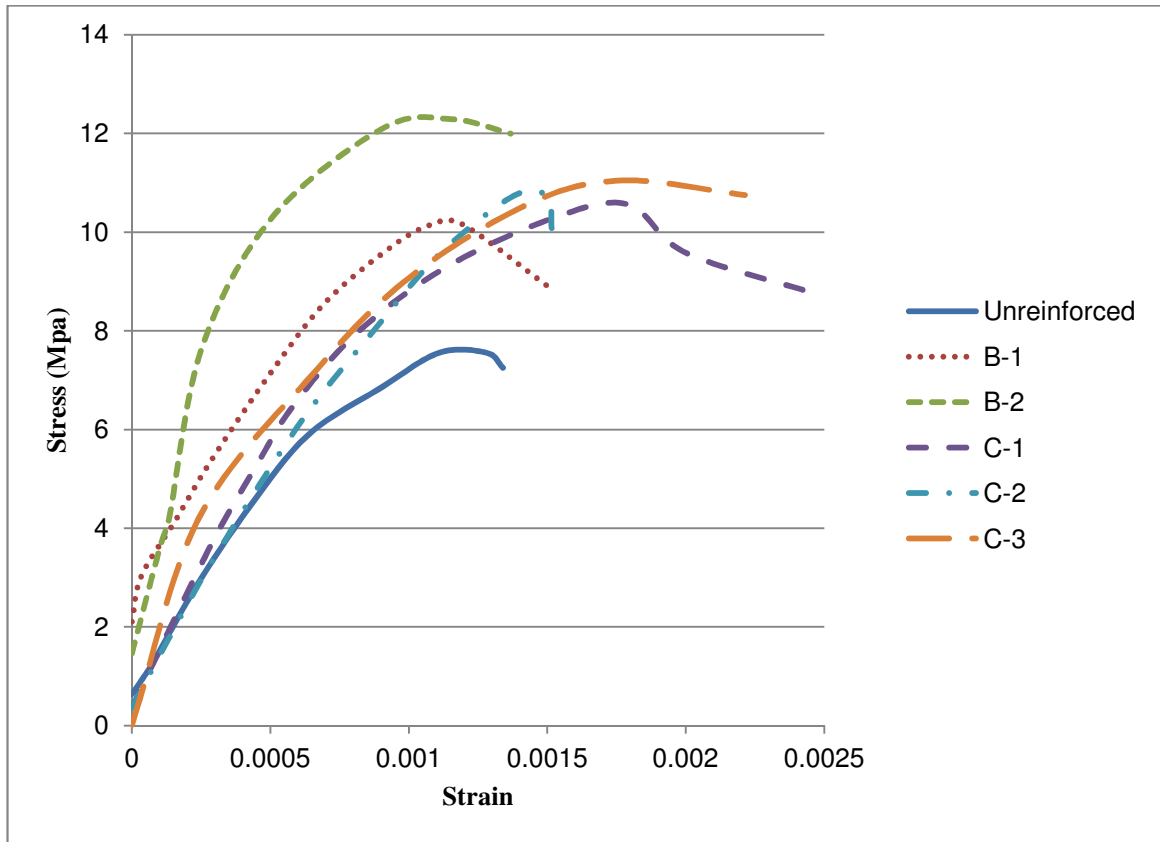


Figure 4-6: Stress vs. Strain for Assemblages Under Axial Compression

4.7 Conclusions

Based on this preliminary study that examined the effects of polyurethane reinforcement on the compressive of masonry, it is clear that this type of reinforcement technique can greatly increase the performance of a URM wall reinforced with polyurethane foam. The average ultimate compressive strength of the reinforced assemblages showed an increase by 42 times over the URM specimen. With the specimens showing an increase in compressive strength from 31 times to 59 times the unreinforced specimen, it is clear that even the lower density polyurethane foam specimens can contribute to a higher compressive strength and significant increases in compression strength can be reached.

Beyond the increases in compressive strength, the ability of each of the compression assemblages reinforced with polyurethane foam to remain completely intact upon failure shows great promise for this type of new reinforcement. Given that URM buildings experience such drastic brittle failure during earthquakes, which can lead to catastrophic collapse, the ability of the polyurethane foam to keep all of the broken debris together while still maintaining some residual compressive strength is extremely promising. If polyurethane foam is able to keep entire sections of wall together and support a light roof post-disaster, then such new reinforcement material could be of great use in how we design buildings in seismic regions in the future.

5 Main Experimental Program—Full Scale Walls

5.1 Introduction

In this chapter, the in-depth testing and analysis of polyurethane foam reinforcement within masonry construction is carried out. Based on the preliminary wallette testing, full-scale models were built using the more promising polyurethane foams. The best performing foam out of these out-of-plane wall tests was used in further investigative testing using common rope as reinforcement in addition to the polyurethane foam.

It was necessary to test full-scale wall specimens which were built to imitate a 1m section of wall within a typical single-storey dwelling. Polyurethane foam as a reinforcement material is still a new concept, so it was necessary to conduct full-scale testing to better understand how the material would bond to the masonry and act in a real-world style application when an out-of-plane load is applied.

5.2 Materials

5.2.1 Concrete Blocks

Standard hollow concrete block units with frogged ends manufactured by Boehmer Block were used in the construction of the masonry assemblages. The full-size blocks had dimensions of 190mmx190mmx390mm with a gross area of 75,250mm², a normal weight block density and a minimum specified gross concrete compressive strength of 15MPa, meeting Canadian CSA A165.1 standards.

5.2.2 Masonry Mortar

Type S mortar (for structural application) was used in the fabrication of all wall specimens. The mortar for the Company B walls was mixed from base ingredients, while the mortar for the remaining walls was made from a factory produced pre-mix. Each type

of mortar was mixed and prepared by experienced masons who then constructed the walls. As groups of these walls were constructed at different times, thirteen different batches of mortar were used. Three 50mm cubes were cast from each batch (39 in total) and were tested so as to determine the properties of each batch of mortar.

5.2.3 Urethane Polymer

The B-1 and B-2 polyurethane foams supplied by Company B were used in addition to three different polyurethane foams supplied by Company C, polyurethane foams of low, medium and high density. C-1, C-2 and C-3.

5.2.4 Polypropylene, Nylon and Polyester Ropes

In order to enhance the potential of the polyurethane foam reinforcement, the idea was conceived to additionally reinforce the foam-filled walls with rope, similar to the normal reinforced masonry system whereby walls are reinforced with steel and filled with grout. In addition to providing extra load capacity for the wall system, the rope reinforcement would keep the parts of the wall together upon failure. The wallette testing showed that out-of-plane wall failure would result in the top and bottom sections of the wall separating into two detached sections, with the separate sections of the wall staying completely intact. In the context of a building, the tension in the rope and the bond of the foam to the rope would keep these separated sections from falling out of the wall, providing a further level of *Life Safety* in addition to complete loss of structural integrity of the system. To keep this system at a low-cost and easy to use, the ideal rope would be a strong commonly used low-cost rope.

In order to determine the optimal rope to be used in the design, several different ropes were tested of various materials, sizes and cost ranges so as to determine their ultimate load capacity. As the safe working load data that is provided by the manufacturer is often significantly lower than the actual capacity of a rope, it was necessary to determine how the rope would actually perform when stretched to its maximum capacity. As the ropes differed significantly in price, with the ropes with a

lower safe working load costing from \$0.02-\$0.07 per ft (ropes A-G) and the higher capacity ropes costing \$2.00-\$3.00 per ft (ropes H-J), it was necessary to study the behaviour of each rope, and compare the rope's performance to its price.

Rope H is made from one of the strongest and lightest fibres available. It is a specially processed polyethylene fibre that is pound-for-pound fifteen times stronger than steel and three times more durable than polyester. With excellent toughness and outstanding visco-elastic properties, this type of fibre can withstand high-load strain-rate velocities. Similar to steel, this fibre has low elongation of just 3 percent. Rope H has a high resistance to abrasion, and excellent vibration damping, flex-fatigue and internal fibre-friction characteristics. This type of rope is hydrophobic, and will not absorb moisture, nor deteriorate in water. In addition to water, it exhibits a high resistance to chemicals and ultraviolet light. The fibre that Rope H is made from is commonly used for high-performance applications including police and military ballistic-resistant vests, helmets and armored vehicles, as well as sail cloth, fishing lines, marine cordage, lifting slings, and cut-resistant gloves and apparel (Honeywell, 2011).

Rope I is made from an organic aramid fibre that is used in several industries, from mountaineering ropes and fishing lines to electro-mechanical cables and fine gauge cables for electronic device applications. Like Rope H, this type of fibre is stronger and lighter than steel on an equal weight basis. These aramid fibres also produce a product with a high modulus, high tensile strength at low weight, high chemical resistance, low thermal shrinkage, and a high toughness. These qualities produce a high-strength rope that is ideal for realizing the maximum potential of a rope when being used as reinforcement, as in this case (Dupont, 2011).

To test the ultimate capacity of each rope, the rope was stretched using the tinius compression machine. As shown in Figure 5-1 below, the rope being tested was tied around a steel cylinder using a clove hitch knot, creating a loop. This loop was then threaded through the center of the tinius machine and secured and made taut by

suspending another steel cylinder through the lower section of the loop, and raising/lowering the tinius machine until the rope became taught, which is shown in Figure 5-2. By increasing the distance between the two sections of the tinius, the rope became increasingly taught until failure was reached. Failure normally occurred at the top of the loop where the clove hitch overlapped, however there were instances where the rope broke at the very bottom of the loop. There were also cases when the ropes failed prematurely; when the outer material of the rope was too slippery, which under extreme tension caused the knots in the rope to come undone. In the case of ropes that have an outer layer and an inner core, the outer core tended to break first, leaving the remaining inner core completely intact – which then required additional testing of the inner core on its own.



Figure 5-1: Clove Hitch Knot

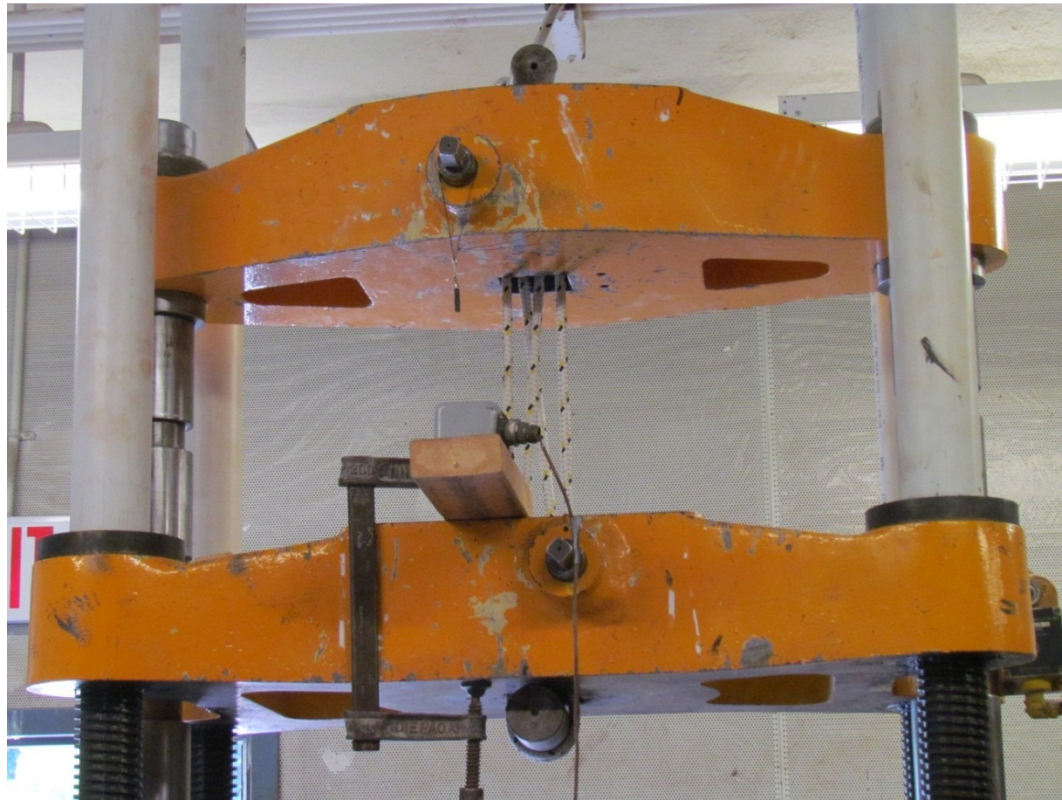


Figure 5-2: Rope Test Set-up

The testing of the different kinds of rope yielded some interesting results, which are summarized below in Table 5-1. As expected, the less expensive ropes were able to support smaller loads than the more costly H-J ropes. However, many of the cheaper ropes were able to carry loads far exceeding expectations, with some ropes carrying eight to ten times their labelled safe working load. In contrast, ropes H-J failed before reaching their safe working load, with each rope failing long before this threshold. A reason for this peculiar behaviour may be the test setup itself, where there was an imposed weakness due to the rubbing and force at the knot, or there may have been slipping, due to the smooth outside surface of the ropes. In the case of rope H, only the outer shell of the rope failed, leaving the inner core intact. Upon testing of this inner core alone, no distinct data was able to be obtained, as the rope was very slippery and the rope repeatedly failed prematurely, with the knot undoing itself upon the application of significant tension.

Table 5-1: Rope Test Results

Rope Label	Type of Rope	Size	Safe Working Load (N)	Ultimate Load (N)
A	Twisted Propylene	3/16"	314	greater than 1746
B	Solid Braid Polypropylene	3/8"	1079	4648
C	Braided Nylon	5/16"	843	3147
D	Twisted Propylene	3/8"	1089	10591
E	Braided Polyester	3/8"	843	4246
F	Braided Nylon	3/8"	1089	3295
G	Solid Braid Nylon Polyester Polypropylene	7/16"	1334	10699
H	Polyethylene	7/16"	NA	greater than 20015
I	Aramid Fibre	7/16"	52485	29165
J	Polyethylene/Aramid Fibre	7/16"	51151	33097

In order to select the appropriate rope to use in conjunction with the polyurethane foam to reinforce masonry walls, it was important to use a rope that would not fail during the testing of the masonry walls. The use of the rope in this test is to provide tension to the foam/masonry system – acting as steel re-bar does when it is reinforced with grout in current masonry construction. Keeping this in mind, the high strength rope I was used in the construction of the masonry walls reinforced with rope and polyurethane foam. This rope was the less expensive of the high-performing ropes, at a cost of \$2 per foot, and also had a braided outer covering of its thick, braided aramid fibre inner core, which provided an excellent surface for the polyurethane foam to bond to. The stress vs. strain diagram of the selected rope is shown below in Figure 5-3. The rope was able to withstand a stress of 307MPa before it severed due to the applied tensile force.

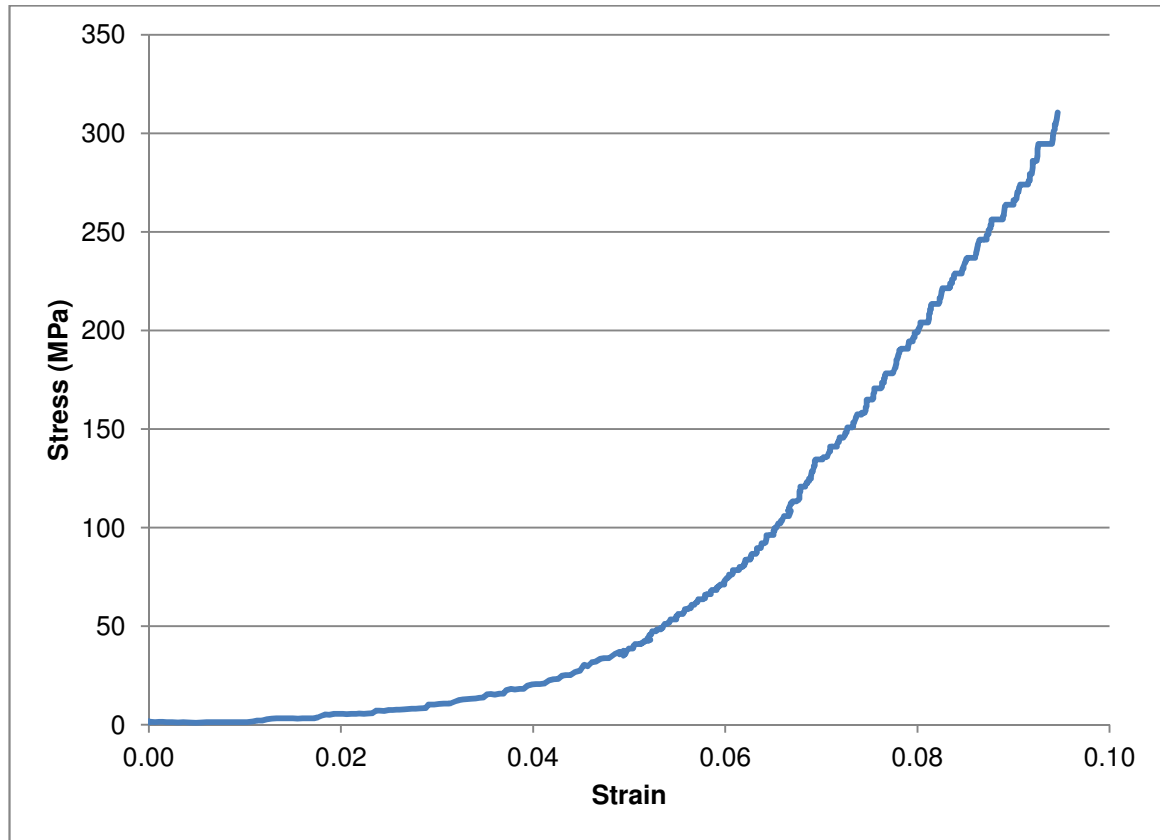


Figure 5-3: Stress vs. Strain of Rope I

5.3 Specimen Selection and Construction

The out-of-plane strength of unreinforced masonry walls depends on the tensile strength of masonry blocks, mortar, and the bond between them. Given that the tensile strength of mortar is generally very weak, masonry performs very poorly in the out-of-plane direction. A tension failure is characterized by a rocking behaviour and most often leads to the complete collapse of the wall.

The fifteen course high wall was selected to represent an average 1m strip of wall in a single-storey dwelling. The walls consist of full size 390mmx190mmx190mm block and standard construction 10mm mortar joints resulting in overall wall dimensions of 3mx1m. For the initial full-size wall tests using the B-1 and B-2 polyurethane foams,

walls eleven courses high were used. These walls consisted of the same block as the rest of the walls, and had overall dimensions of 2.2mx1m. These walls were initially used as they were already build and on-site. The walls were constructed by experienced masons according to standard industry practice. The joints were tooled to ensure mortar compaction and to provide a suitable wall finish.

5.4 Urethane Polymer Injection

The use of polyurethane foam as a reinforcement material in masonry construction is a very new concept and the process of building with these two materials has not yet been refined. Initially, the polyurethane foam is a free-flowing liquid, which can flow through any opening it encounters. However, as the polymers react with one another, the liquid quickly expands and solidifies into the polyurethane foam. As the polyurethane foam can expand at a quick rate, and can exert a great deal of force on the masonry block if it is confined, a great deal of care and precision needs to be taken in the polyurethane foam injection process to ensure that just the right amount of material is being injected into the wall. If too much material is injected, it can run out of room to expand, leaving nowhere for the material to go but out through the mortar joint, thereby destroying parts of the wall.

5.4.1 Polymer Injection Methods

There are two main ways of injecting polyurethane foams into masonry cells. The simplest method is to inject the foam into an open masonry cell from the top of the wall. This allows you to visually see the foam as it rises, and control the amount of material input. The other methods involve drilling a hole in either the mortar joint or the masonry face shell, and injecting the foam through this opening. This allows for more control during the injection process, and can be done in a variety of ways.

There are a few general problems that can be encountered in the injection process. Modern masonry construction methods stipulate that mortar be placed along the face shells with a 10mm mortar joint. As mortar is not placed along the inner web of the

masonry block, small air voids are formed which connect the hollow core columns to each other. When the polyurethane foam is initially injected it is a liquid product. It therefore can travel through any opening that is in its path, including the open air voids between the different cores. This can result in the liquid foam travelling horizontally across the wall instead of vertically upwards, causing potential blockages. If foam from previous injections makes its way into an empty cell and seals it off, it will create a blockage for future injections, making it likely that foam will not reach certain areas of that cell in the wall. If these hollow areas form at critical points in the wall, the structural performance of the wall could be greatly compromised.

5.4.1.1 Injection Method I—Top-Down Injection

In this method, each cell of the masonry wall is filled individually. A copper rod is inserted down the length of the masonry cell to approximately mid-height. A nozzle is attached to the top end of the rod, connecting the rod to the hose where the polyurethane foam is pumped in from a truck. This method can be seen in Figure 5-4. The foam is then injected, and the liquid polymer flows to the very bottom of the cell. As more material is injected, the foam begins to rise and the copper rod is withdrawn as the rising foam reaches its bottom tip.



Figure 5-4: Top-Down Injection

There are many flaws with this method of injection. Firstly, this method allows the polyurethane foam to freely expand upwards as it fills the masonry cells. This means, that the density of the foam product is that of its free-blown density. If this foam was made to be confined, it can reach much higher densities, which can invariably lead to much higher strengths within the material. If say, the top of the wall was made to be closed off and no longer open to the air, and then a hole drilled at the top through which one could insert the copper rod, this method would result in much denser foam.

Another potential problem with this type of injection method is that foam can easily travel between cores when it is in its liquid state, thereby cutting unfilled cell channels off mid-height. This would make it so that the top-down injection method

would only be able to fill that cell with foam from the blockage upwards. This would necessitate using injection method two or three to fill in the resulting voids.

5.4.1.1.1 Injection Method II – Single Injection Point

This method utilizes the air voids between the cores, by specifically planning for the liquid foam to travel across the cells. For the single injection point method, one hole is drilled into either the mortar bed or the face shell of the masonry block at the base of the wall. The pressurized hose is then inserted into the drilled hole, and the foam is injected into the opening as can be seen in Figure 5-5. Enough material is injected into the wall to appropriately fill the entire wall.



Figure 5-5: Injection Apparatus and Set-up

This method is only suitable for smaller walls that are only a block or two wide, so as to avoid hollow voids within the walls. In order to check if foam has been able to

reach all extents of the wall, holes can be drilled throughout to check for foam behind the face shell. Also, if the top of the wall has remained open, one can visually assess if foam has been able to reach all the way to the top of each cell.

5.4.1.1.2 Injection Method III – Multiple Injection Points

This method is the same as the single injection point method, only with multiple injection points. The multiple injection points can be chosen in a pattern that is at the discrepancy of the builder. For the purposes of these tests, it was necessary to ensure that each cell was filled with material. For some of the walls, points were drilled at every other face shell at the base of the wall and at 4-6 courses above those base points. Foam material was then injected into the base holes and allowed to rise up until foam visibly reached the mid-height holes above. Holes were then drilled 1-2 courses up from the base of the wall for the two remaining hollow cores. These holes were not drilled at the base, as foam material in its liquid state is generally able to travel through the air voids and help fill up the remaining base blocks. Also, any unfilled areas that remain will generally be filled by the falling liquid from the holes drilled above. Holes are also drilled 4-6 courses above these holes to track the foams progress up the wall. Once all bottom cores have been filled, then the top holes are filled with enough foam to fill the remaining hollow cores above. This scattered layout can be seen in Figure 5-6, along with a different two row layout. Injection points were placed in each cell across the lower third of the wall, and used corresponding mid-height holes in a similar manner as the previous layout.

This method utilizes both the liquid properties of the foam, allowing the foam to travel horizontally through different cores, and also the expansive properties of the foam. As the liquid reacts with itself it forcibly expands and rises throughout the wall. This makes it possible for the liquid to be injected at the bottom of the wall, but still fill those cells above the injection point.

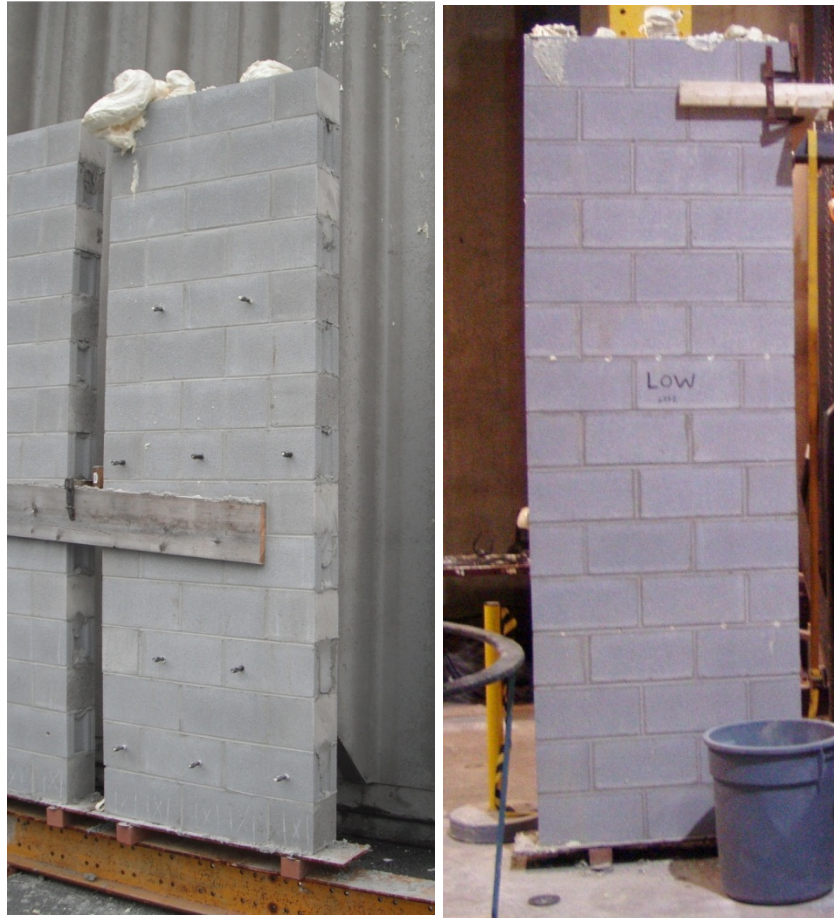


Figure 5-6: Multiple Injection Points with Scattered and Two Row Layout

5.4.1.2 Polymer Injection Into Test Walls

The walls injected with B-1 and B-2 polyurethane foams were both pre-existing walls built by a previous student. They are 1m (two and a half blocks) wide and 2.2m (11 courses high). These walls were filled using method number one, the top-down injection process. As these were the first walls injected with foam, the injection techniques had not yet been perfected. These 2.2m walls were built leaving open air voids where any half block was exposed to the outside edge of the wall. This meant that liquid polyurethane would make its way out of these openings, which would result in a great loss in material, and also would decrease the confining effect that the masonry is supposed to have on the foam so as to densify it. To counteract this problem, small pieces of foam tubing were

stuffed into these openings and secured with duct tape, which can be seen below in Figure 5-7. In some places, the pressure of the expanding polyurethane foam after injection was able to push out the foam tubing and remove the duct tape from the wall, showing the force and power it can have.



Figure 5-7: Injection Preparation For Walls With Company B Polyurethane Foam

All remaining walls were built by masons, under the instruction of the author. These walls were 1m (two and a half blocks) wide and 3m (15 courses) high. These walls were built using the multiple injection point method. The low, medium and high density Company C walls were filled with polyurethane foam using the two row layout shown in Figure 5-6. The 3m tall B-2 walls were all filled with foam using the scattered layout. The two B-2 walls that were additionally reinforced with rope required wood to be placed along the base and top of each wall in an order to attempt to confine the foam, while keeping the rope in place in the center of the masonry cells.

Two walls were built using the B-2 polyurethane foam and rope reinforcement. One wall was fully reinforced, with rope being woven down the center of each of the five

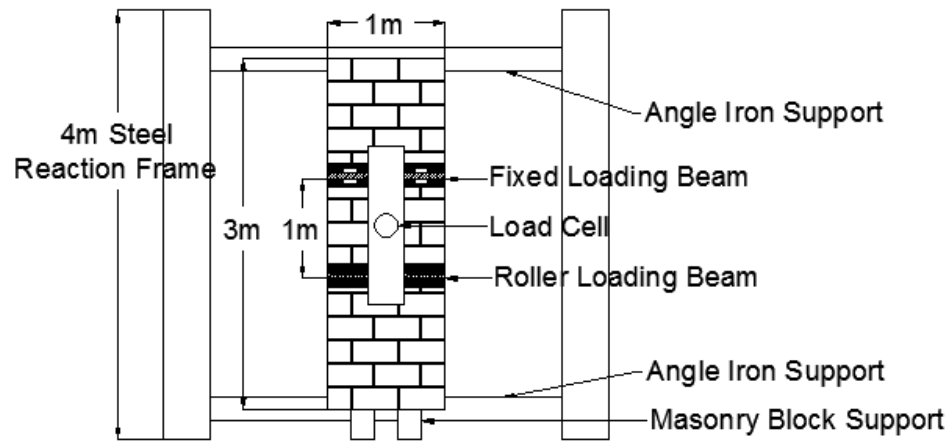
cells, while the other wall contained rope in three cells, weaving through every other cell. In order to secure and tighten the rope, knots were tied at each end of the rope, and a wedge was inserted between the wooden top and bottom and the knot end in order to give the rope tension and keep it in place while the foam was being injected. Once the foam was injected in the wall, these wooden wedges were kept in place in order to provide consistent tension in the case of rope slippage during testing.

5.5 Test Set-up and Instrumentation

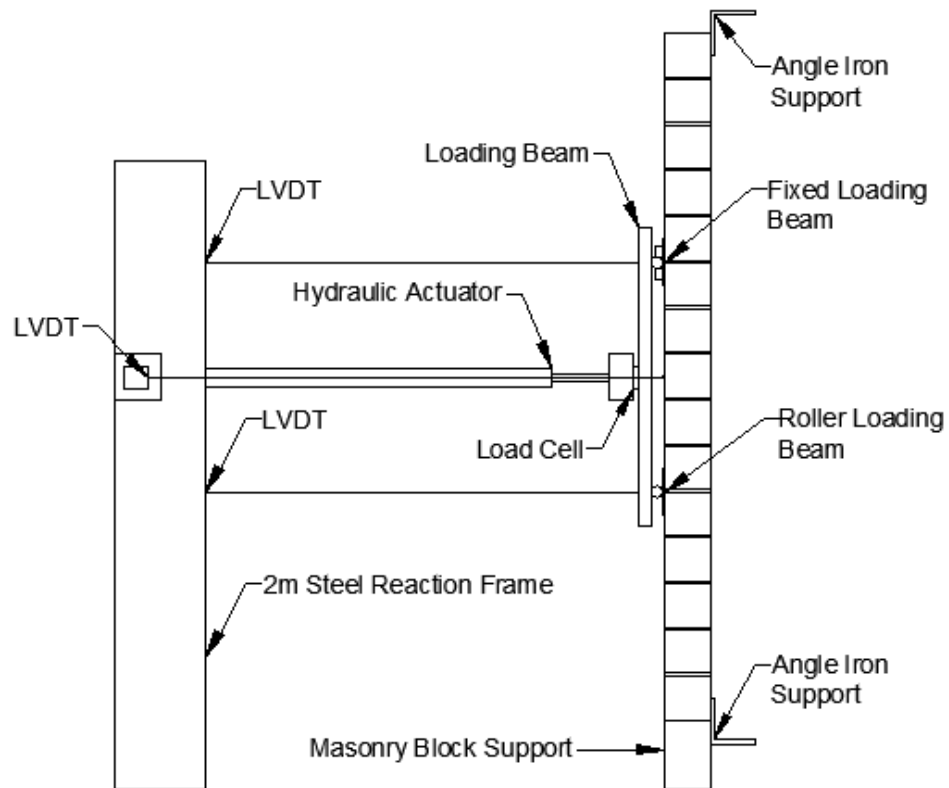
The test setup is shown in Figure 5-8 which illustrates the configuration of the masonry wall within the test frame. The main frame consisted of two 12ft columns, connected to the laboratory strong floor with two angle irons spanning between them at the top and bottom of the wall to create a pin-pin connection. When inserted into the set-up, the wall rests upon two masonry blocks and a block of wood, and is supported by these angle irons on one side, and by the loading beam on the other. To support the loading beam, another 9ft tall column is connected to the strong floor at the back of the set-up area. A single-ended hydraulic actuator was connected to this 9ft column at the mid-height location of the test wall. The hydraulic actuator had a 500mm stroke. This amount of stroke exceeded the expected deflection required to test the masonry, but due to the potentially deflection capacity of the polyurethane foam, it was necessary to over-estimate the stroke capacity. A load cell was mounted on the end of the hydraulic actuator, and then attached to the loading beam which consisted of a 300mm wide piece of steel, with a pipe welded to its upper end. Along with a fixed joint attached to the wall itself and a loose pipe wedged between the loading beam and the wall, the loading beam was able to mimic a pin-roller loading condition. The roller and the pin connection were placed exactly one third of the wall height apart, so that the constant moment region would occur in the middle third of the wall. The entire setup was strengthened by strong chains joining all columns together, and supporting the end of the hydraulic actuator and the load cell, so that the load cell was not stressed from supporting its own weight. Connected to the hydraulic actuator was a manually pumped jack which was used to

apply the load to the test wall. The applied load was monitored by the load cell and outputted to a data acquisition unit.

Linearly variable displacement transducers (LVDT's) were secured to the test wall to provide the necessary information as to the out-of-plane deflections of the specimen. Two LVDT's were located at the mid-height of the specimen for all testing, and an additional LVDT was located at both the top third of the wall and the lower third of the wall.



(a) Front View



(b) Side View

Figure 5-8: Out-of-Plane Full Scale Test Set-up

5.6 Experimental Results of Full Scale Walls

In this section, the results and observations derived from the full size wall tests are presented. The main findings and conclusions drawn from this testing phase are discussed with the assistance of graphs and tables, with a more in-depth analysis of the testing of each wall and the observed modes of failure and cracking patterns given in Appendix B.

The purpose of testing various polyurethane foams of different densities and from different companies was to create a range of data that would provide insight into the general behaviour of polyurethane foam when it is used as a reinforcing material in masonry construction. As both the strength and the cost of the foam are directly related to the density of the foam, it was crucial to test and compare the results between different densities of foam. Polyurethane foam from Company C was used for this purpose. Three foams were chosen for these tests—an extremely low density foam (C-1), extremely high density foam (C-3), and a foam that had an average density in the middle range of the other selected foams (C-2). So as to compare the characteristics of foam from different companies, B-2 foam supplied by Company B was used which was also a medium density polyurethane foam. Previous to the testing of the 3m walls, a comparison was done between Company B B-1 and B-2 polyurethane foams so as to determine the more ideal B-2 polyurethane foam to work with further, and to test out the concept in general.

In order to further develop the polyurethane foam reinforcement system, rope I was used to reinforce walls so as to determine the effect that the addition of the rope to the system would have on positively enhancing both the strength and the damage tolerance or resiliency of the system. Two walls were tested with B-2 polyurethane foam and rope I reinforcement, one half-roped with rope in the core of every other cell (three cells in total), and another wall that was fully roped with rope in all five cells of the wall specimen.

5.6.1 Preliminary Full-Scale Out-of-Plane Wall Tests Using Company B Polyurethane Foam

In order to investigate how polyurethane reinforcement could improve the performance of URM walls in the out-of-plane direction, preliminary testing was conducted using the B-1 and B-2 polyurethane foams. An eleven course high wall was selected to represent a 1m strip of wall in a single-storey dwelling. The walls consist of full size 390mmx190mmx190mm block and standard construction 10mm mortar joints resulting in overall wall dimensions of 2.2mx1m.

As loading was applied to each wall specimen, an extensive crack pattern developed, leaving at least two layers of mortar in the center region of the wall completely cracked. Once the full crack pattern had developed, each wall experienced a significant stepped drop in load capacity. As loading of the wall specimen continued, each wall continued to deflect while exhibiting a somewhat linear decline in load capacity. When the masonry was fully cracked and no longer capable of carrying any loading, the polyurethane foam then carried the remaining load until ultimate failure was reached. Shortly before reaching ultimate failure, both specimens exhibited unexpected behaviour. The load capacity of each wall increased by approximately 1 kN while it experienced its last 50 mm-100 mm of deflection. The cracking capacity and ultimate capacity of each specimen is shown in Table 5-2.

Table 5-2: Comparison of Out-of-Plane Behaviour of Wall B-1 and Wall B-2

	Cracking Capacity (kN)	Deflection at Cracking (mm)	Ultimate Capacity (kN)	Deflection at Ultimate (kN)	Energy Absorption (Nmm)
Wall A-1	3.63	12.37	1.48	195.80	184,224
Wall A-2	5.83	27.23	1.30	354.14	300,727

From the load versus deflection diagram in Figure 5-9, it can be seen that the B-2 polyurethane foam achieved a significantly higher load and energy absorption capacity than that of B-1. When the wall with the B-1 reinforcement began to fail during testing, the masonry and the foam cores acted as separate systems, with the masonry failing first, followed by the failure of the foam. As the foam cores were in fact not sufficiently bonded to the masonry, they were not able to act together as a system to take on the high loads being applied to the wall. In contrast, when the wall containing the B-2 foam was tested, the foam was fully bonded to the masonry and together they worked as a system to resist the applied loading. The B-2 foam which was of a medium density was able to withstand 60% more lateral force than the lower density B-1 foam, and was able to absorb 63% more energy. Compared to the case of an unreinforced specimen, that when cracked exhibits sudden and complete failure, these specimens reinforced with polyurethane foam exhibit a much more ductile failure, and provide some residual strength in the specimen after the full crack-pattern has developed. This positive preliminary study requires further analysis into the potential out-of-pane load capacity that this type of reinforcement could offer.

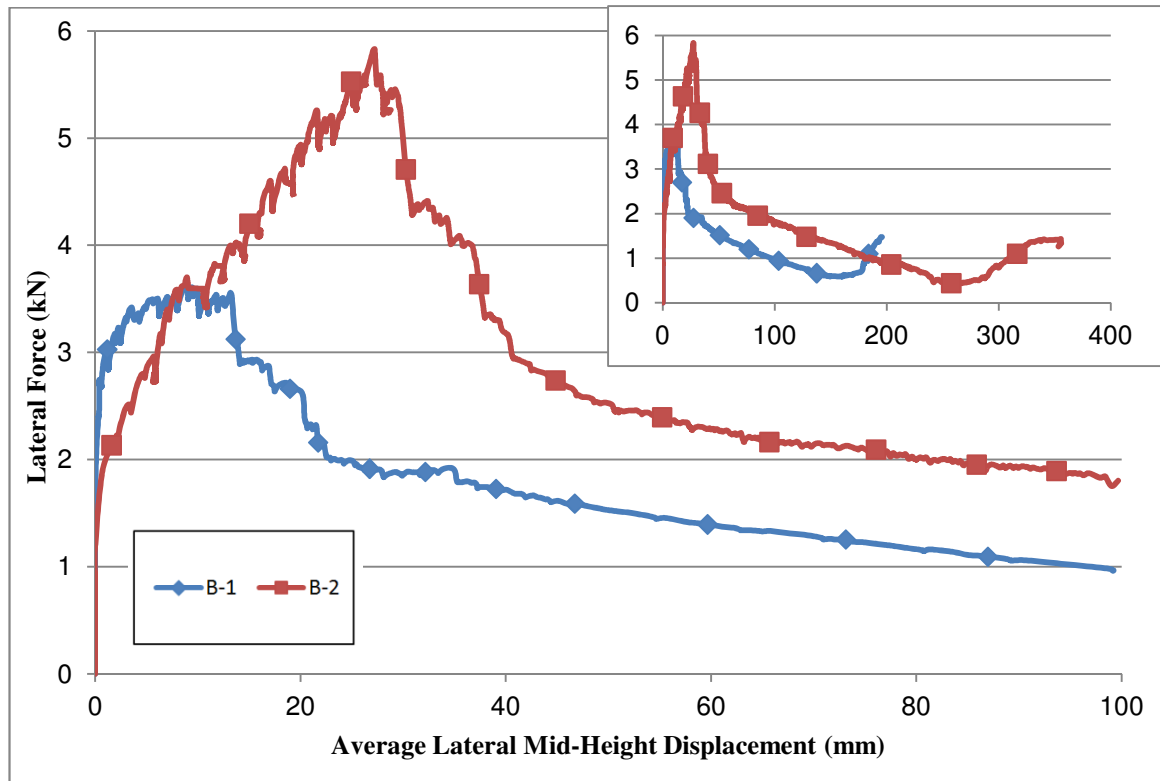


Figure 5-9: Comparison of Lateral Force vs. Average Lateral Mid-Height Displacement of B-1 and B-2 Walls

5.6.2 Full Scale Out-of-Plane 3m Wall Test Analysis

As can be seen in Figure 5-10 the 3m unreinforced wall specimen was able to withstand a loading of only 1.65 kN before a crack along its full width opened up and gave way. Once a crack developed in the wall, there was no residual strength remaining in the wall. This opening of the crack pattern resulted in the ultimate failure of the unreinforced specimen after deflecting only 6.6 mm at mid-height, and the dissipation of only 7840 Nmm of energy. Any strength remaining in the wall after the opening of the crack pattern was a result of the stability of the test apparatus and a minimal resistance from the remaining intact mortar. The overall strength of the wall system was provided by the resistance of the wall due to its heavy self-weight, along with minimal resistance provided by the mortar. The inability of this type of wall system to carry any significant

load or dissipate energy shows how weak this type of building system is, and that there is a lot of room for improvement with different reinforcement technologies.

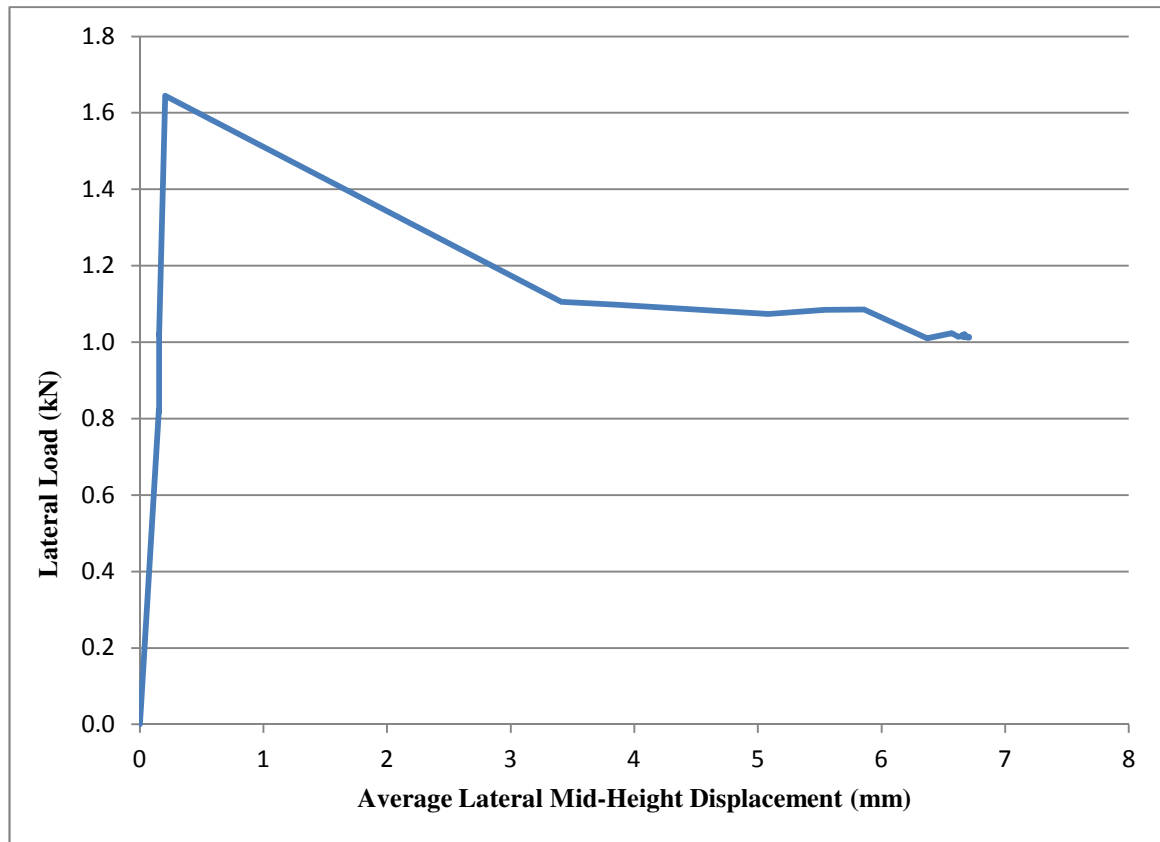


Figure 5-10: Lateral Load vs. Average Mid-Height Displacement Curve for the Unreinforced Control Wall

Comparing all of the different foamed walls to each other, it can be seen that each of the walls experienced somewhat similar behaviour as the walls approached their cracking capacity. They each experienced a gradual increase in load capacity as the walls started to deflect at mid-height. Upon reaching the cracking capacity, each wall also experienced a sudden large drop in load capacity, followed by a very gradual further loss in load capacity until ultimate failure was reached. However, as much as the load-deflection relationships are comparable prior to reaching the cracking capacity, the

comparison of the post-cracking behaviour of the walls yields far less conclusive analysis. After the drastic loss in load capacity of each of the walls, it is low density C-1 wall and the medium density B-2 wall that demonstrate the most residual strength, followed by the high density C-3 wall and the medium density C-2 wall. This result was unexpected, as the higher density walls were expected to have the highest amount of residual strength, followed by the medium density walls and so on. This change in the data shows that the residual strength left in the walls post cracking may not be conclusive. Depending on the crack pattern and particular conditions of the specimen, each may experience a different residual strength, regardless of foam density of the specimen.

As can be seen easily in Figure 5-11, the testing of the 3 m walls showed that the maximum lateral load that the walls were able to carry depended on foam density. The high density C-3 foam was able to reach a capacity of 6.49 kN while the low density C-1 foamed wall was able to reach a capacity of only 4.96 kN. The two walls that had medium density foam in the masonry were able to reach capacities almost exactly between these two values, with the medium density C-2 and B-2 walls reaching capacities of 5.69 kN and 5.75 kN respectively. As the C-2 and the B-2 medium density walls otherwise behaved quite differently, with the B-2 wall experiencing significantly greater deflection than the Company C walls, the fact that each wall reached a similar cracking capacity shows that the cracking capacity must be directly related to density, and less dependent on the other variables in the polyurethane foam.

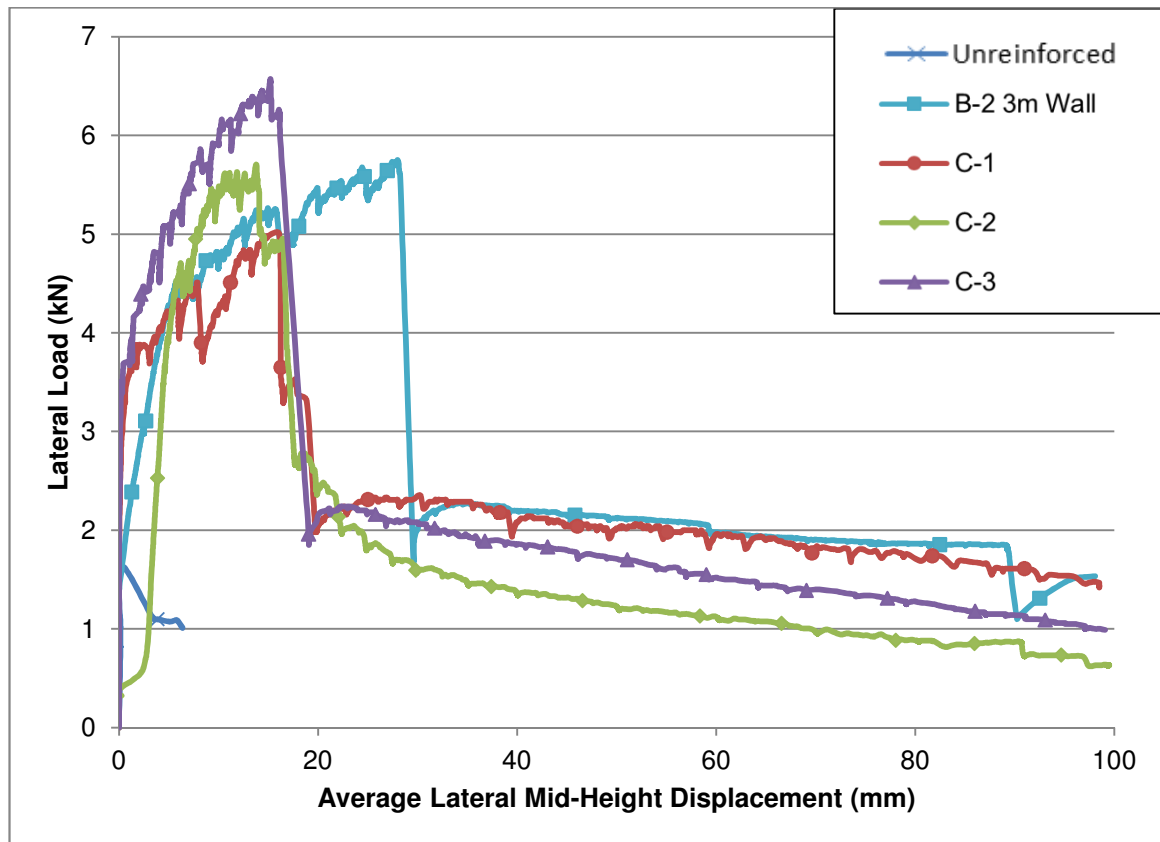


Figure 5-11: Comparison of Lateral Load vs. Average Lateral Mid-Height Deflection for Different Types and Densities of Polyurethane Walls

It can also be seen from the above load-deflection diagram that each of the Company C walls reached their cracking capacity at approximately the same deflection (within a tolerance of 1.5 mm). Given that each of these walls experienced a different cracking pattern and experienced a main failure plane between different rows of masonry, this result is quite remarkable and would imply that this brand of polyurethane foam has a deflection threshold at which the cracking capacity will be reached.

Looking at the energy absorption of each of the walls in Table 5-3, it should be noted that the higher density walls are not necessarily able to absorb more energy than lower density walls. In fact, the low density C-1 wall was able to dissipate 33.8% more

energy than the medium density C-2 wall. The high density C-3 wall was only able to dissipate 6.5% more energy than the low density C-1 wall, showing that the energy absorption capabilities of the specimen did not directly relate to the polyurethane foam density of the specimen.

Table 5-3: Comparison of Different Types and Densities of Polyurethane Reinforced Walls

	Cracking Capacity (kN)	Deflection at Cracking Capacity (mm)	Energy Absorption (Nmm)
Unreinforced	1.65	0.20	7840
B-2	5.75	28.08	264,145
C-1	4.96	14.85	234,869
C-2	5.69	13.72	175,576
C-3	6.49	15.10	250,194

By looking at the energy absorption of each specimen, one can also conclude that the B-2 polyurethane foam specimen is superior to the other Company C foamed walls. Under the same level of loading, the B-2 wall is able to deflect 28 mm before the main crack pattern gave way and opened up, compared to the medium density C-2 wall which reached this same state at a deflection of only 13.72 mm, less than half of the displacement of the B-2 wall. The superiority of the B-2 wall is again reinforced by comparing the energy absorption of the two walls. The B-2 wall was able to absorb 50.44% more energy than the medium density C-2 wall, with the C-2 wall absorbing 175,576 Nmm of energy, compared to 264,145 Nmm in the B-2 wall. The comparison of the energy dissipating capabilities of each type of foam can again be seen in Figure 5-12, where the energy absorption capacity of each wall has been normalized to the unreinforced specimen. This graph shows again that out of all of the foams being tested, the B-2 polyurethane foam is able to dissipate the most energy. However, this graph also shows that each foam is able to provide the unreinforced masonry system with 22-34 times more energy dissipation capacity than it would have had otherwise.

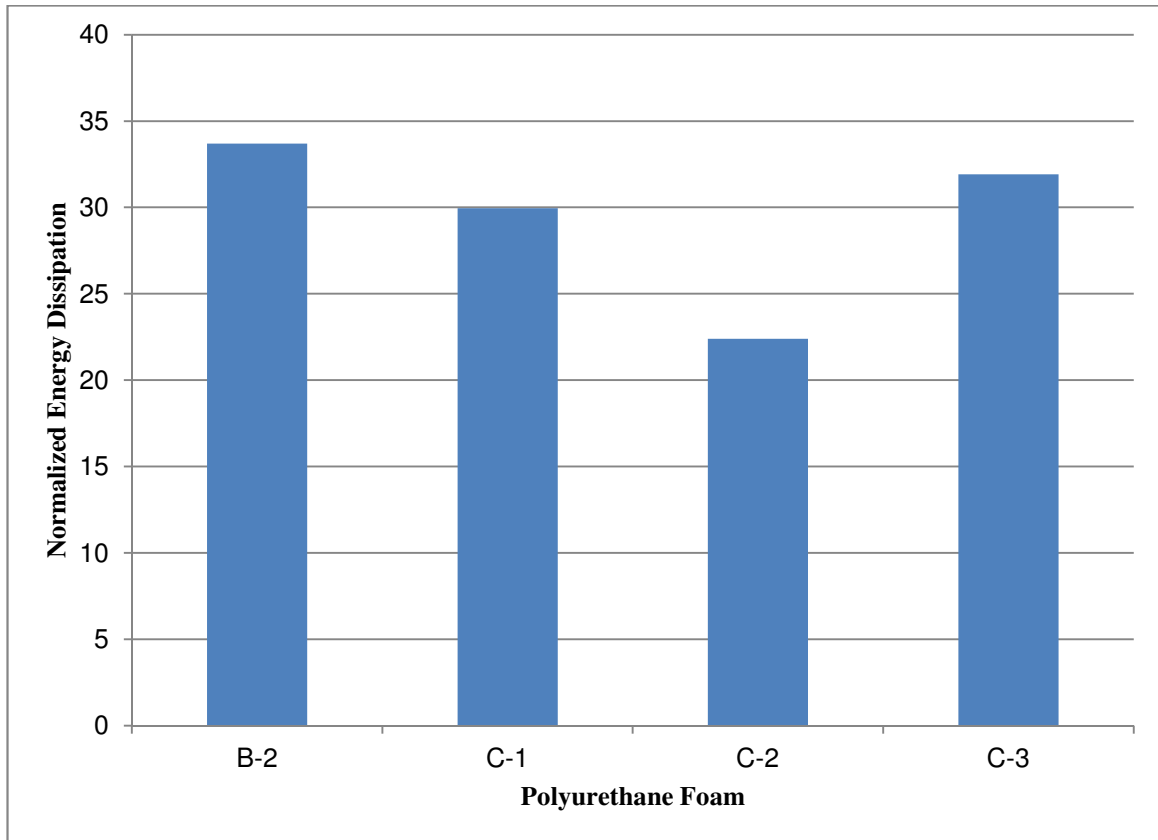


Figure 5-12: Comparison of Energy Absorption of 3m Walls, Normalized to Unreinforced Specimen

The comparison of each wall's performance can further be seen in Figure 5-13 which shows the work done by each wall specimen. All walls initially have the same work vs. displacement profile, showing the similar capacities of each foam at small deflections. However, as deflection increases, medium density B-2 foam outperforms the other wall

specimens, with the wall being able to absorb substantially more energy.

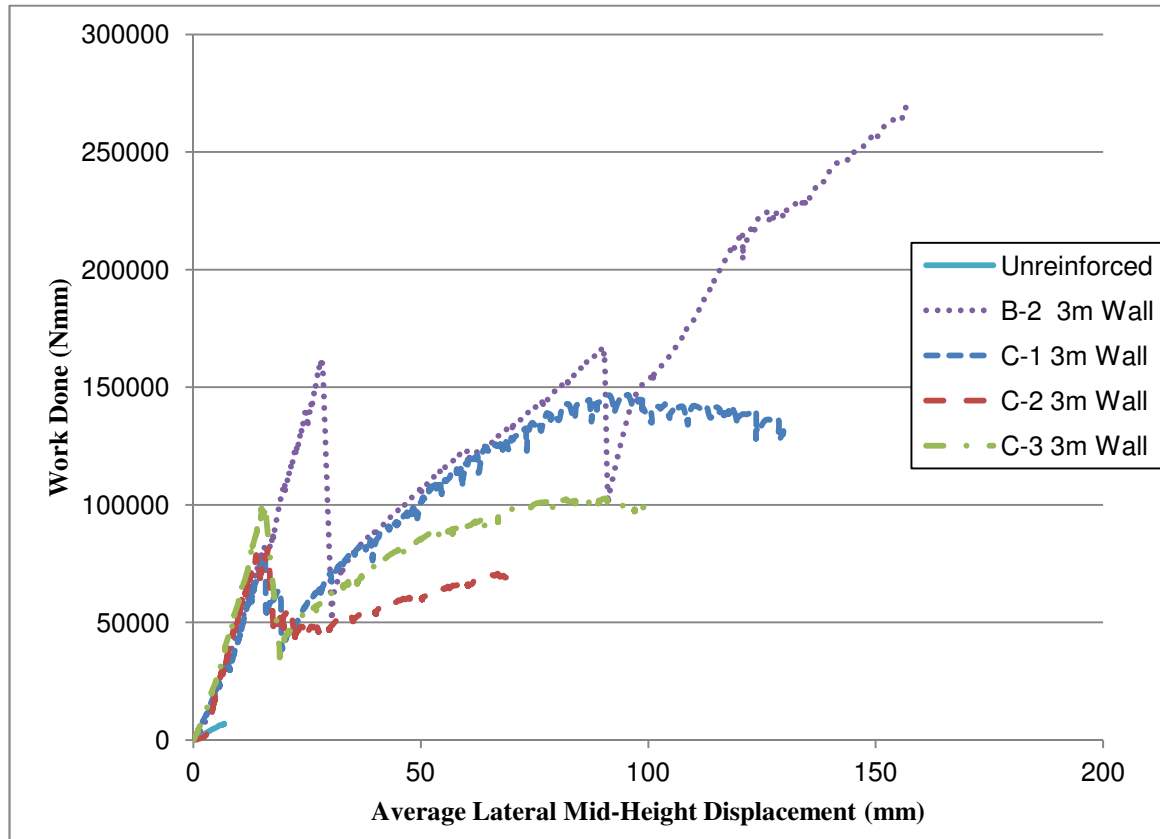


Figure 5-13: Work vs. Displacement for 3m Polyurethane Foam Reinforced Walls

5.6.2.1 Comparison of B-2 2m and 3m Walls

The comparison of the testing of the B-2 2 m and 3 m walls yield some interesting and somewhat unexpected results. Prior to testing, it was hypothesized that the 3m wall would experience a greater amount of deflection, and would experience a load-deflection curve similar to the green curve in Figure 5-14 below. However, the 3 m B-2 wall behaved in a very different pattern.

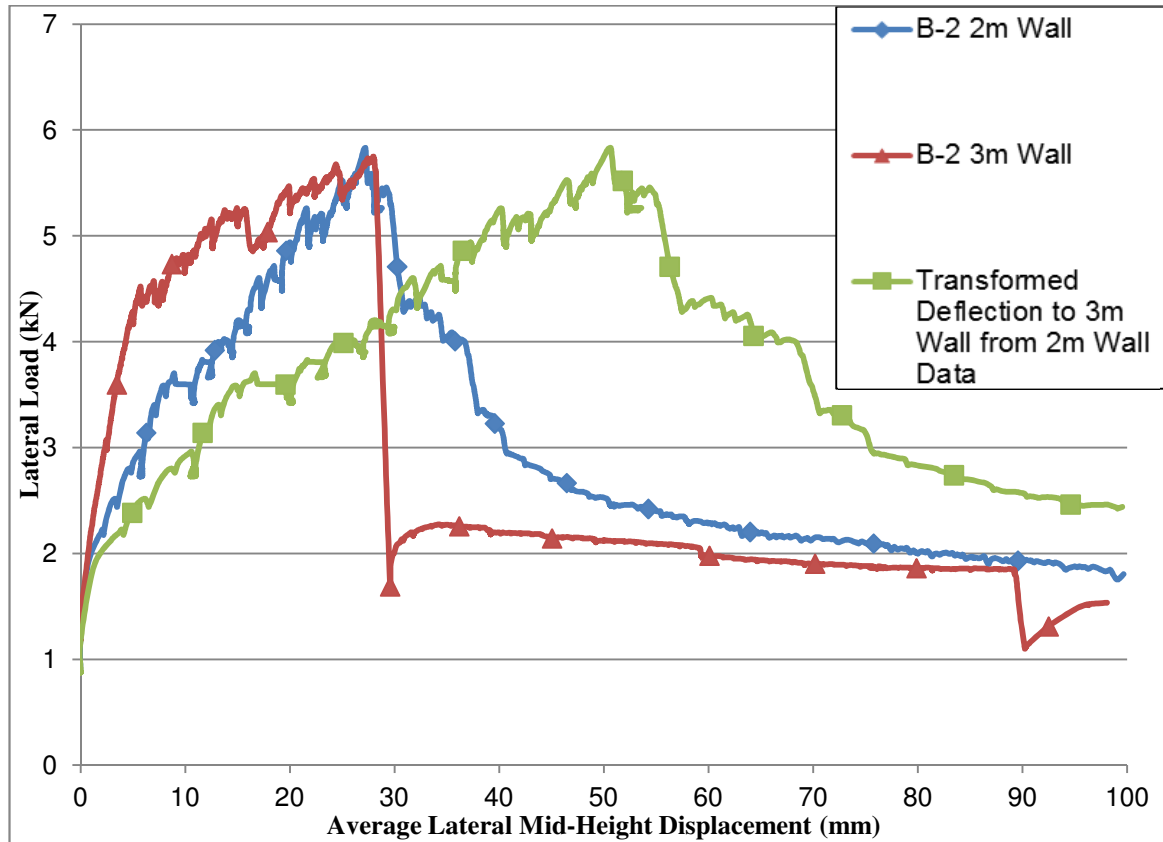


Figure 5-14: Comparison of Lateral Load vs. Average Lateral Mid-Height Deflection of B-2 2m and 3m Walls

Instead of a very gradual increase in load and deflection, the wall was initially able to take on more loading while exhibiting smaller deflections than the 2 m wall. However, as different as the load paths of the two walls were, they both were able to reach relatively the same peak load while undergoing the same amount of deflection. In the future, this similarity may prove to show that as long as the wall height is within a certain range, it will experience the same peak loading at similar mid-height displacements.

The post-cracking load behaviour of the 3 m wall is significantly different from the 2 m wall. After the full cracking pattern in the 2 m wall had developed, the wall lost

strength as the main crack opened up. However, it lost strength incrementally, with the wall abruptly losing some strength, followed by a more gradual loss, and then again by another sudden loss in strength. This made the failure of the specimen considerably more gradual overall. The 3 m wall, instead of following this similar pattern, simply lost all of its strength as soon as its full cracking pattern developed. This showed that there was much less residual strength left in the wall post-cracking.

A better comparison between the walls can be found in the analysis of their energy absorption when normalized to unreinforced wall data. As can be seen in Figure 5-15, the 2 m wall specimen was able to absorb 13.7 times more energy than the 3m wall. Initially the 3 m wall was able to absorb more energy than the 2 m wall, however after the walls were fully cracked, the 2 m wall was able to absorb substantially more energy than the 3 m wall as it approached failure. The 2 m wall behaved in a more ductile manner which is highly more desirable than the sudden and more drastic failure of the 3 m wall specimen.

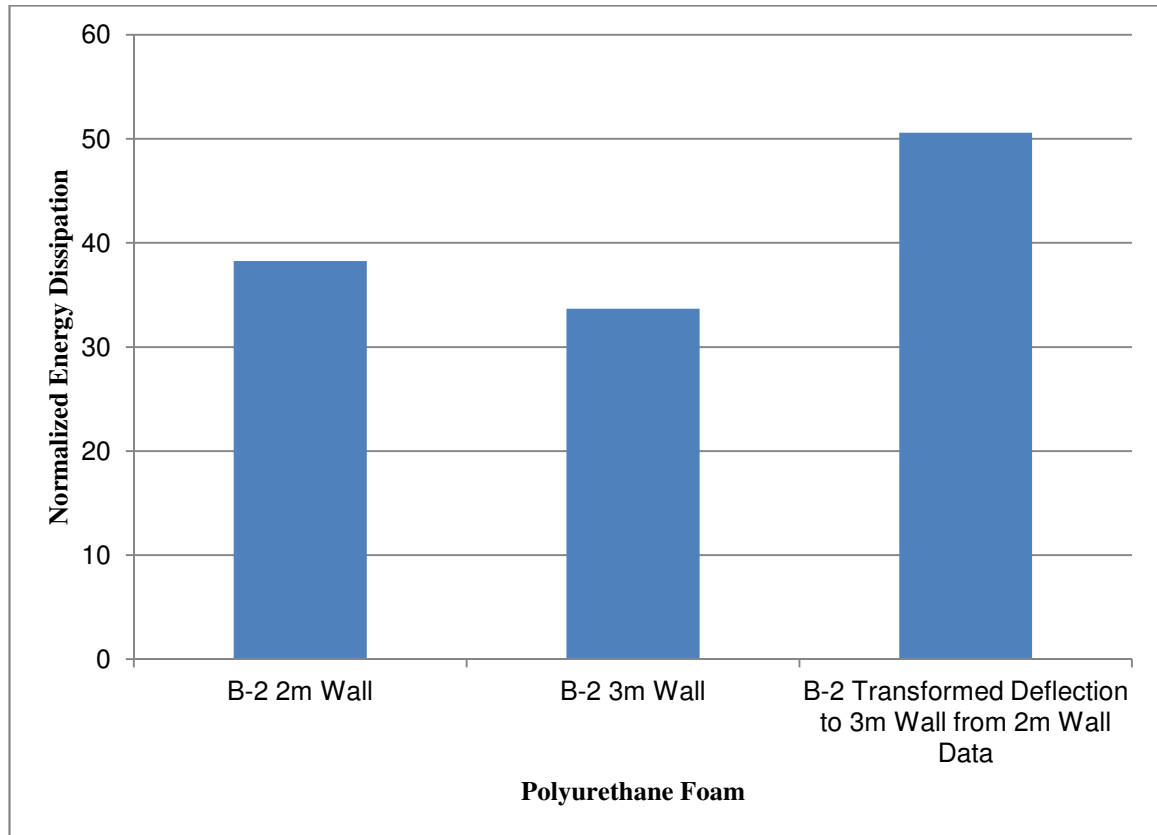


Figure 5-15: Comparison of Energy Absorption of B-2Walls, Normalized to Unreinforced Specimen

5.6.3 Full Scale Out-of-Plane 3m Wall Analysis of Rope I Reinforced Walls

A comparison of the B-2 polyurethane foam and rope I reinforced walls shows that as additional reinforcement in the form of rope I is added to the cells of the wall, the wall as a whole becomes progressively stronger, as can be seen in Figure 5-16. Intuitively, this was an expected result. What can be learned of this comparison analysis is the extent that this additional rope reinforcement enhances the lateral load capacity of the wall, and the behaviour of such a wall under out-of-plane testing.

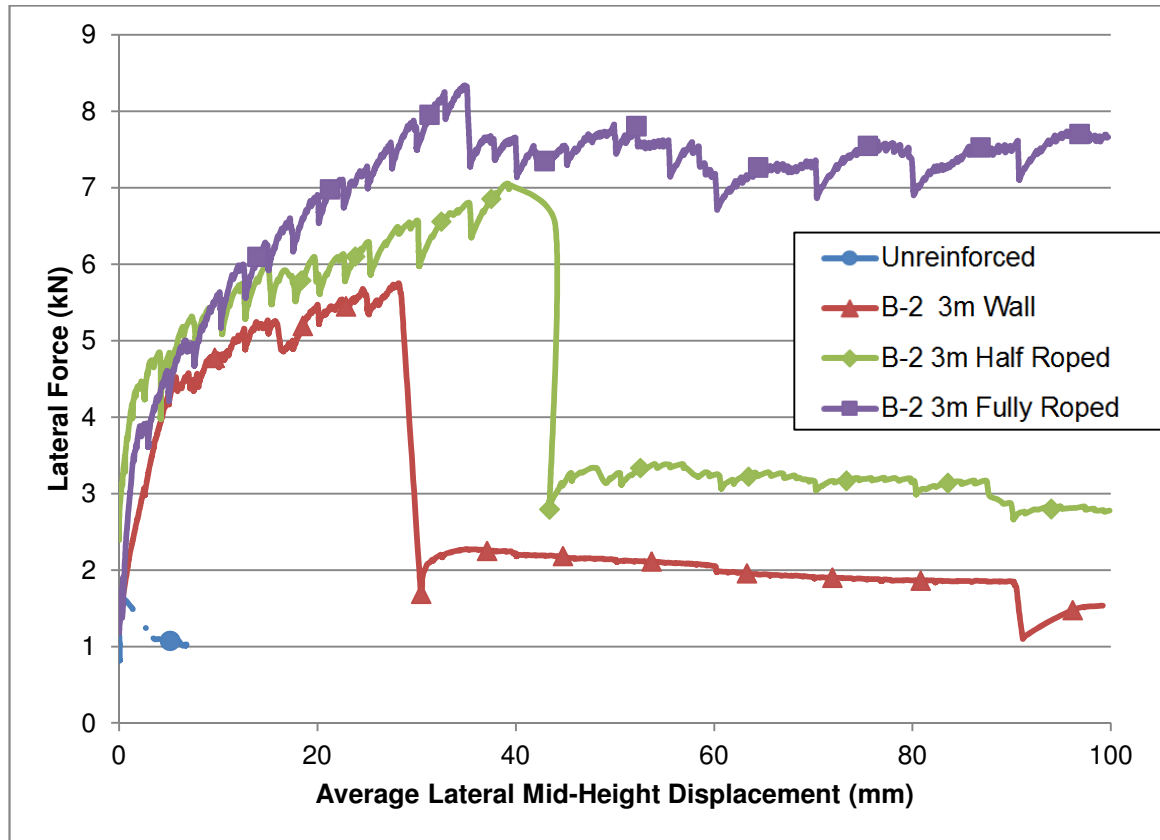


Figure 5-16: Comparison of Lateral Load vs. Average Mid-Height Displacement for B-2 Reinforced Walls

The addition of 3 columns of rope reinforcement to the B-2 polyurethane foam reinforced wall increased the maximum lateral load capacity by 22.6%, and the addition of another two columns of rope to make the specimen fully roped increased the maximum lateral load capacity by 47.3% as compared to the B-2 wall with no rope reinforcement. These maximum loads occurred at mid-height deflections between 28 mm and 39 mm. Surprisingly, the wall containing only 3 cells of rope reinforcement was able to experience the most deflection while at its cracking capacity. This is made even more unexpected, as this was the wall that had already cracked due to the over-expansion of foam when the walls were injected with the B-2 polyurethane foam. However, as all of the walls reached their cracking capacity while experiencing deflections that are in such a

small range from each other, it is to be expected that if different numbers of rope reinforcement are used, they would experience deflections that are within or near this 11mm range when they reach their cracking capacity. Also, as the cracking capacity of the specimen increased as the B-2 wall became more and more reinforced with rope I, an assumption can be made that a wall containing only one of two columns of rope reinforcement would experience a cracking load between that of the plain B-2 specimen and that reinforced with only three cells of reinforcement (between 5.75 kN and 7.05 kN). Likewise, a wall containing four cells of reinforcement should experience a cracking capacity between that of the wall with 3 cells of rope and the fully roped wall (between 7.05 kN and 8.47 kN).

As can be seen in Table 5-4, the energy absorbed by the specimens over the same amount of deflection, becomes increasingly larger as more rope reinforcement is added to the trench foam walls. The wall containing three columns of rope is able to absorb 50% more energy than the plain B-2 wall, and the fully roped wall is able to absorb 78% more energy on top of that, absorbing 167% more energy as compared to the plain foamed specimen. This shows a drastic increase in the capability of the masonry/foam system to dissipate the energy being applied to the wall. This relationship can be seen even clearer in Figure 5-17 where, when normalized to the 3m unreinforced wall specimen, the energy absorption capacity of each roped specimen is significantly higher than that of the plain B-2 polyurethane foam specimen. Considering that the B-2 polyurethane foam was the highest-performing of all the wall specimens, the fact that the half roped and fully roped specimens were able to outperform the B-2 specimen by 17 times and 56 times, respectively, in their energy absorption capabilities, this data shows the true potential of this polyurethane foam system when used in conjunction with rope I.

Table 5-4: Comparison of B-2 Reinforced Walls

	Cracking Capacity (kN)	Deflection at Cracking Capacity (mm)	Energy Absorption (Nmm)
B-2	5.75	28.08	264,145
B-2, Half Roped	7.05	39.15	395,639
B-2, Fully Roped	8.34	34.15	704,166

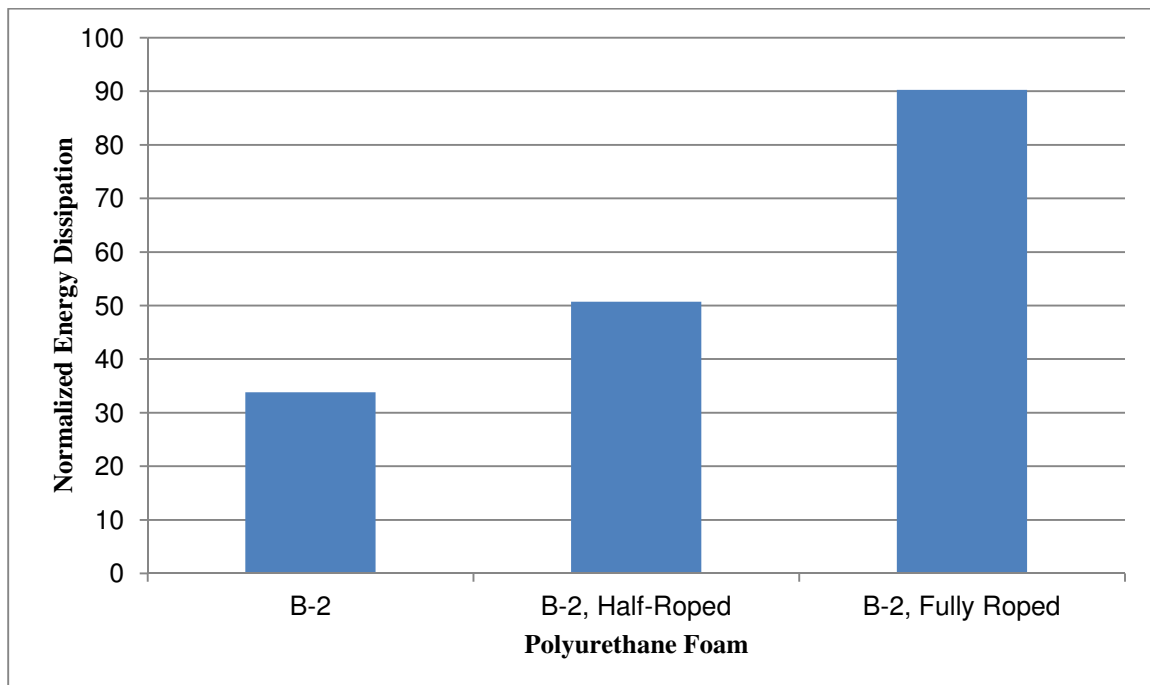


Figure 5-17: Comparison of Energy Absorption of All B-2 3m Walls, Normalized to Unreinforced Specimen

The post-cracking behaviour of these specimens is also significant. The fully roped wall is able to withstand peak loading for the duration of the post-cracking period, right up until the point of failure. Figure B-0-31 in Appendix B shows that the high level of loading is maintained, and even surpassed on two occasions. Although there are dips and fluctuations in the loading, it remains relatively constant at such a high level of loading. When comparing this fully roped case to the half-roped case, it is clear that there is a significant loss in energy absorption capacity between the two cases. When the half-

roped wall experienced its cracking capacity, it then experienced a significant loss in strength more reminiscent of how the foamed walls behaved without any reinforcement. This half roped wall was able to take on a higher level of load while undergoing higher levels of deflection; however it was not able to maintain such high loading. This could partially be due to the premature failure of the half-roped specimen during the foam injection, which led to a weaker test specimen. Further investigation needs to be done to see whether the half-roped specimen would exhibit less of a loss in loading after reaching its cracking capacity, and exhibit behaviour more akin to the fully roped specimen, if the half-roped wall would have been fully intact upon testing.

5.7 Categorization of Out-of-Plane Wall Behaviour

As the use of polyurethane foam as reinforcement in masonry construction is a new concept and has yet to have specific codes and guidelines regarding the use of this material as reinforcement, it does not yet meet the literal requirements of the buildings code. However, as polyurethane foam reinforcement proves itself to be capable of performing as well as or better than conventional reinforcement, it will prove to be a candidate within the context of performance-based design.

Performance-based design approaches are regularly being used for the structural and seismic design of new buildings as well as for seismic evaluations and upgrades of existing buildings. In performance-based design, the designer selects a target performance level that the building should meet if it is subjected to an earthquake with a specific intensity. The designer selects a level of damage to the building that is acceptable to the client, and then designs the building accordingly. In conventional design there is a focus on collapse prevention. However, with different design approaches, other goals can be met which can leave the building in a functioning state in need of only minor repairs after an earthquake instead of in a state where the collapse of the building was prevented but

still requires costly and time-consuming repairs, or in some cases where the building is too damaged to remain safe and occupied (Hamburger, et. al., 2011).

As clients of buildings can desire various different post-earthquake scenarios, there are a variety of damage states that have been developed so that the designer can select a specific performance design level, varying from only a small amount of acceptable damage in the forms of small cracks in the masonry, to the allowance of a great deal of damage to the building with the buckling of vertical reinforcement (Hamburger, et. al., 2011).

Procedures have been developed to identify the damage states in-depth. The Federal Emergency Management Agency (FEMA) has developed document FEMA 306 which details the evaluation of earthquake damaged concrete and masonry wall buildings, and provides guidelines for evaluating the level of structural damage which correlates to a specific damage state in performance-based design. For each individual component of the structural system, there is a classification of damage given a particular behaviour mode. This selected behaviour mode is indicative of the type of damage that a component could sustain as a result of earthquake forces and subsequent displacements. For each component of a building, the severity of damage is classified according to the damage levels given in Table 5-5 (ATC, 1998).

Table 5-5: Component Damage Classification (ATC, 1998)

Level of Damage	Description
Insignificant	Damage does not significantly affect structural properties in spite of a minor loss of stiffness. Restoration measures are cosmetic unless the performance objective requires strict limits on nonstructural component damage in future events.
Slight	Damage has a small effect on structural properties. Relatively minor structural restoration measures are required for restoration for most components and behavior modes.
Moderate	Damage has an intermediate effect on structural properties. The scope of restoration measures depends on the component type and behavior mode. Measures may be relatively major in some cases.
Heavy	Damage has a major effect on structural properties. The scope of restoration measures is generally extensive. Replacement or enhancement of some components may be required.
Extreme	Damage has reduced structural performance to unreliable levels. The scope of restoration measures generally requires replacement or enhancement of components.

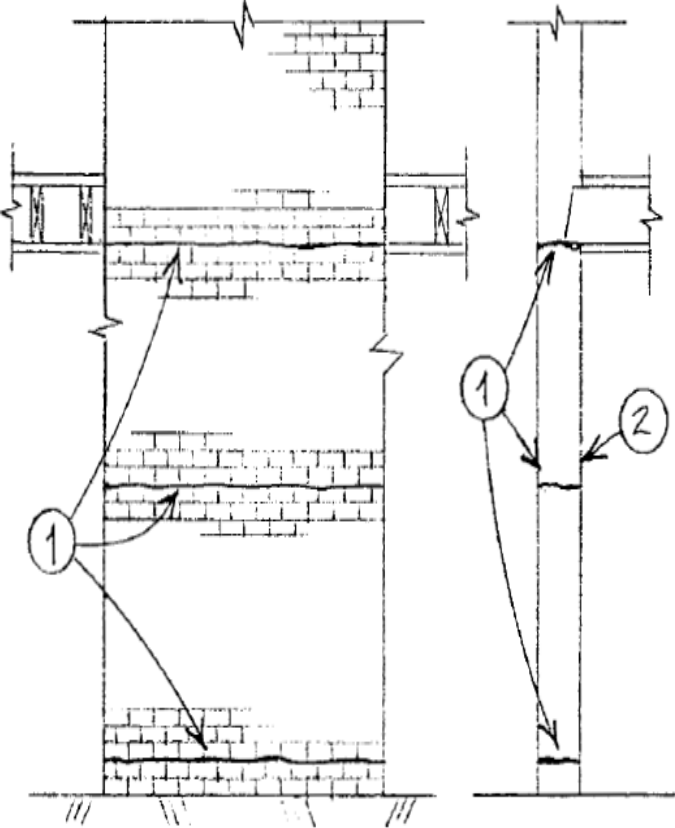
The polyurethane foam reinforced masonry walls were tested in the out-of-plane direction, and demonstrated similar failure patterns to unreinforced out-of-plane wall failure, so in order to classify these walls, the URM component damage classification guide within FEMA 306 was used, using the out-of-plane flexural response behaviour mode. The component damage within this behaviour mode is described as rigid-body rocking motion occurring on three cracks: one at the top of the wall, one at the bottom, and one at mid-height. As rocking increases, the mortar and masonry units at the crack locations may degrade, and residual offsets can occur at the crack planes. The ultimate

limit state of the component is reached when the wall rocks too far or overturns. As in this testing phase of the polyurethane reinforced masonry walls, the main wall failure was due to a mid-height crack, as just described, this component classification guide was used to categorize and describe the failure that occurred (ATC, 1998).

In Table 5-6, each level of damage for this behaviour mode is described, along with the rotation of each wall at the point when it was experiencing each level of damage. With this categorization, and the comparison of angles of rotation, general observations about the level of damage incurred upon a certain level of deformation can be made. Although each wall cracked at a different wall height and was reinforced with different polyurethane foams, the walls collectively reached each damage state at almost exactly the same angle of rotation. This shows that while the various polyurethane foams exhibited different properties and strengths, the relationship between the amount of cracking of the polyurethane foam and the angle of top rotation is more dependent on the geometry of the test set-up than on the strength of the foam itself.

In the cases of the walls that were half- and fully-reinforced with rope, the walls were able to experience higher top angles of rotation when reaching each level of damage. The same classification guide was used for these walls, as similar repairs would need to be done to the rope-reinforced walls as to the plain polyurethane foam reinforced walls. However, as the rope reinforcement is flexible, even in the extreme damage state, the rope is never damaged. This implies that if this classification guide was used in the context of a building, where the test wall is not allowed to deflect freely, then it is expected that even higher levels of deflection and angles of rotation can be achieved for each damage state due to the extra strength and deflection capacity of the rope reinforcement.

Table 5-6: Out-of-Plane Flexural Response Classification Guide for Polyurethane Foam Reinforced Masonry (ATC, 1998)

Level of Damage	Description	Angles of Rotation
<p>Insignificant</p>	<p><i>Criteria:</i></p> <ol style="list-style-type: none"> 1. Hairline cracks at floor/roof lines and mid-height of stories 2. No out-of-plane offset or spalling of mortar along cracks 3. Polyurethane Foam has not cracked. <p><i>Typical Appearance:</i></p> 	<p>0°-1.0°</p> <p>Half-reinforced with rope: 0°-1.5°</p> <p>Fully-reinforced with rope: 0°-1.9°</p>

Slight	<p><i>Criteria:</i></p> <ol style="list-style-type: none"> Cracks at floor/roof lines and mid-height of stories may have mortar spalls up to full depth of joint. Polyurethane foam has begun to crack up to ¼ of the depth of masonry. 	<p>1.0°-1.9°</p> <p>Half-reinforced with rope: 1.5°-2.7°</p> <p>Fully-reinforced with rope: 1.9°-3.1°</p>
Moderate	<p><i>Criteria:</i></p> <ol style="list-style-type: none"> Cracks at floor/roof lines and mid-height of stories may have mortar spalls up to full depth of joint. Polyurethane foam has begun to crack up to ½ the depth of masonry. 	<p>1.9°-2.6</p> <p>Half-reinforced with rope: 2.7°-3.8°</p> <p>Fully-reinforced with rope: 3.1°-4.6°</p>
Heavy	<p><i>Criteria:</i></p> <ol style="list-style-type: none"> Cracks at floor/roof lines and mid-height of stories may have mortar spalls up to full depth of joint. Polyurethane foam has begun to crack up to ½ the depth of masonry. 	<p>2.6°-3.4°</p> <p>Half-reinforced with rope: 3.8°-5.4°</p> <p>Fully-reinforced with rope: 4.6°-6.5°</p>
Extreme	<p><i>Criteria:</i> Vertical-load-carrying ability is threatened</p> <ol style="list-style-type: none"> Cracks at mid-height of stories have fully opened up. Polyurethane foam has begun to crack up to ¾ of the depth of masonry. 	<p>≥3.4°</p> <p>Half-reinforced with rope: ≥ 5.4°</p> <p>Fully-reinforced with rope: ≥ 6.5°</p>

5.8 Conclusions

As out-of-plane failure can often be the most hazardous type of failure during an earthquake, the positive performance of masonry walls reinforced with polyurethane foam shows great potential applications. Given that each type of polyurethane foam reinforced wall was able to far outperform the URM specimen, this full-scale proof of concept stage shows that polyurethane foam reinforcement can be used to provide a great more resiliency and strength to URM buildings, as well as make them more damage tolerant.

A great deal of information was learned from this part of the study. The effect of density on a given polyurethane foam was able to be properly judged, to create a range of data showing the density needed in order to maintain a certain level of loading. Polyurethane foams of similar density were able to be compared, so as to determine an optimal polyurethane foam to work with for future research. The higher level of resiliency of the B-2 polyurethane foam showed that a great deal of energy could be absorbed during the failure of this type of system. With the addition of rope reinforcement to the polyurethane foam system, this new reinforcement system took on a load-displacement curve more similar to conventional steel-reinforced masonry, with no drastic drop in force with the failure of the masonry. The ability of simple rope to carry and maintain high loading after the masonry had fully cracked, shows that this rope and foam system should be looked at in-depth to come up with an optimal, inexpensive system that can rival conventional reinforcement in providing adequate safety to masonry buildings that are seismically vulnerable.

The classification of the tested data into performance-based parameters aids in the future use of this data in developing a full polyurethane foam reinforcing system. As polyurethane foam reinforcement is unconventional and does not follow normal code guidelines, it is within the performance-based design framework that it will be able to flourish and eventually be implemented on a large scale.

6 Conclusions

Earthquake damage to URM buildings has shown that the outside perimeter walls of a building are particularly susceptible to out-of-plane failure. The new first-world building codes require masonry buildings to be reinforced with a system of steel re-bar and grout to minimize the effect of seismic forces on a building in the event of an earthquake. However, as these building materials are expensive and not always readily available, an inventive approach needs to be taken to look for alternative reinforcement techniques for implementation in developing countries. The reinforcement of URM buildings with steel re-bar can be very specific, with certain guidelines needing to be followed. In an unmonitored environment, these guidelines can often be ignored which can lead to disastrous consequences, as was experienced in Haiti in January of 2010. For those who tried to reinforce their homes with re-bar and grout, it was often done improperly, which rendered the reinforcement incapable of properly supporting a home during a strong earthquake. This highlights the need for an inexpensive and easy to implement URM reinforcement system, which a common person could implement with little training. This study was carried out to develop and test a new reinforcement system that would fulfill these requirements.

A polyurethane foam reinforcement system was developed, which involved the analysis of different polyurethane foams, a study of different foam injection methods, and a study of the capacity of each polyurethane foam to improve the compressive and the critical out-of-plane strength of masonry. As a reinforcement, polyurethane foam has the advantage that it is inexpensive and available world-wide, it can easily be applied to both new construction and retrofit projects, and it is easy to use. This material is also strong, and provides a glue for the URM system to keep it all together, with the system becoming even stronger and more ductile with additional rope reinforcement.

Wallettes were constructed of third-scale block to test the foaming properties of different types of polyurethane foams so as to determine which would be viable products to use in full-scale testing. The effectiveness of each foam was tested under simply-supported monotonic loading.

Compression assemblages reinforced with the selected polyurethane foams were tested so as to determine the increase in strength that the reinforcement would provide to the system. The adhesion effect of the foam to the masonry was also studied. The test results demonstrated that the foam reinforcement was able to significantly increase the compressive capacity of the wall. Of greater significance was the ability of the failed compression assemblages to stay together, with the polyurethane foam acting as glue holding all of the broken pieces of the assemblage together.

Nine full-scale walls were constructed of standard masonry block and were built to represent a one-meter section of a single-storey dwelling. The effectiveness of the developed technique was tested under out-of-plane monotonic loading with a pin-roller system. One of the test walls was an unreinforced control specimen, and another two walls were further reinforced with rope in addition to polyurethane foam.

The test results showed the incredible potential of this reinforcement technique. Significant increase in ultimate capacity, energy dissipation and deformability were achieved compared to the URM specimen. Despite the absence of a post-peak plateau in the load-displacement response (apart from the full rope-reinforced case), the polyurethane foam-reinforced masonry showed the significant capability to absorb large amounts of energy through large deformations, before reaching ultimate failure.

It was concluded that reinforcing masonry walls with polyurethane foam is an effective and inexpensive way to enhance the out-of-plane seismic resistance of URM. Due to its higher strength and deformation and energy dissipation capacity, the system of polyurethane foam with additional rope reinforcement is the highest performing system and should be looked at in more depth.

The implementation of this new type of reinforcing system could have a significant impact on the improvement of seismically vulnerable housing in developing countries. Since this system is inexpensive, easy to use and quick to implement, the implementation of this system could result in a much greater percentage of homes being properly prepared for a future earthquake, which would significantly increase the safety of the occupants if such an event were to occur. As the developed techniques can be implemented anywhere, this technique can be further developed to be integrated into the Canadian building code in the future adoption of performance-based design.

REFERENCES

ATC 1998: Applied Technology Council, “FEMA 306 – Evaluation of Earthquake Damaged Concrete and Masonry Wall Buildings, Basic Procedures Manual,” Redwood City, CA, 1998.

Badoux, M., ElGawady, M., and Lestuzzi, P. “A Review of Conventional Seismic Retrofitting Techniques for URM,” in Proc. 13th IB2 MaC, Amsterdam, Holland, 2004.

Badoux, M., ElGawady, M., and Lestuzzi, P. “Retrofitting of Masonry Walls Using Shotcrete,” in Proc. 2006 NZSEE Conference, Paper 45.

Bhattacharya, S. and Macabuag, J. 2009. “Extending the Collapse Time of Non-Engineered Masonry Buildings Under Seismic Loading,” in Proc. EWB-UK Research Conference 2009, January.

Boen, T. 2001. “Earthquake Resistant Design of Non-Engineered Buildings in Indonesia,” in Proc. EQTAP Workshop IV, Dec 3-4.

Bruneau, M. “State-of-the-art Report on Seismic Performance of Unreinforced Masonry Buildings,” J. Structural Eng (ASCE), v. 120, issue 1, pp. 230-251. (January 1994).

Charleson, A.W. 2009. “Research on Used Car Tyre Strap Reinforced Adobe Construction in Peru,” in Proc. 2009 NZSEE Conference.

Concresive 1210 IUG. BASF: Shakopee MN, June, 2010.

Concresive 1230 IUG. BASF: Shakopee MN, June, 2010.

Concresive 1250 IUG. BASF: Shakopee MN, June, 2010.

Dowling, D.M., " Adobe housing in El Salvador: Earthquake Performance and Seismic Improvement," Natural Hazards in El Salvador, Ed. William Ingersoll Rose, USA: Geological Society of America, Inc., 2004, pp. 281-300.

Dupont. (1998). "Properties of Rigid Urethane Foams," Freon Product Information, BA-13.

Göralmiş, M. and Turer, A. "Scrap tire ring as a low-cost post-tensioning material for masonry strengthening," Materials and Structures. V. 41, pp. 1345-1361. (November 2007).

Guragain, R., Megura, K., Mayorca, P., et al. "Experimental Study on In-Plane and Out-of-Plane Behaviour of Masonry Wallettes Retrofitted by PP-Band Meshes," University of Tokyo, October 2005.

Hamburger, R. O. and Whittaker, A. S. (2011), "The ATC-58 Project: Development of Next Generation Performance-Based Seismic Criteria for Buildings." Retrieved November 10, 2011, from Consortium of Organizations for Strong Motion Observation Systems Website: www.cosmos-eq.org

Ing, Christopher Tyler. Application of Expanding Polyurethane Foam for Upgrading the Seismic Resistance of Unreinforced Masonry Structures. M.A.Sc. University of Western Ontario, London, ON, 2010.

NCFI-24-010. NCFI Polyurethanes: Mount Airy, NC, September, 2010.

NCFI-24-014. NCFI Polyurethanes: Mount Airy, NC, September, 2010.

POLARFOAM PF-6304-0. Polyurethane Foam Systems Inc.: Waterloo, ON, February, 2011.

POLARFOAM PF-6313-0. Polyurethane Foam Systems Inc.: Waterloo, ON, February, 2011.

POLARFOAM PF-6352-0. Polyurethane Foam Systems Inc.: Waterloo, ON, February, 2011.

Redman, T., and Smith, A. 2009. “A Critical Review of Retrofitting Methods for Unreinforced Masonry Structures,” in Proc. EWB-UK Research Conference 2009, January.

Shutov, Fyodor A. “Integral/Structural Polymer Foams: Technology, Properties and Applications.” Germany: Springer-Verlag Heidelberg, 1986.

Thomson, Timothy. “Polyurethanes as Specialty Chemicals: Principles and Applications.” New York: CRC Press, 2005.

APPENDIX A: TESTING SCHEME FOR WALLETTE SPECIMENS

Table A-1: Ratios of Blowing Agent and Accelerant Used in A-2 Mixes

		BLOWING AGENT		
		Small (A) 5% (15mL)	Medium (B) 7.5% (22.5mL)	High (C) 10% (30mL)
ACCELERANT	Small (4) 1% (3mL)	4A	4B	4C
	Medium (5) 5% (15mL)	5A	5B	5C
	High (6) 10% (30mL)	6A	6B	6C











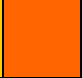
Table A-2: Ratios of Blowing Agent and Accelerant Used in A-3 Mixes

		BLOWING AGENT		
		Small (A) 5% (15mL)	Medium (B) 12% (36mL)	High (C) 20% (60mL)
ACCELERANT	Small (1) 4% (12mL)	- little to no reaction, - flows out of bottom	- liquid when poured in - did not seep through joints - foamed at fast rate	- foamed at very fast rate - foam has airy consistency - did not seep between blocks
	Medium (2) 10% (30mL)	2A	2B	2C
	High (3) 16% (48mL)	3A	3B	3C

APPENDIX B: Full Experimental Results of Full Scale Walls

In this chapter, the results and observations derived from the full scale wall tests that were described in Chapter 5 are presented. The test results are discussed with the assistance of illustrations and graphs, with sets of lateral load versus lateral displacement curves as well as drawn illustrations and photographs of cracking patterns. The illustrations of crack patterns are drawn using the scale shown in Table B-1, which associates a colour with a particular level of mid-height deflection. The modes of failure and the observed crack patterns are discussed, with the main findings and conclusions drawn from this phase of the testing program having already been presented in Chapter 5.

Table B-1: Colour Scheme of Crack Pattern Figures

Colour												
Mid-Height Deflection (mm)	2.5	5	7.5	10	12.5	15	17.5	20	22.5	25	27.5	30

B-1 Polyurethane Foam Reinforced 2.2 m Test Wall

When the B-1 polyurethane foam 2.2m wall was initially loaded it experienced an impact load of 3.5kN. As cracks began to form and the wall started to deflect it was able to sustain this level of loading, as can be seen below in Figure B-0-1. At a deflection of 12.5mm the wall experienced a drastic drop in force capacity from 3.5kN to 2kN as the specimen became fully cracked. Under continued loading, the ratio of the lateral load to the mid-height displacement of the wall became relatively linear. Once the wall had fully cracked and reached its cracking limit, the strength of the masonry was no longer contributing to the walls resistance against the lateral load that is was experiencing. At this point, the foam cores were acting together in tension to resist these forces. This behaviour can be seen by the rise in load capacity of the B-1 foam wall as the wall approached ultimate failure.

Due to the nature of the B-1 foam, which rises and travels through the masonry cores within seconds of initial injection, the foam does not bond well to the sides of the masonry cells as can be seen in Figure B-0-2. This photograph is taken looking down on the top exposed section of the wall prior to testing. It can be seen that the foam core remains relatively separate from the masonry, which may lead to them acting as two separate systems upon testing. This could suggest that the masonry would first fail during testing, while the foam cores may remain intact up to a certain point—which in the case of this test is what seemed to happen.

Another drawback of the foam expanding so quickly upon injection is that it can often miss cells while spreading between different foam cores. After testing, it was discovered that there was a large section of one core that was not filled, which can also be seen in Figure B-0-1. These empty cells happened to pass through the critical failure plane, thereby negatively affecting the masonry-foam systems performance. If this was remedied and all cells were fully filled, one could expect a slightly higher strength performance from the wall specimen.

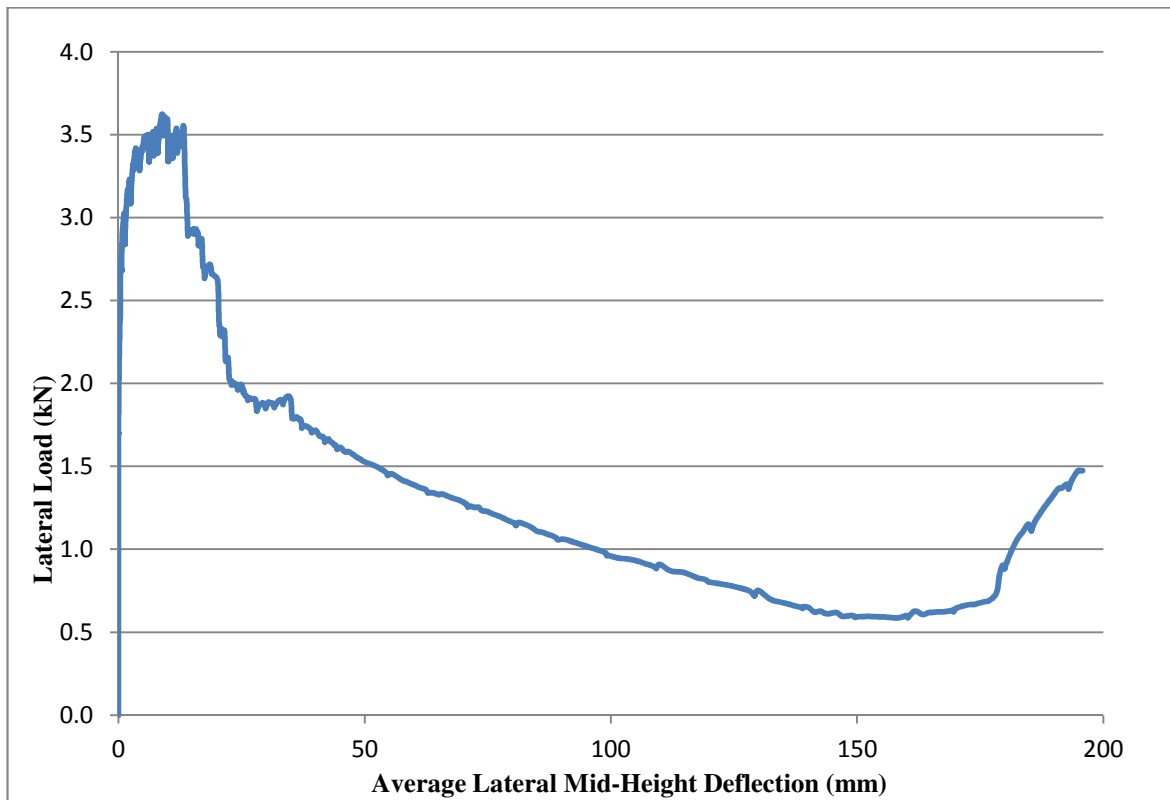


Figure B-0-1: Lateral Load vs. Average Lateral Mid-Height Deflection of B-1 2.2m Wall

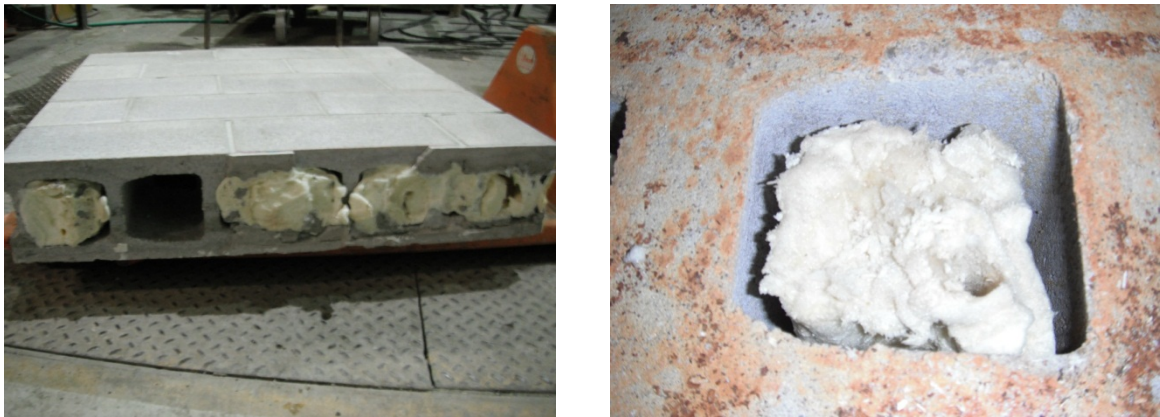


Figure B-0-2: Inside of Failure Plane of B-1 2.2m Wall

As the wall specimen experienced its period of high loading, the complete crack pattern was able to form. Within the first 2.5mm of deflection, the crack pattern shown below in Figure B-0-3 had formed, forming cracks travelling across the entire width of

the wall between the fifth and sixth rows of blocks. As loading continued, this same crack pattern further developed and spread out. Between a deflection of 10mm and 12.5mm an additional crack pattern formed between the sixth and seventh layer of blocks which almost exactly mirrored the initial crack pattern that had first formed at a deflection of 2.5mm. After the formation of this extra row of cracks, the wall lost its strength as both rows of cracks opened up. Upon continued loading, the initial crack pattern governed and gradually opened up as deflection increased. The evolution of this crack pattern can be seen in Figure B-0-4 and Figure B-0-5.



Figure B-0-3: Close-up of Initial Crack Pattern at a Deflection of 2.5mm of B-1 2.2m Wall

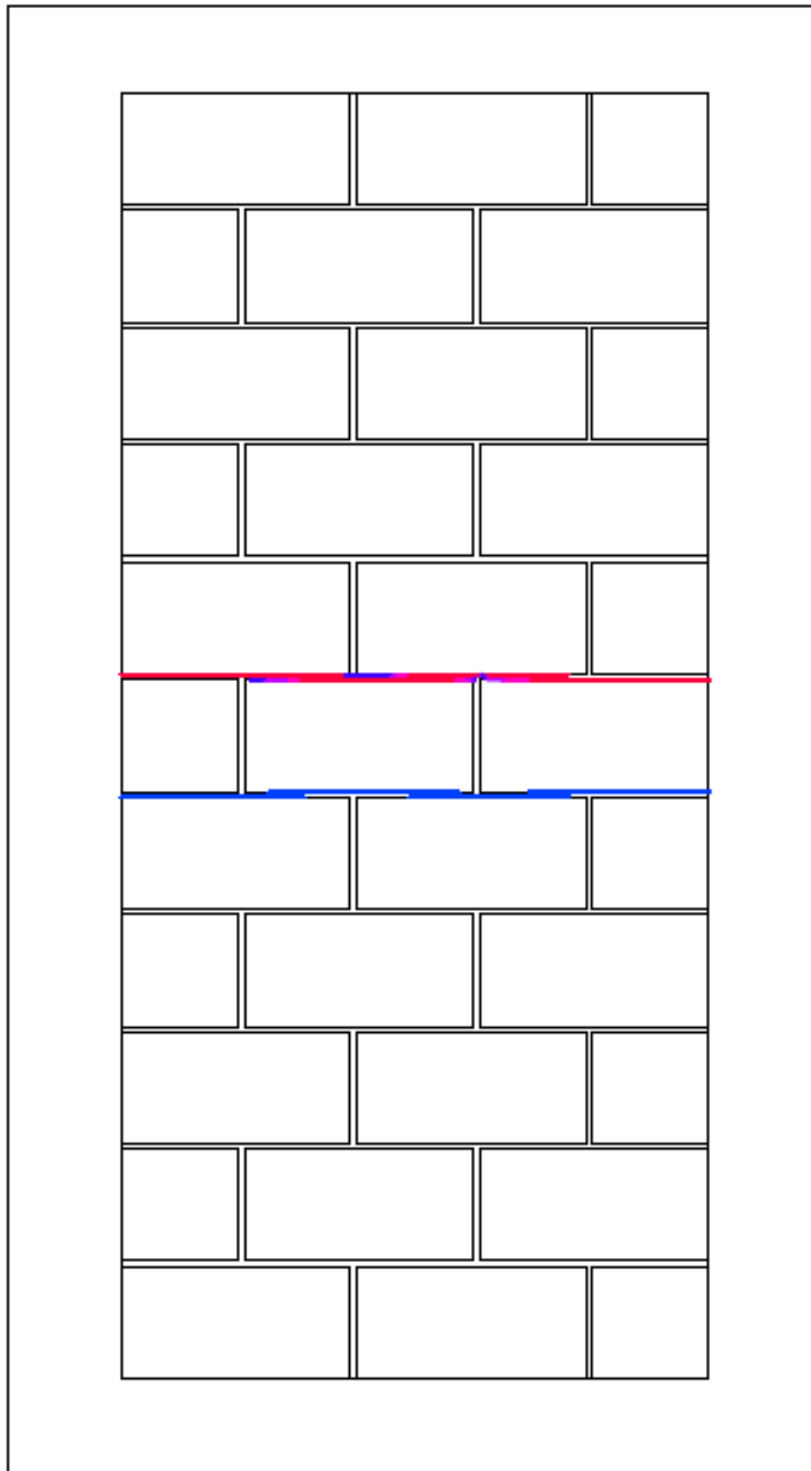


Figure B-0-4: Cracking Pattern of B-1 2.2m Wall

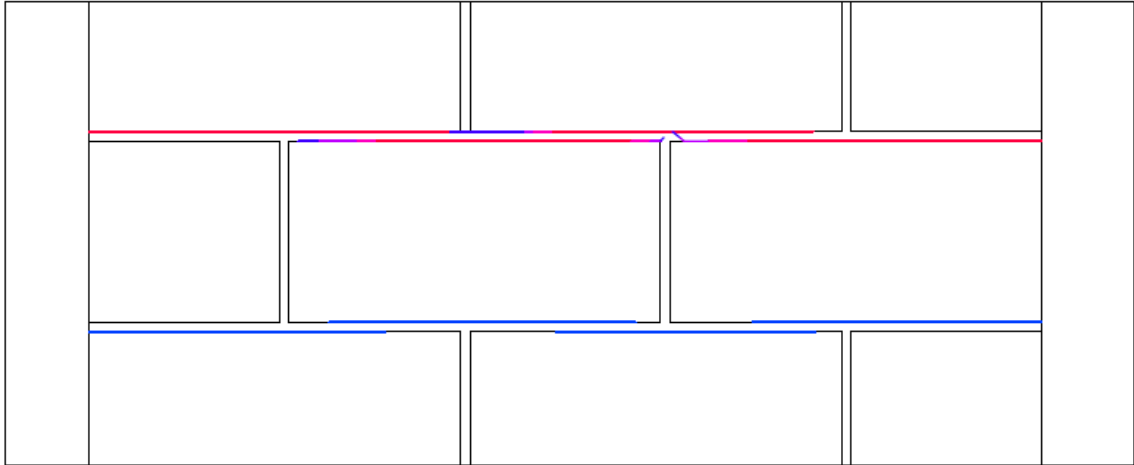


Figure B-0-5: Close-up of Crack Pattern of B-1 2.2m Wall

B-2 Polyurethane Foam Reinforced 2.2 m Test Wall

The B-2 2.2m wall specimen behaved slightly different from any other tested specimen. When the specimen was first loaded, the relationship between the lateral load and the mid-height displacement of the wall increased in a relatively linear pattern until peak loading was reached at a loading of 5.83kN and a mid-height deflection of 27.23mm, as can be seen in Figure B-0-6. At this point in time, the full crack pattern of the system had nearly developed, and as the specimen continued to deflect while gradually losing load capacity, the remainder of the crack pattern developed while the cracks between the fifth and sixth layers, as well as the sixth and seventh layers of blocks opened up.

At a deflection of 50mm, the crack pattern between masonry layers six and seven began together, thereby closing up the crack between the fifth and sixth layers. This point also marks a transition on the load versus displacement graph. Up until a deflection of

50mm, the continued loading/deflection relationship of the specimen after peak loading was reached was almost exactly a mirror image of the load/deflection relationship as the specimen was first loaded. This is significant, as other tested specimens exhibited a much more drastic and immediate drop in load capacity after the formation of the main crack pattern.

After this transition point, the B-2 2.2m wall specimen behaved similarly to the B-1 wall specimen. As the main crack pattern in the wall continued to steadily open up, the wall exhibited a linear decline in strength as deflection increased. Also, as in the case of the B-1 wall, when the masonry was no longer able to carry further loading, the polyurethane foam system took over, allowing the specimen to carry more load up until the point of ultimate failure.

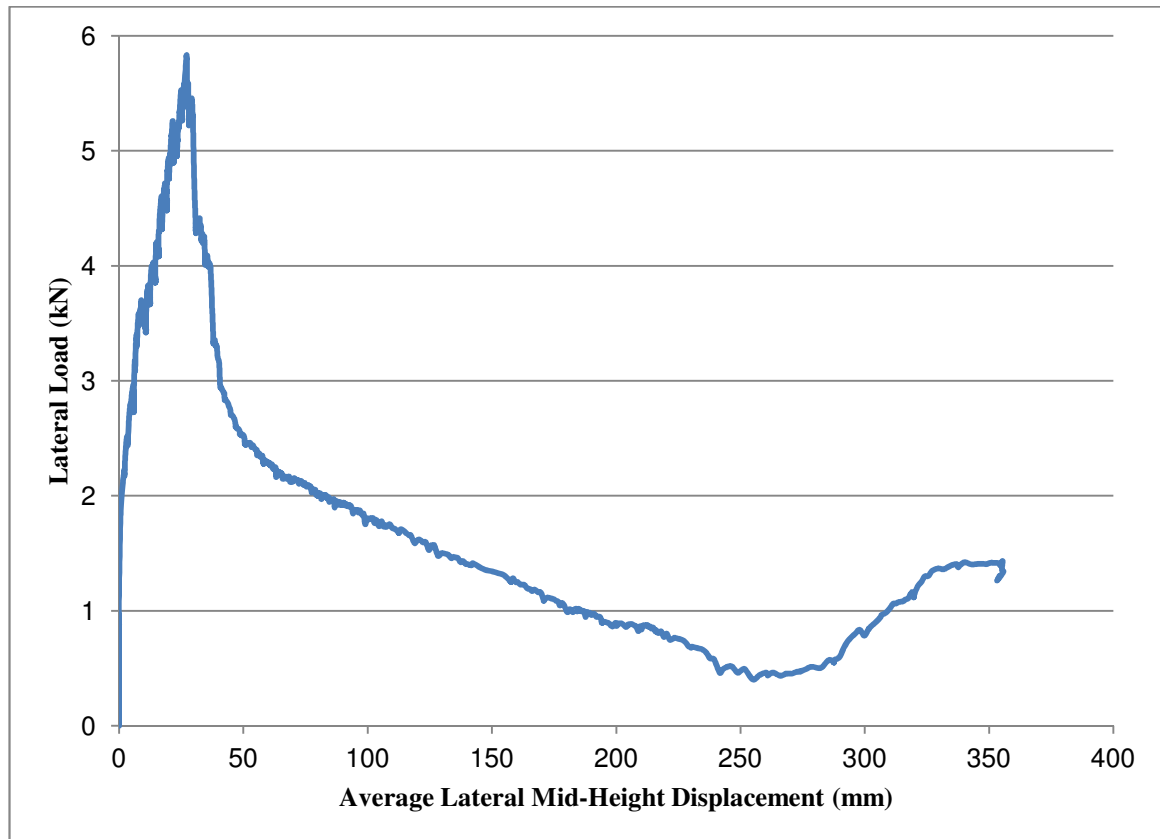


Figure B-0-6: Lateral Load vs. Average Lateral Mid-Height Deflection of B-2 2.2m Wall

After only 5mm of deflection, the wall had developed a crack pattern travelling the full width of the wall between the sixth and seventh row of masonry blocks. The wall did not exhibit any major new cracks until a deflection of 17.5mm was reached. At this time, the original crack pattern spread slightly, and an entirely new row of cracks formed between the fifth and sixth rows of masonry, which can be seen in Figure B-0-7 and Figure B-0-8. As loading continued, these existing crack patterns spread slightly, while new rows of cracks continued to form. At a deflection of 25mm a smaller crack pattern formed along the mortar joint between the fourth and fifth rows of masonry, while at a deflection of 27.5mm, the final row of cracks formed between the seventh and eighth row of blocks. Upon continued loading, the initial two cracks started to slightly widen, with the initial crack between the sixth and seventh row eventually governing and widening as loading and deflection continued.

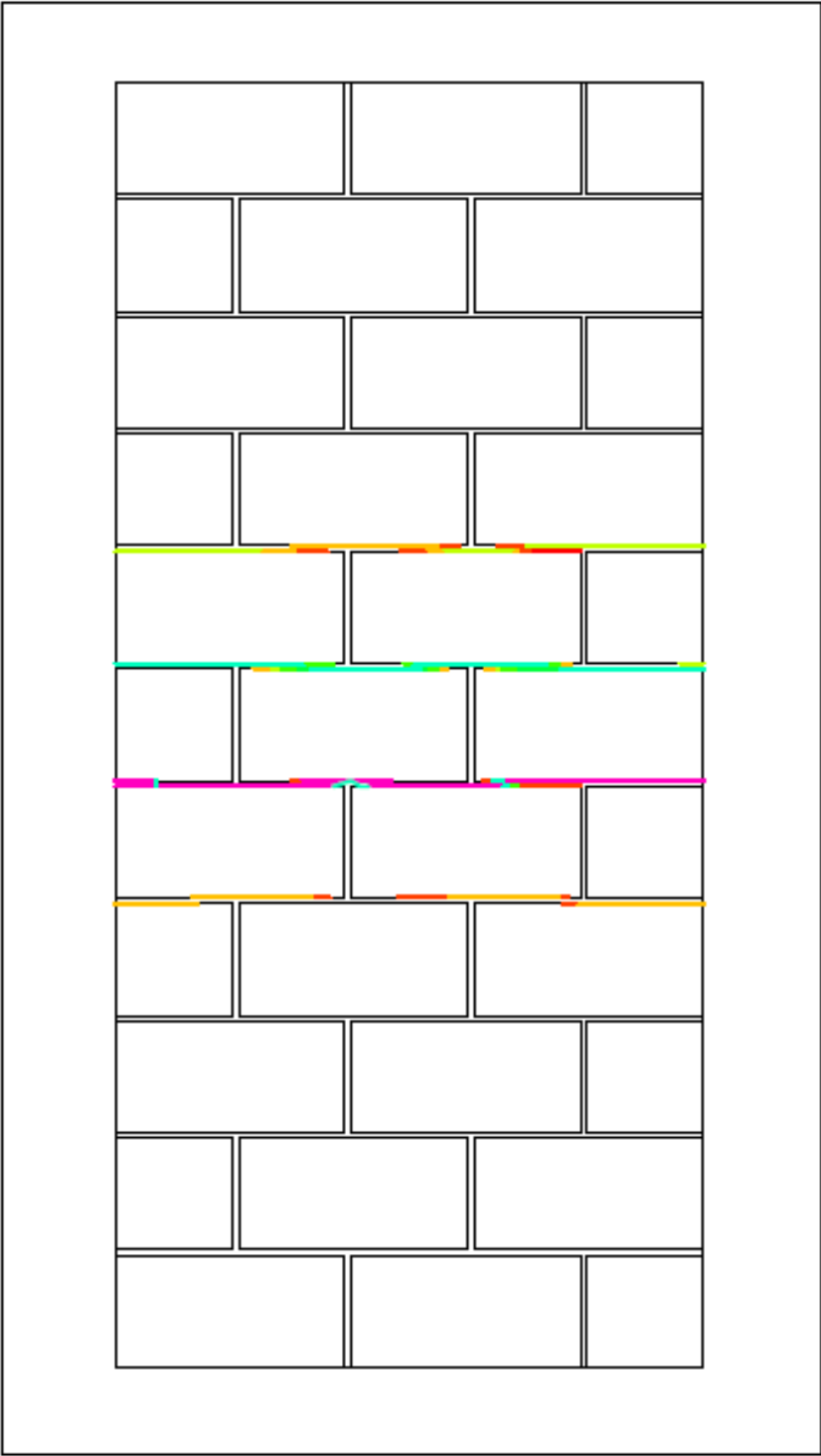


Figure B-0-7: Cracking Pattern of B-2 2.2m Wall



Figure B-0-8: Close-up of Crack Pattern of B-2 2.2m Wall

Unreinforced Test Wall

The lateral load versus lateral deflection relationship of the unreinforced 3m control wall is shown in Figure B-0-9. When load was first applied to the specimen, the wall was able to withstand an increase in load of approximately 0.8 kN before it formed its first crack, which is evidenced by the drastic drop in loading on the wall and the increase in deformation experienced at mid-height. At this point in time, within a 2 second period in time, the load on the wall increased from 1.02kN to 1.65kN and then decreased back to 1.1kN. Likewise, the deflection on the wall increased greatly from 0.2mm to 3.4mm as this first crack formed. This crack continued to propagate until the wall lost all of its load carrying capability after deflecting 6.6mm at mid-height. The unreinforced wall specimen was only able to dissipate 7840 Nmm of energy before reaching ultimate failure, showing how weak this type of building system is.

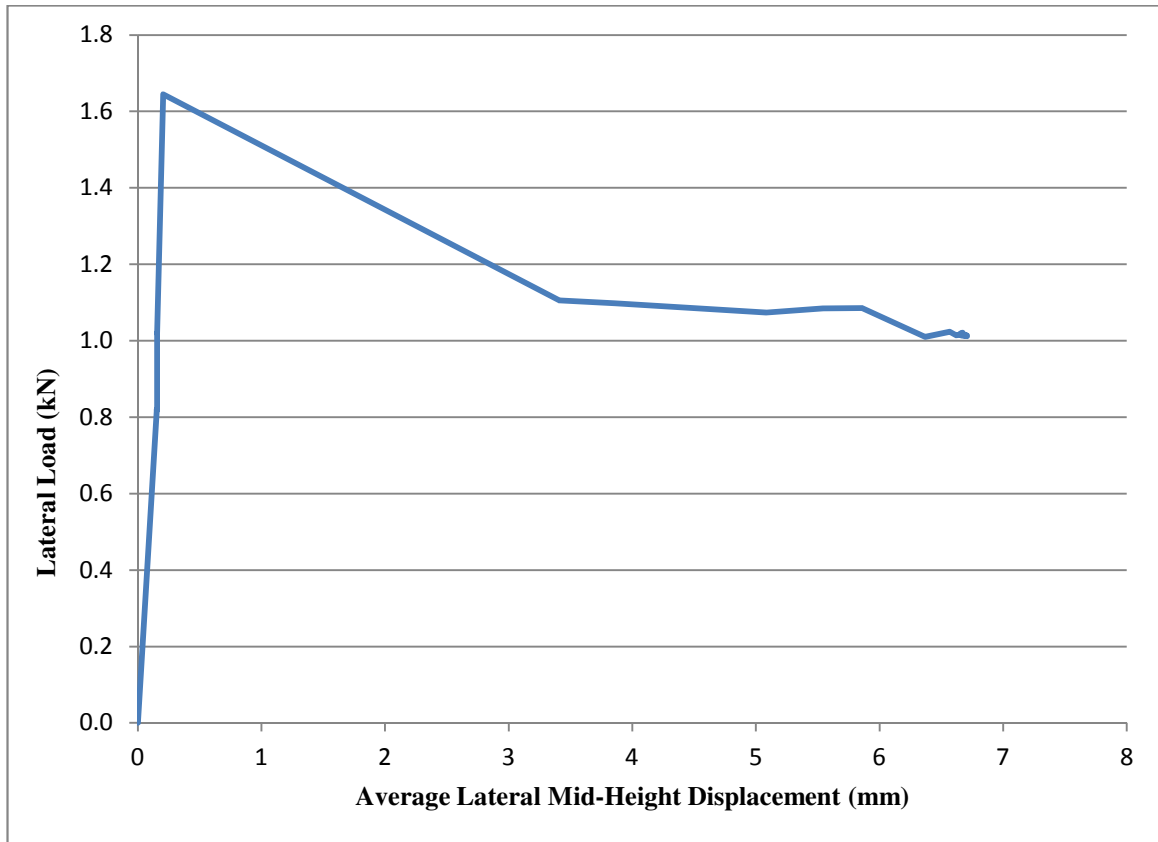


Figure B-0-9: Lateral Load vs. Average Mid-Height Displacement Curve for the Unreinforced Control Wall

The crack pattern shown below in the photograph in Figure B-0-10 was the first crack in the wall and the formation of this crack can be seen graphically in the first peak of the load-displacement curve above. Following the formation of this crack, no new cracks formed. Instead, this one crack simply widened, leading to the collapse of the wall. The crack occurred between the seventh and the eighth row of blocks which is within the expected cracking region of the middle third of the wall, and is in fact as close to the middle of the wall as possible. The crack pattern can also be seen in Figure B-0-11 and Figure B-0-12.



Figure B-0-10: Cracking Pattern of Unreinforced 3 m Control Wall

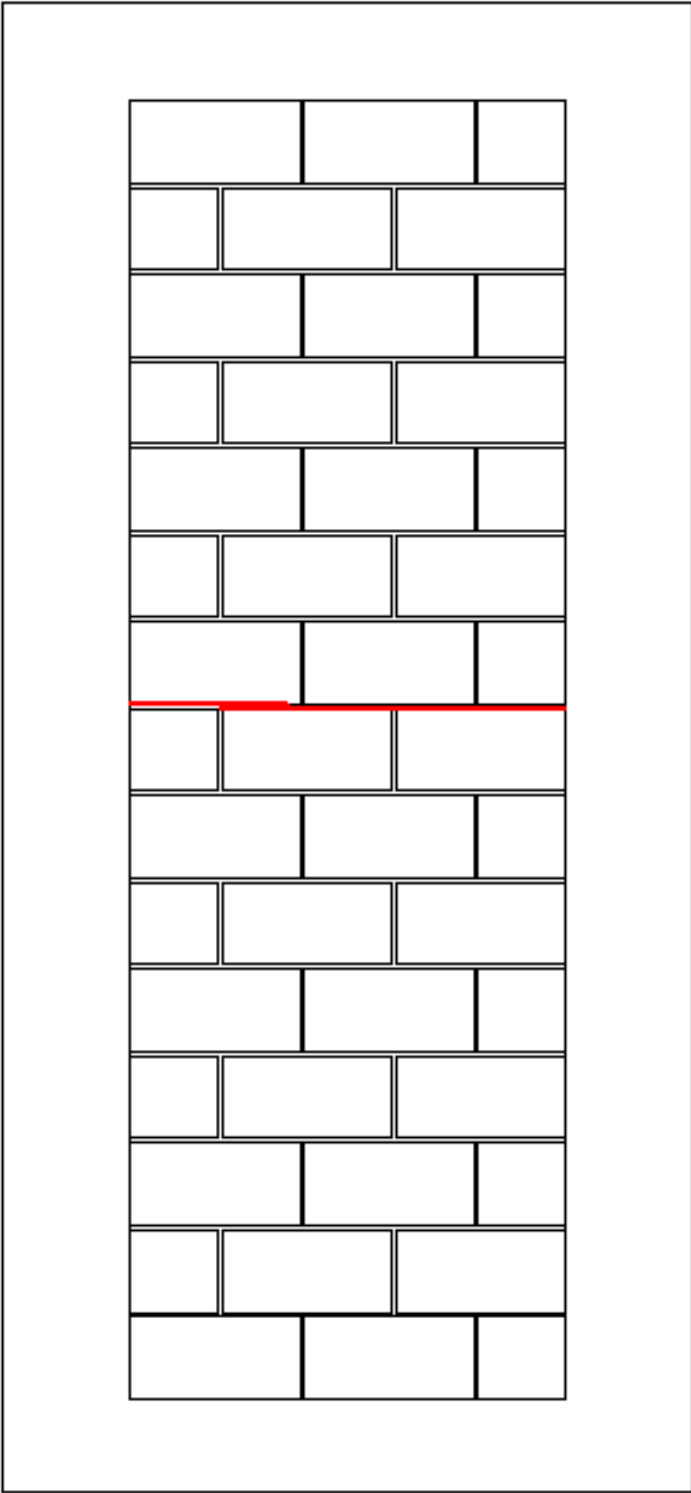


Figure B-0-11: Cracking Pattern of Unreinforced 3m Control Wall

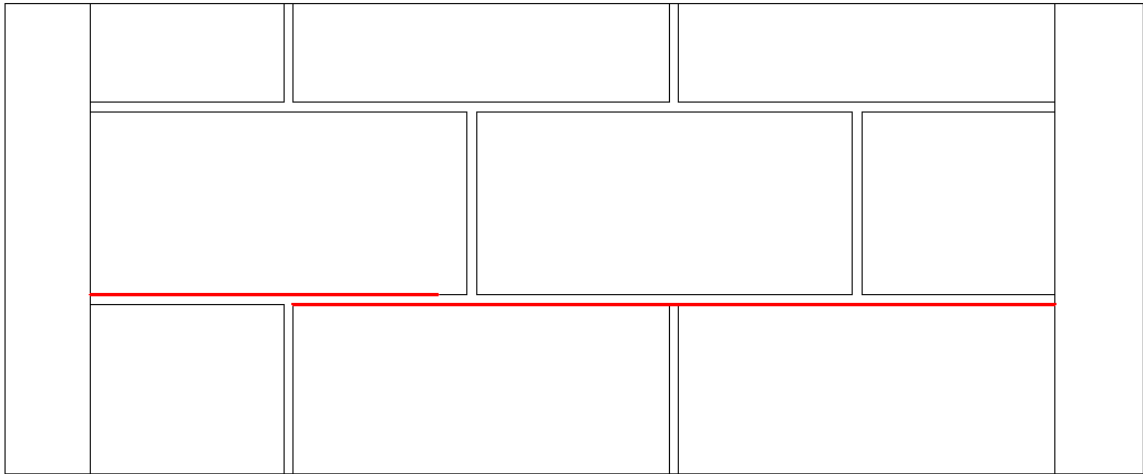


Figure B-0-12: Close-up of Crack Pattern of Unreinforced 3m Control Wall

B-2 Polyurethane Foam Reinforced 3m Test Wall

The B-2 3m wall exhibited slightly different behaviour than the 2.2m specimen. In the 2.2m specimen, the wall experienced a linear relationship between load and deflection as the wall was first loaded—showing that the wall experienced greater deflections at the application of lower loads. However, the 3m specimen was able to sustain a higher loading before this same level of deflection occurred. As can be seen below in Figure B-0-13, the wall is able to carry a load of 4.5kN which causes the wall to deflect only 5.5mm at mid-height. The 2.2m wall had reached a deflection of 16.5mm at this same loading.

The B-2 3m wall displayed behaviour more similar to the other 3m walls that were tested, by experiencing a high level of initial loading as the crack pattern developed, followed by a sudden loss in strength as the crack started to open up. This wall was able to carry a load of 5.75kN before it lost strength at a deflection of 28mm. However, as much as the two B-2 walls of different heights had different load/deflection patterns up to peak loading, they both lost strength at almost the same loading and deflection, with the 2.2m wall losing its strength at a loading of 5.83kN at a deflection of 27.23mm.

After the large drop in loading, the 3m B-2 wall again exhibited similar behaviour to the other 3m foam-reinforced walls. Over time, as the crack pattern opened up and mid-height wall deflection increased, the wall exhibited a gradual loss in strength until ultimate failure was reached.

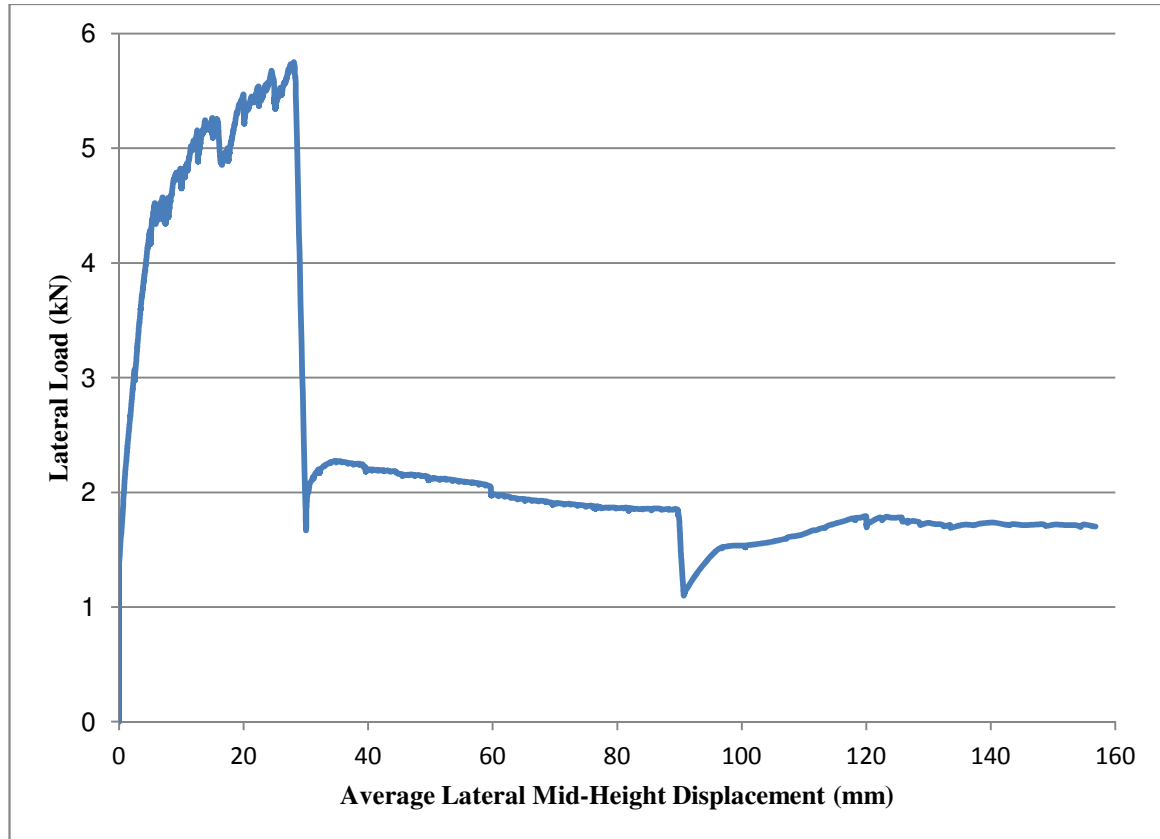


Figure B-0-13: Lateral Load vs. Average Lateral Mid-Height Deflection of B-2 3m Wall

Upon first loading the specimen and only after 2.5mm deflection, an extensive crack started to form between the tenth and the eleventh row of masonry blocks, as can be seen below in Figure B-0-14 and Figure B-0-15. At a deflection of 7.5mm another crack pattern developed between the sixth and seventh row of blocks while the initial crack continued to propagate and slightly widen. Between 7.5mm and 15mm of wall deflection, the existing cracks continued to open and no new crack patterns formed. However, at a deflection of 17.5mm and 20mm, cracks formed between the seventh and eighth row of

blocks and the eighth and ninth rows of masonry respectively. Over the entire course of loading, the crack that had first formed between the tenth and eleventh row of blocks had continued to open up, and after the specimen developed its full crack pattern, this crack governed until the ultimate failure of the wall specimen.

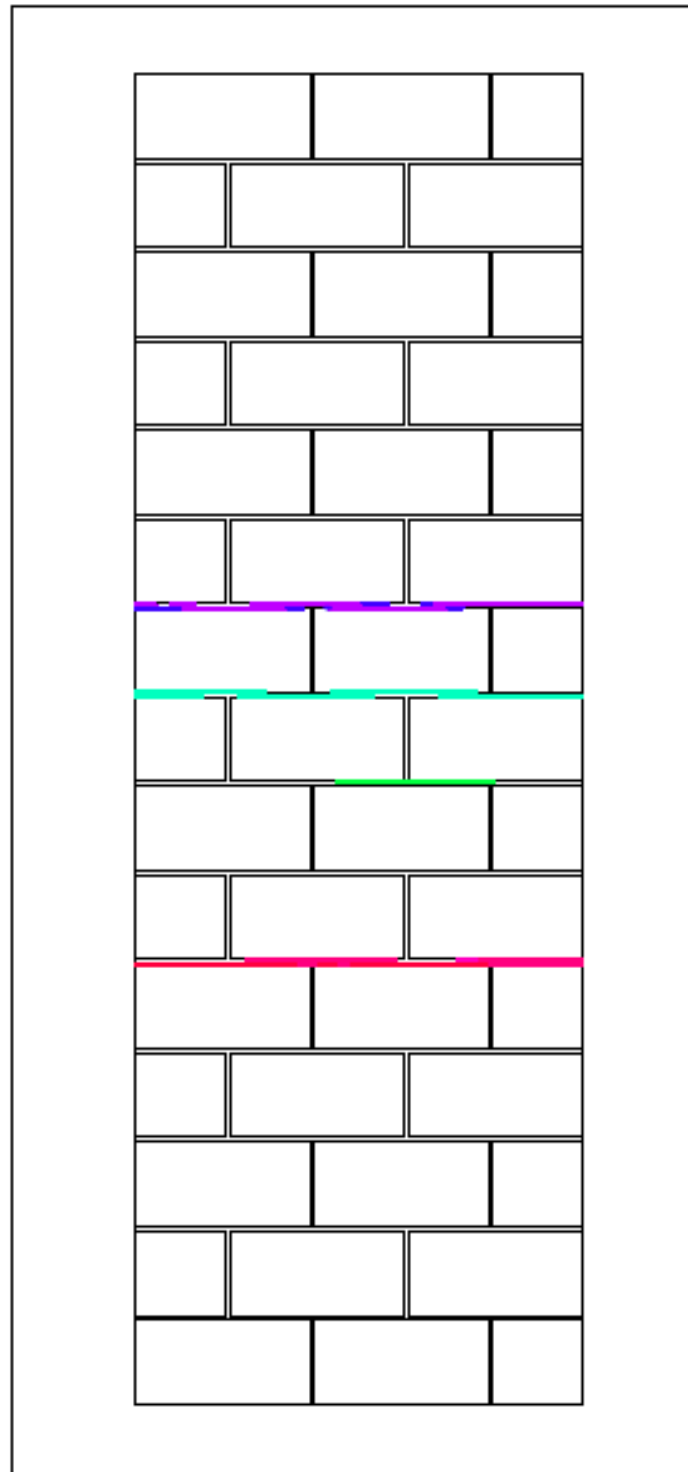


Figure B-0-14: Cracking Pattern of B-2 3m Wall
123

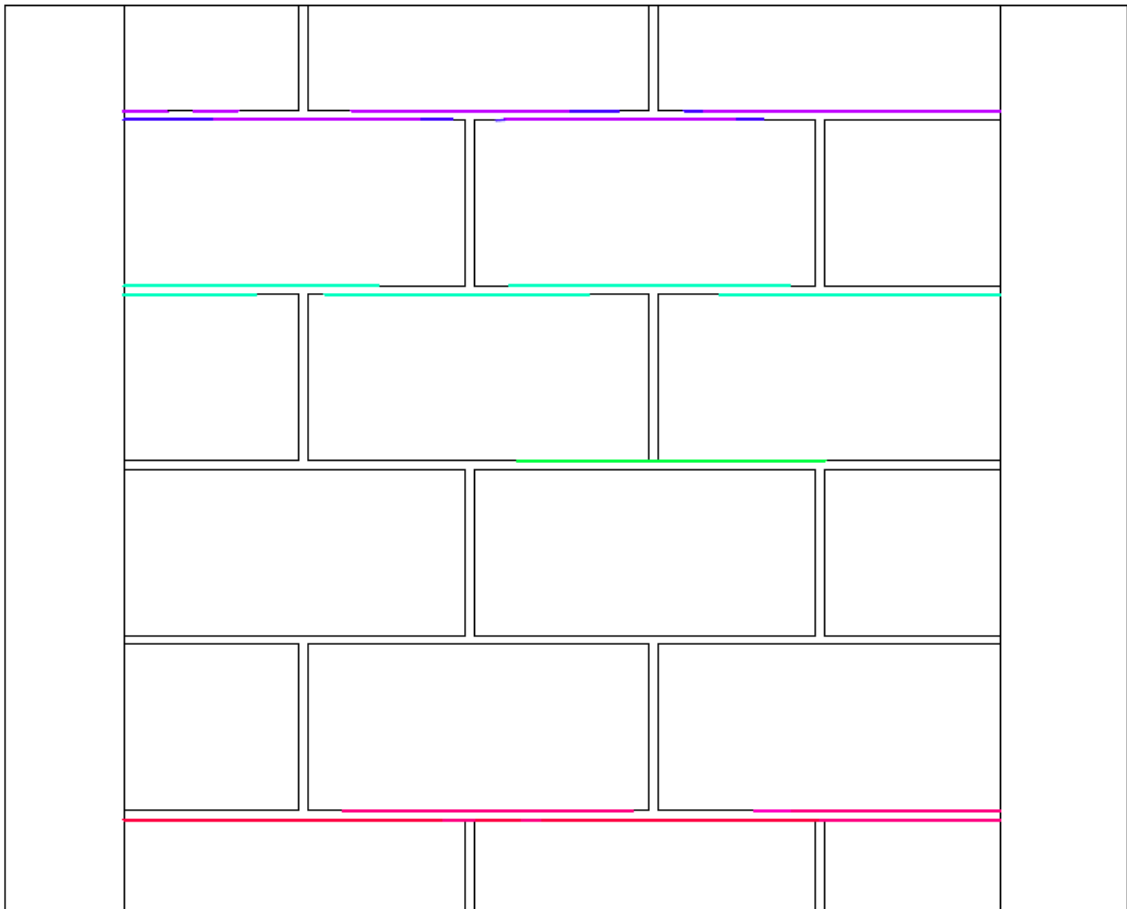


Figure B-0-15: Close-up of Crack Pattern of B-2 3m Wall

C-1 Low Density Polyurethane Foam Reinforced 3 m Test Wall

The low density 3m Kepler wall was able to take a 5kN force and deflect 16mm before the first visible crack was formed. The formation of this crack led to a drastic decrease in force on the wall down to only a 2kN load as can be seen in Figure B-0-16. This was followed by a gradual small increase in force to a high of 2.3kN as the foam cores carried the load. Over this period of time, further cracks did develop, however the increase in load carrying capacity within the foam was able to counteract what would have been further losses in strength. Once the wall was fully cracked, the wall gradually

lost strength in a somewhat linear fashion as these cracks widened and reached ultimate failure at a deflection of 130mm.

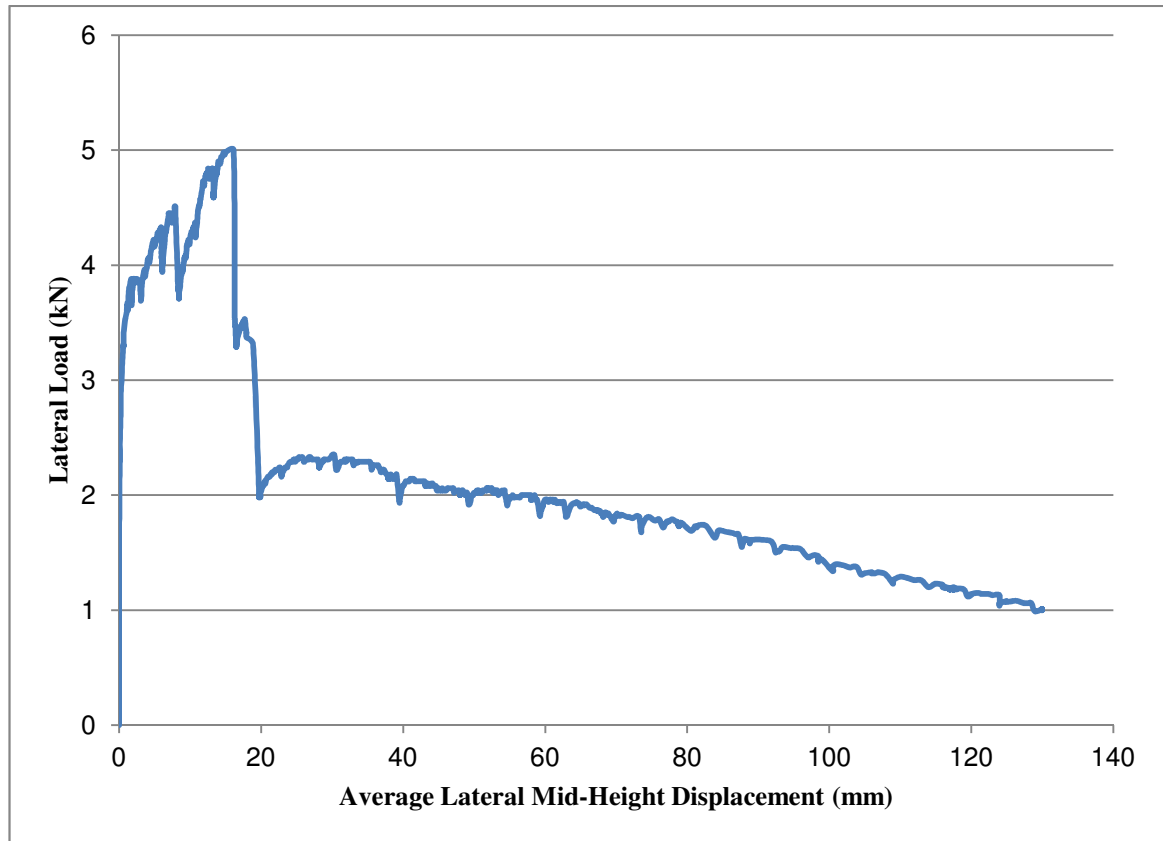


Figure B-0-16: Lateral Load vs. Average Lateral Mid-Height Displacement for C-1 3m Wall

The cracks shown along the mortar joints at the top and bottom of the seventh row of blocks from the top were the first cracks to be formed, at a deflection of 16mm. Along this top mortar joint the mortar bed had been previously weakened by the drilling of holes into each cell which had been used to inject the polyurethane foam. As these first cracks formed in a pattern which connected these holes to each other along the width of the wall, it may suggest that the existence of these holes inherently weakened the strength of the wall. To avoid this weakened mortar bed, a future suggestion could be to drill foam injection holes directly into the masonry face shells and not into the mortar bed.

Following this large initial crack formation, at a deflection of 20mm, cracking occurred between the eighth and ninth row of blocks. Under continued loading, this crack continued to propagate and widen. As the bottom row of cracks widened, the previous cracking pattern above and below the seventh row of blocks closed up. The evolution of this crack pattern can be seen below in Figure B-0-17 and Figure B-0-18. These cracks occurred within the center third of the wall, which was expected due to the test conditions.

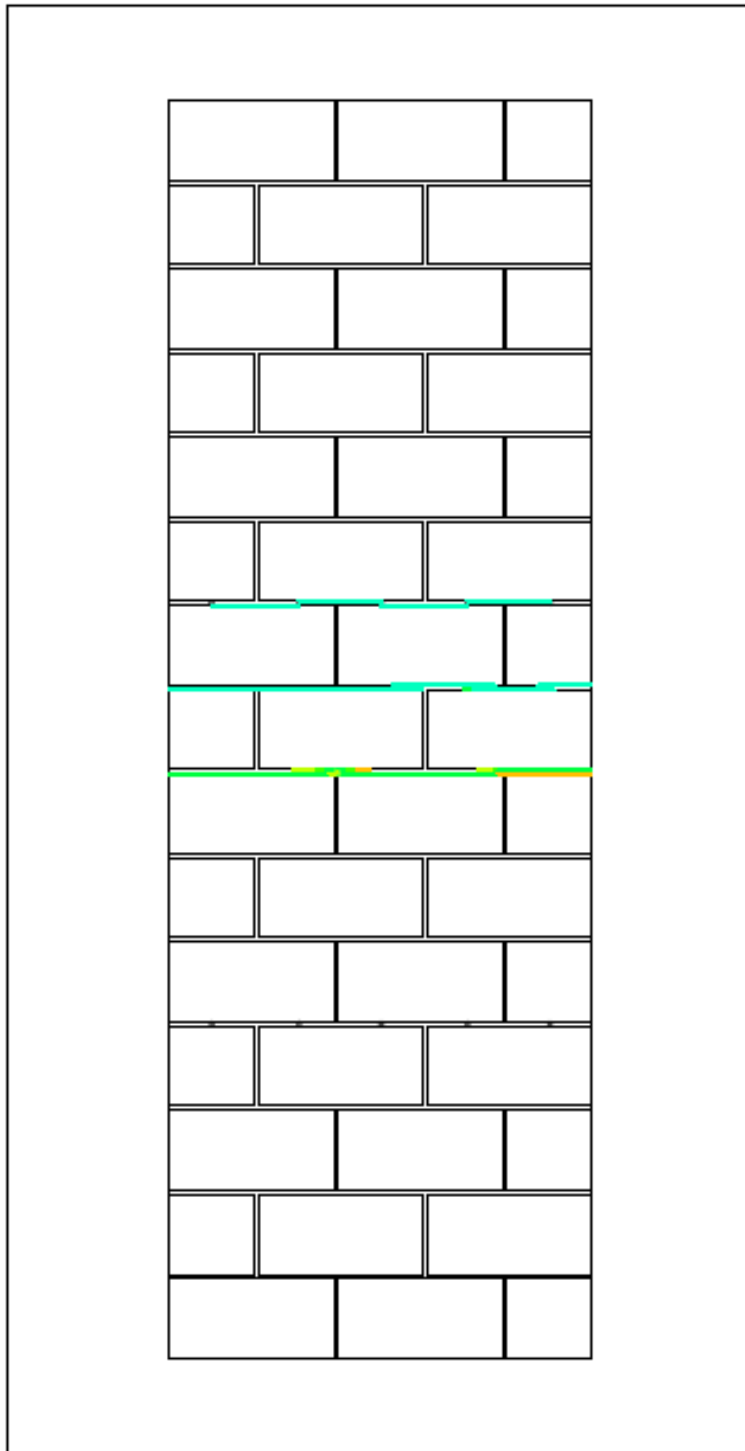


Figure B-0-17: Cracking Pattern C-1 3m Wall

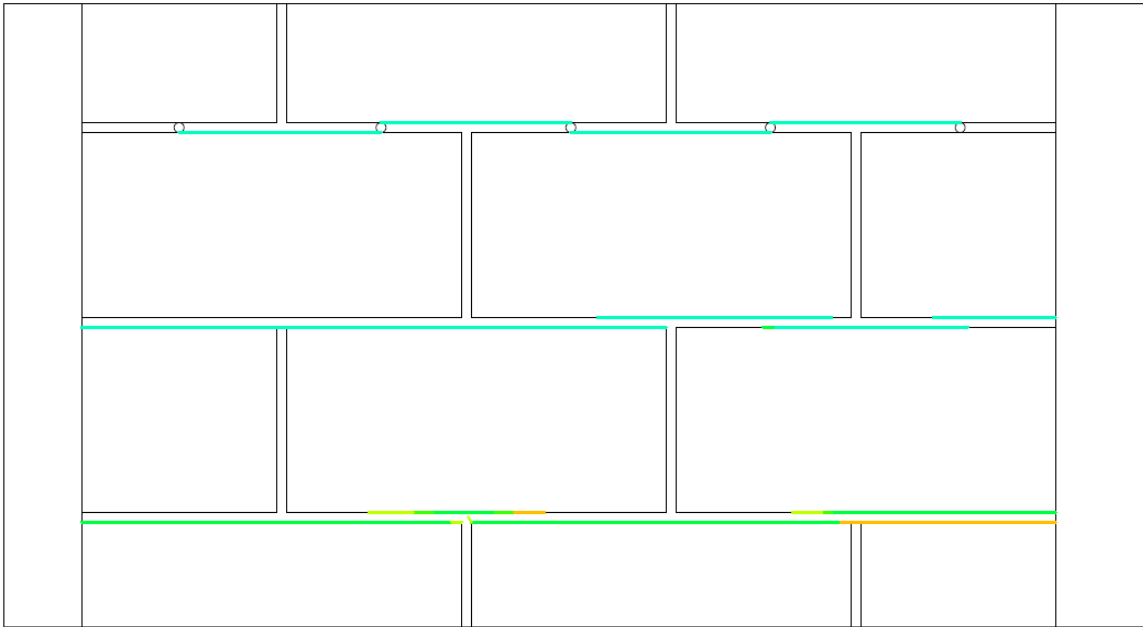


Figure B-0-18: Close-up of Crack Pattern of C-1 3m Wall

C-2 Medium Density Polyurethane Foam Reinforced 3 m Test Wall

The medium density polyurethane foam reinforced 3m C-2 test wall exhibited similar behaviour to the low density C-1 wall. In the lateral load versus average lateral mid-height deflection diagram shown in Figure B-0-19, it can be seen that the wall was able to withstand a lateral force of 5.5 kN before it experienced the same drop in force as a result of cracking. Upon continued loading, the wall lost strength gradually, in a somewhat linear fashion. However, what was different from the previous tests was that the medium density specimen was able to withstand a greater amount of force than its low density counterpart. This was expected, as denser foam should be stronger.

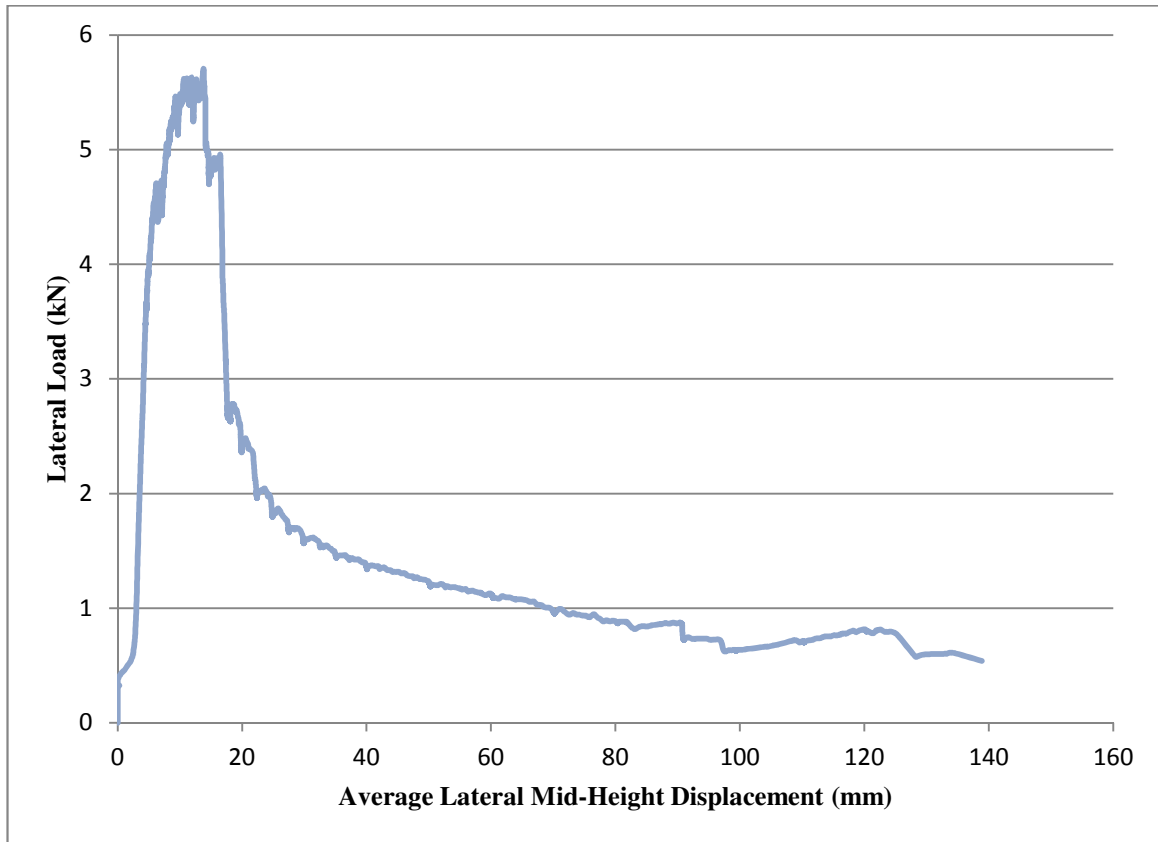


Figure B-0-19: Lateral Load vs. Average Lateral Mid-Height Displacement of C-2 3m Wall

The crack pattern and how it developed was significantly different from the previous low density test. At the time of testing, pre-existing cracks were noticed in the top left corner of the wall. These cracks did not widen or lengthen during testing, and were incurred during the process of moving the walls into place. New cracks started to develop at a deflection of less than 7.5mm. The effects of the development of these cracks can be seen in the left section of the load-displacement graph where there is a brief drop in load on the upward curve at a deflection of approximately 6mm and 4.6kN. This first crack developed between the fifth and sixth row of blocks, whose location can be seen more closely in Figure B-0-20 through Figure B-0-22. This main crack location happens to be directly at the point of application of the top section of the loading beam. Due to this crack location, it lies on the very edge boundary of where a crack would be

expected to occur. As the crack occurred so high within this range, it would be expected that this wall behaved at the lower end of its capacity. If the crack would have formed at mid-height as was the case for the low density wall, it could be expected that a greater deflection could have been reached at the point when the wall reduced its loading.

The wall was able to sustain further loading as the crack continued to form along the length of the wall. At a deflection of 15mm the wall was almost fully cracked, and the loss in strength at this point in time can be clearly seen in the lateral load versus lateral displacement graph at this location. Between the displacement of 15mm and 17.5mm the wall cracking became very loud as the mortar split apart, and the crack widened significantly. After this point, under continued loading no new cracks were formed, with the previous crack pattern simply widening over time until the wall reached ultimate failure.



Figure B-0-20: Cracking Pattern of Medium Density C-2 3m Wall

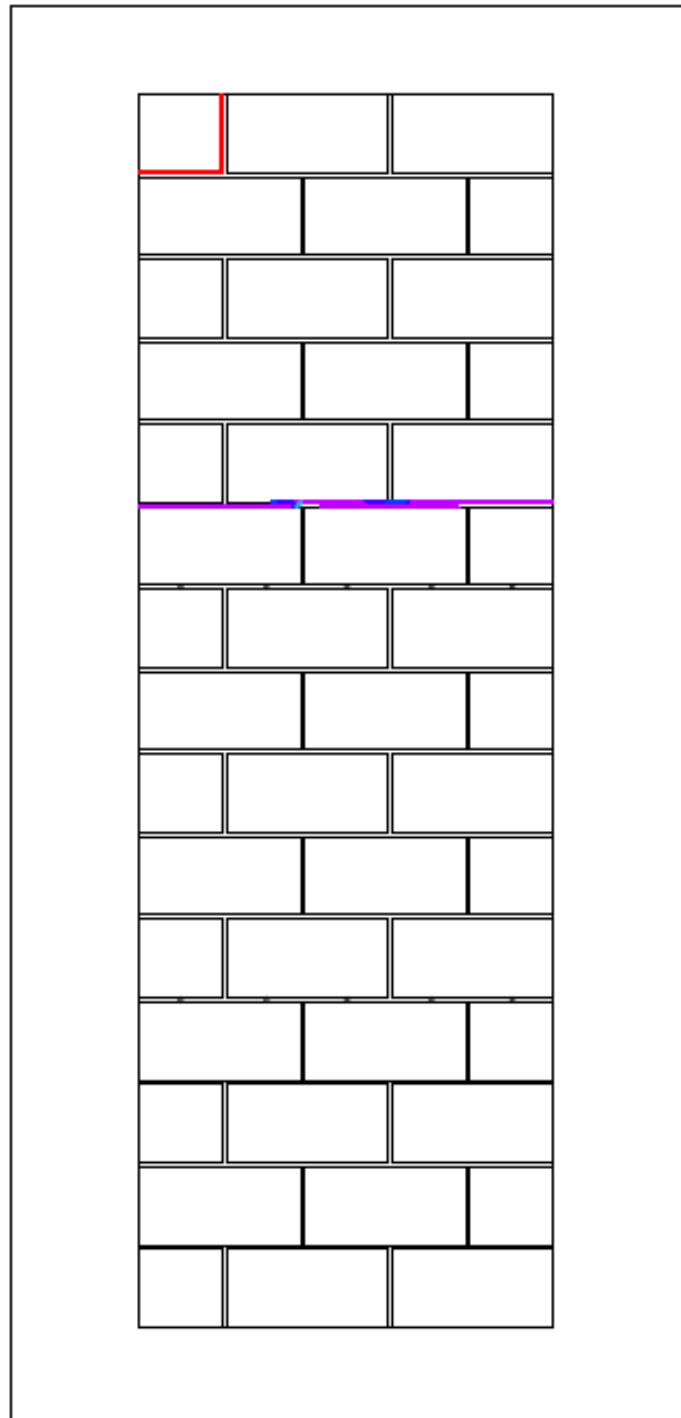


Figure B-0-21: Cracking Pattern of Medium Density C-2 3m Wall

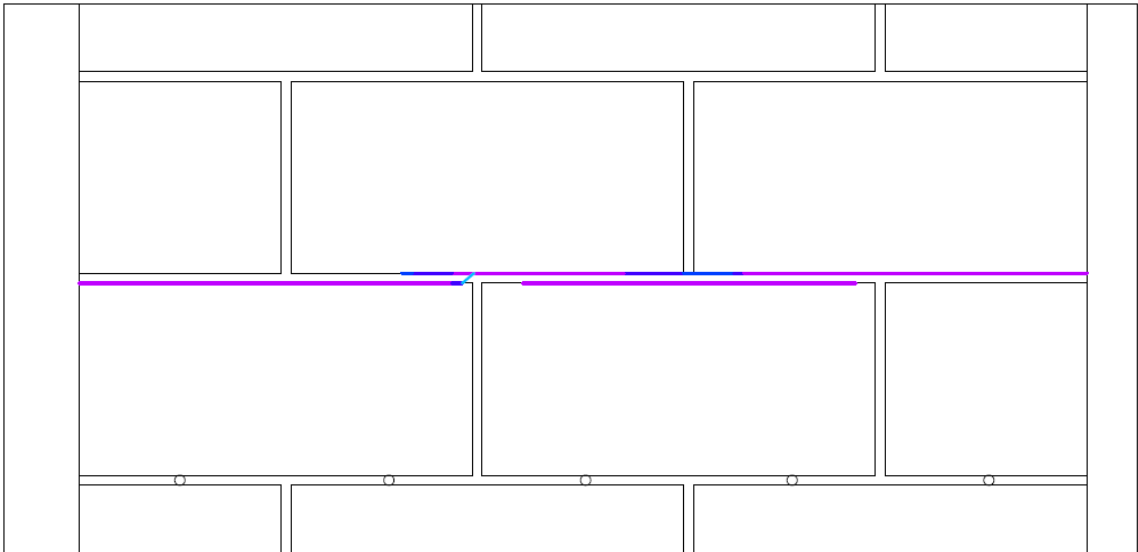


Figure B-0-22: Close-up of Crack Pattern of Medium Density C-2 3m Wall

C-3 High Density Polyurethane Foam Reinforced 3 m Test Wall

The high density polyurethane foam reinforced 3m C-3 test wall exhibited similar behaviour to the other two Company C walls. As can be seen in the diagram in Figure B-0-23, the high density wall fully cracked and widened between 15mm and 17.5mm, which demonstrates the same behaviour as the previous two walls. However, as the foam was of a higher density and therefore stronger, the wall was able to withstand forces of up to 6.5kN. Upon continued loading, the main crack in the wall gradually continued to widen as the force on the wall slowly decreased.

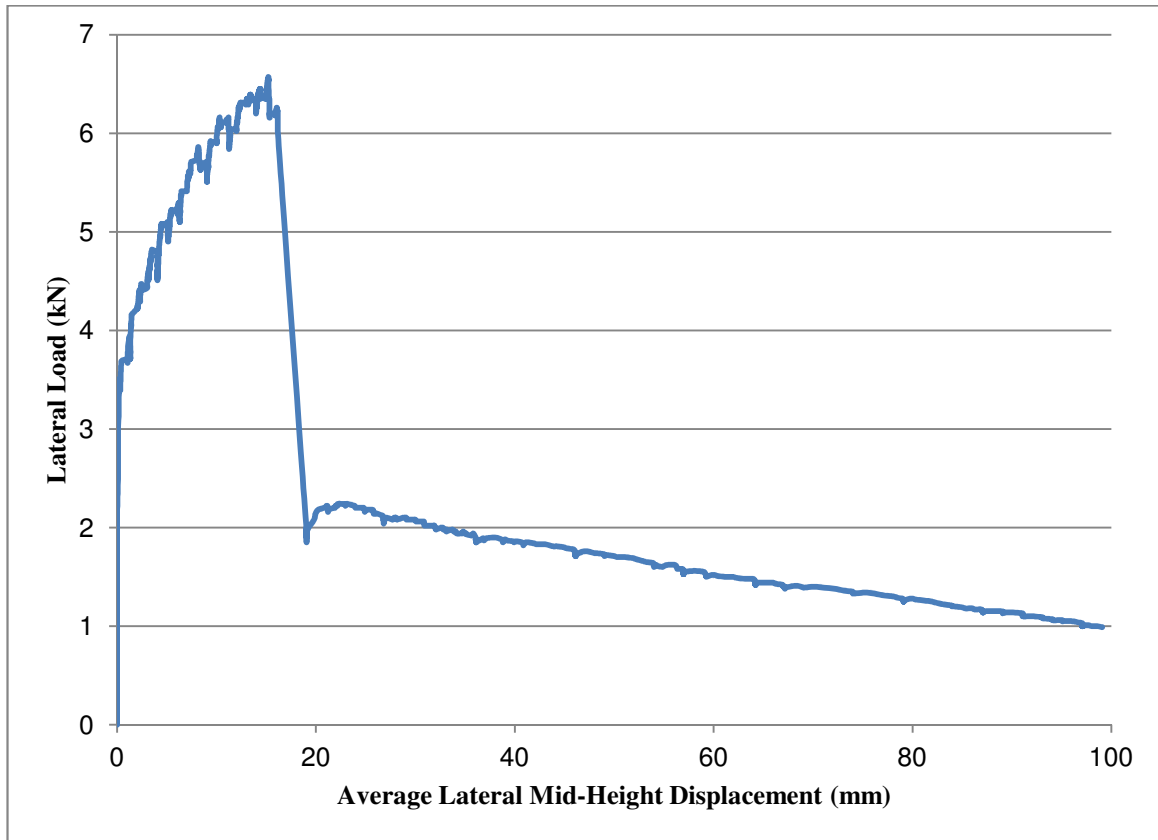


Figure B-0-23: Lateral Load vs. Average Lateral Mid-Height Deflection of C-3 3m Wall

The first cracks in the high density C-3 3m wall occurred between the sixth and seventh rows of blocks after a deflection of only 2.5mm. They first formed in a similar manner to the first cracks in the low density wall, with cracks going between the different holes drilled in the masonry mortar for the polyurethane foam injection. After a mid-height deflection of 5mm, this crack along the drilled holes in the masonry fully cracked along the full width of the specimen. In addition, a further line of cracks developed between the seventh and the eighth row of blocks. As loading continued, these cracks further developed and after a deflection of 10mm further rows of cracks had developed between the eighth and the ninth row of blocks as well as between the tenth and the eleventh row of masonry. These new cracks propagated further over time, until after a deflection of 15mm, the original crack between the sixth and seventh row of masonry

blocks started to govern and gradually open up. At a deflection of 17.5mm this governing crack suddenly widened as can be seen below in Figure B-0-24, increasing the mid-height deflection of the wall by a jump of 3mm. At this point in time, the high density wall experienced a similar linear decline in strength and increase in deflection under continued loading. The development of this crack pattern can be seen in Figure B-0-25 and Figure B-0-26.



Figure B-0-24: Sudden Widening of Main Crack in High Density C-3 3m Wall

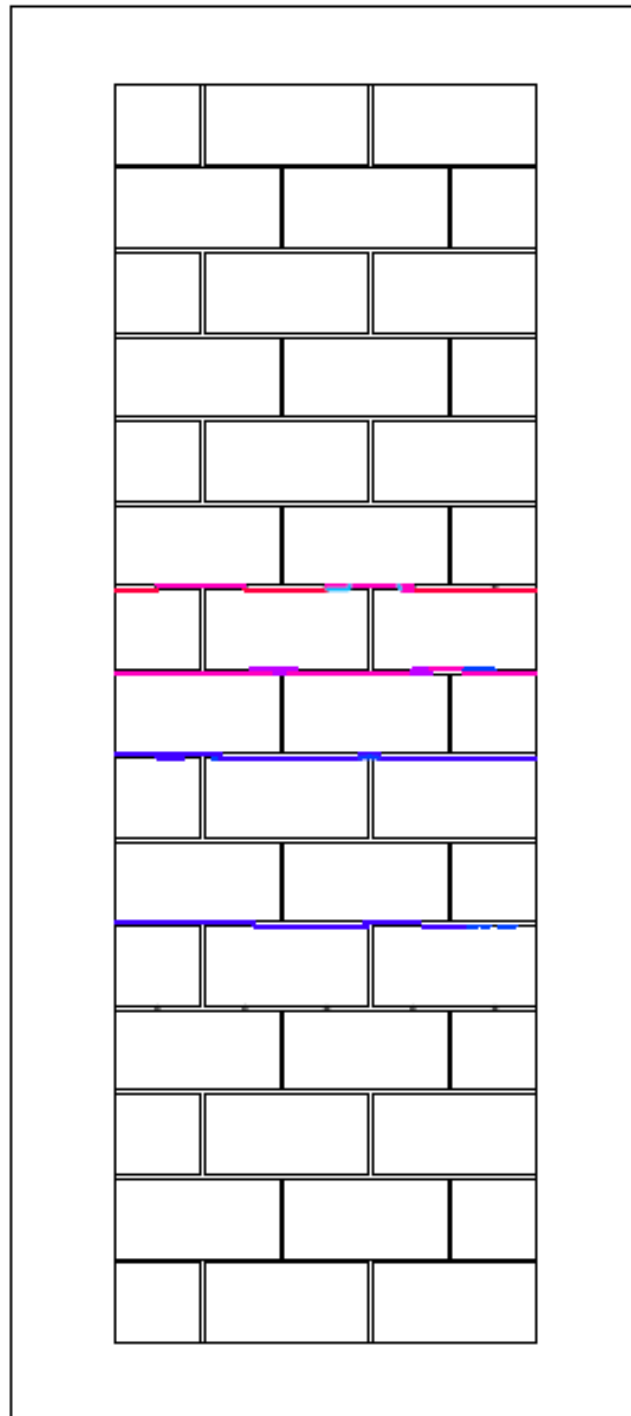


Figure B-0-25: Crack Pattern of C-3 3m Wall

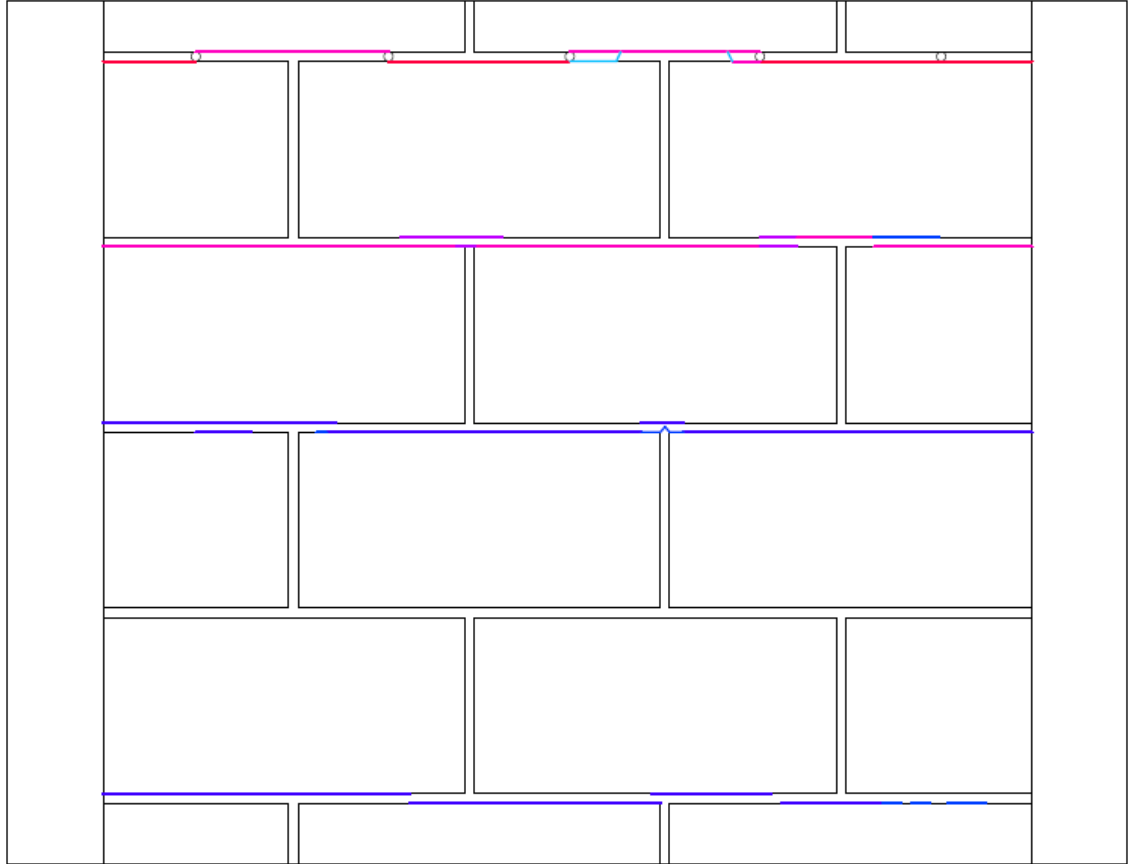


Figure B-0-26: Close-up of Crack Pattern of C-3 3m Wall

B-2 Polyurethane Foam and Rope I Reinforcement—Three Roped Cells

The B-2 wall that contained three cells of rope I reinforcement performed similarly to the B-2 wall without the extra rope reinforcement, except that the rope-reinforced wall was able to carry significantly higher loads for a longer period of time. The half-roped specimen was also able to sustain a higher level of loading after initial failure and reached ultimate failure at a significantly greater amount of deflection.

When the wall was first loaded, it was able to carry a load of 4.0kN before any deflection occurred at mid-height. As cracks began to form after this point, the deflection

in the system gradually increased as the load on the system increased, until the wall reached a maximum loading of 7.05kN at a deflection of 39.15mm as can be seen in Figure B-0-27. At this point, the load on the wall dropped to around 3.25kN and gradually diminished as continued force was applied to the wall. As the foam and rope reinforcement were carrying the majority of the load at this point, the system was able to experience very large deflections before it reached ultimate failure with the complete failure of the masonry block.

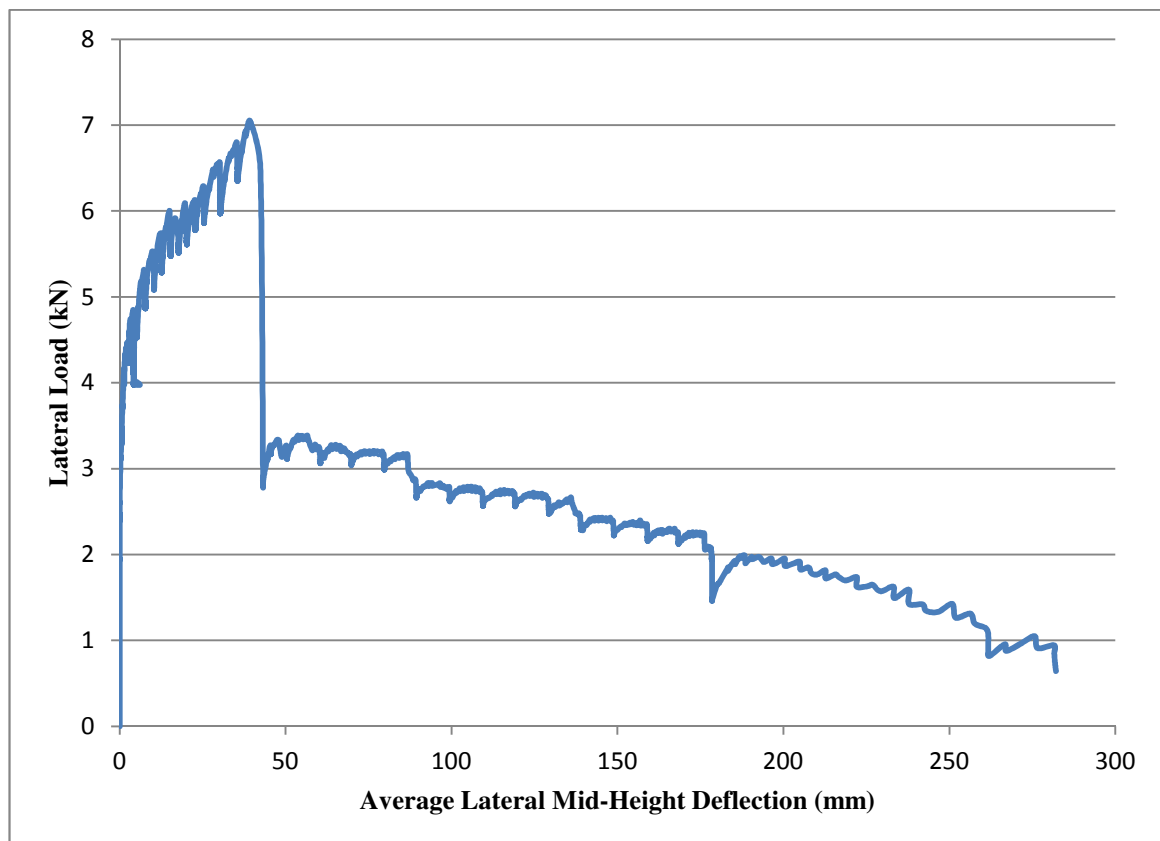


Figure B-0-27: Lateral Load vs. Average Lateral Mid-Height Deflection of B-2 3m Wall with Three Roped Cells

Prior to the start of testing, the wall had already experienced a significant amount of cracking while it was being filled with B-2 polyurethane foam. During foam injection, an appropriate amount of foam was injected into the left-most cell so as to fill it from mid-height and upwards to the top. However, as the foam was expanding upwards, it hit

a blockage which was most probably caused by excessive mortar inside the cell. This blockage caused the foam to no longer travel upwards filling the core, but instead to find other areas to fill, finding any open path it could. However, as there was an abundance of material confined in such a small area, the material had nowhere to expand but outwards, exiting through the masonry joints and cracking many of the mortar/block connections, as can be seen in Figure B-0-28. This large amount of pre-existing cracks between the third and seventh layer of blocks made the top section of the wall weaker, and more susceptible to further cracking during testing.



Figure B-0-28: Pre-mature Failure of B-2 Wall With Three Roped Cells Due to Expansive Force of the Foam

When the wall was first loaded during testing, the first new crack to form covered the full width of the wall between the seventh and eighth row of masonry and occurred at a deflection of only 2.5mm. As loading continued, new cracks extended from the damaged blocks. At a deflection of 5mm, cracks developed between the sixth and seventh row of blocks, continuing the cracking pattern that was already there in addition

to extending the length of the cracks in the new crack pattern between row seven and eight. At a deflection of 7.5mm this crack continuation from the damaged areas happened again, only between the fifth and sixth row of blocks. As these cracks continued to extend from the damaged areas, new cracks formed between the ninth and the tenth row of blocks across the entire width of the wall. As deflection continued, pre-existing cracks continued to lengthen along the width of the wall, and new layers of cracks between the eighth and the ninth row and also between the tenth and eleventh row of blocks began to form. Between a deflection of 15mm and 30mm cracks continued to lengthen, with a particularly large amount of new crack length in the lower regions of the wall. At a deflection of 30mm new cracks were still forming between the eleventh and the twelfth layer of blocks.

The cracking pattern was continuously evolving and expanding as can be seen in Figure B-0-29 and Figure B-0-30, until maximum load capacity reached. At this point in time, the crack pattern along the masonry joint between the ninth and the tenth row of blocks opened up and governed the remaining part of testing.

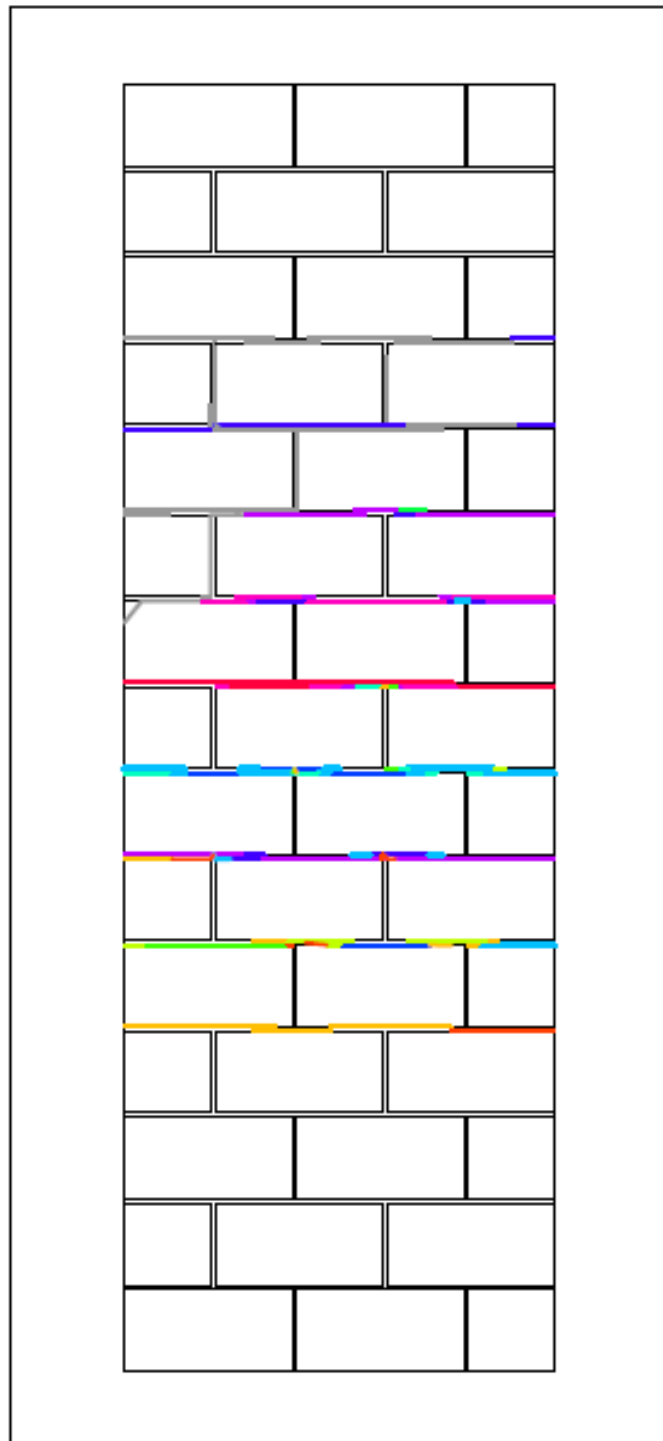


Figure B-0-29: Cracking Pattern of B-2 3m Wall with Three Roped Cells

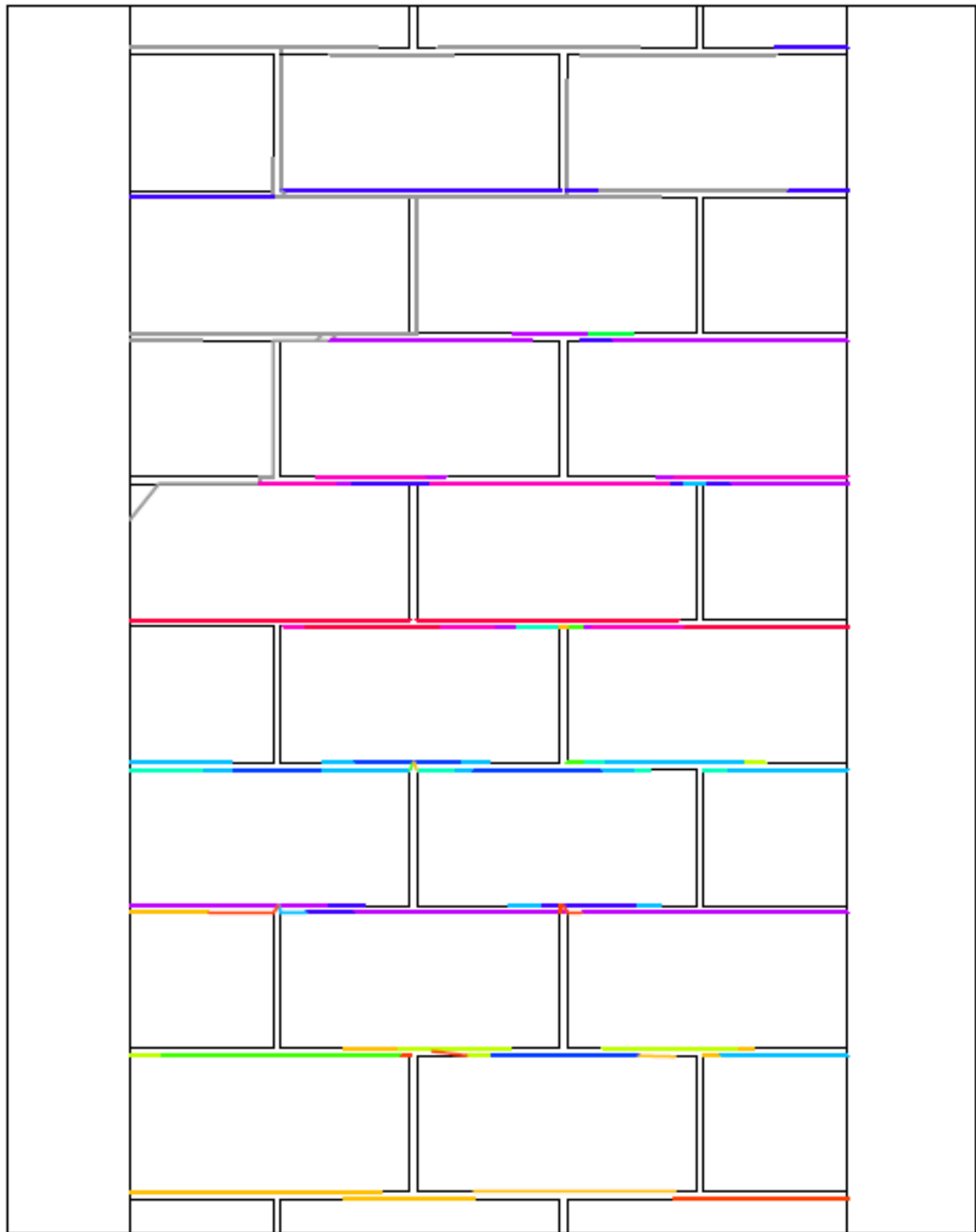


Figure B-0-30: Close-up of Crack Pattern of B-2 3m Wall with Three Roped Cells

B-2 Polyurethane Foam and Rope I Reinforcement—Fully Reinforced

The load-deflection response of the fully rope-reinforced B-2 foam wall was unlike any other foamed wall. The fully reinforced wall reached its cracking capacity at a deflection of 34.15mm. This value is in a similar range to the half-rope wall, which reached its cracking capacity at a higher deflection of 39.15mm. Both of these walls developed their main governing crack between the ninth and the tenth layer of masonry block, making these values directly comparable. As can be seen in the load-deflection curve in Figure B-0-31, the fully-rope wall had a significantly higher cracking capacity than the half-rope wall, reaching this capacity at a load of 8.34kN as compared to 7.05kN. The fact that the wall was able to carry that extra force while maintaining a smaller rate of deflection shows how strong the foam-rope reinforcement is. When this fully rope-reinforced wall is compared to its counterpart without the foam reinforcement, the rope-reinforced specimen shows an increase in cracking capacity of 45%.

The most noticeable difference in the behaviour of this fully-rope wall is its behaviour after it was fully cracked. This wall did not experience the large drop in load capacity that all of the other walls experienced. Instead, it was able to maintain a significant load over the duration of the testing, right up until the ultimate failure of the specimen was reached. After the full crack pattern had developed, the wall specimen did experience a small drop in strength of 1kN, followed by a continuous rise and fall pattern, with some smaller strength losses. However, the wall was able to gradually increase its load capacity not only to the original cracking load, but slightly beyond, reaching loads of 8.45kN. After this high level of loading was reached, the load capacity on the wall again dropped in small increments down to a minimum level of 6.0kN. At this point, the load capacity of the wall increased again, up to the same high value of 8.45 kN. What is remarkable is that this high level of loading was able to be reached and maintained at

such high levels of deflection. As can be seen from the diagram below, the high loading of 8.45kN was reached at mid-height deflections of 128mm and 238mm.

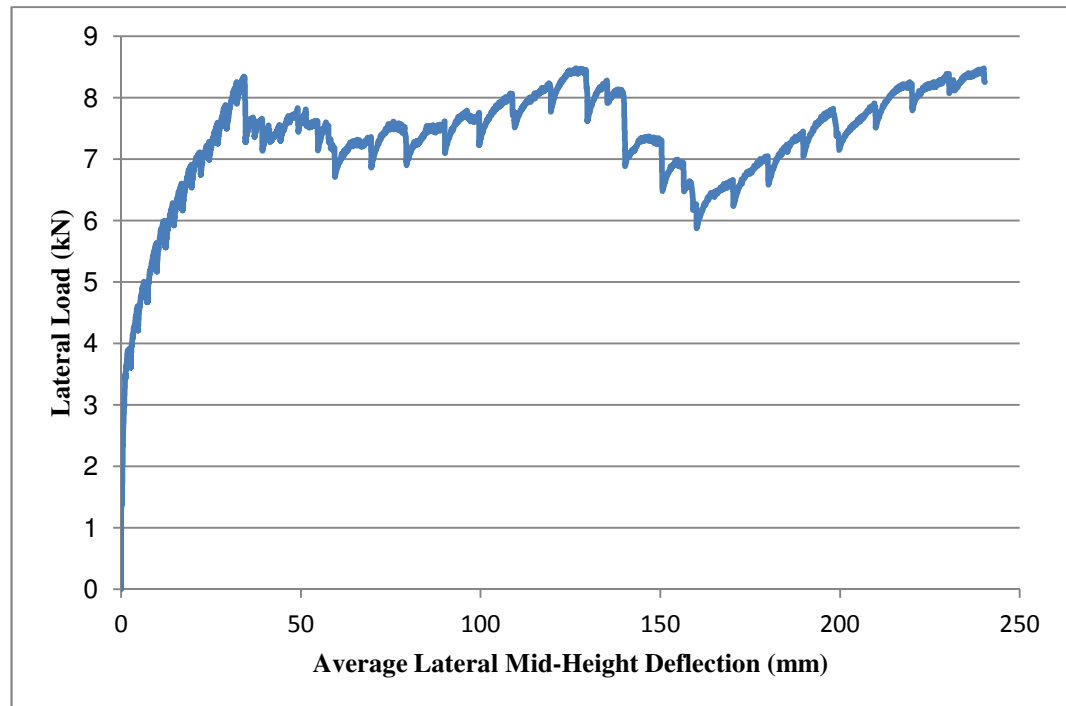


Figure B-0-31: Lateral Load vs. Average Lateral Mid-Height Deflection of B-2 3m Wall with Rope in All Cells

Cracks began to form as soon as the wall started to deflect. After a deflection of only 2.5mm a full crack pattern had developed across the width of the wall between the seventh and the eighth row of masonry. An almost complete crack pattern had also formed between the eighth and the ninth row of masonry. At a deflection of 5mm, cracks started to form between the sixth and the seventh row, and by the time the wall had deflected by 7.5mm this crack had fully developed, in addition to a full crack pattern between the ninth and the tenth row. At a deflection of 10mm, cracks had developed along the masonry joints along the lower section of the wall, with cracks between the tenth and eleventh row, as well as between the eleventh and twelfth row of blocks. Between deflections of 12.5mm and 30mm, this entire crack pattern simply grew larger,

with cracks further extending off of previous patterns and each row of cracks opening up slightly which is depicted in Figure B-0-32 and Figure B-0-33. Immediately prior to a deflection of 35mm, the crack in the ninth and tenth row opened up and began to govern, which could easily be heard by a loud snap in the wall. This large crack opening was also detectable from the load-displacement graph in Figure B-0-31, as the cracking capacity was reached at this point, as discussed earlier. At this time, all the other cracks closed up, except the crack between the seventh and the eighth row of masonry, which remained slightly open for the duration of the testing.

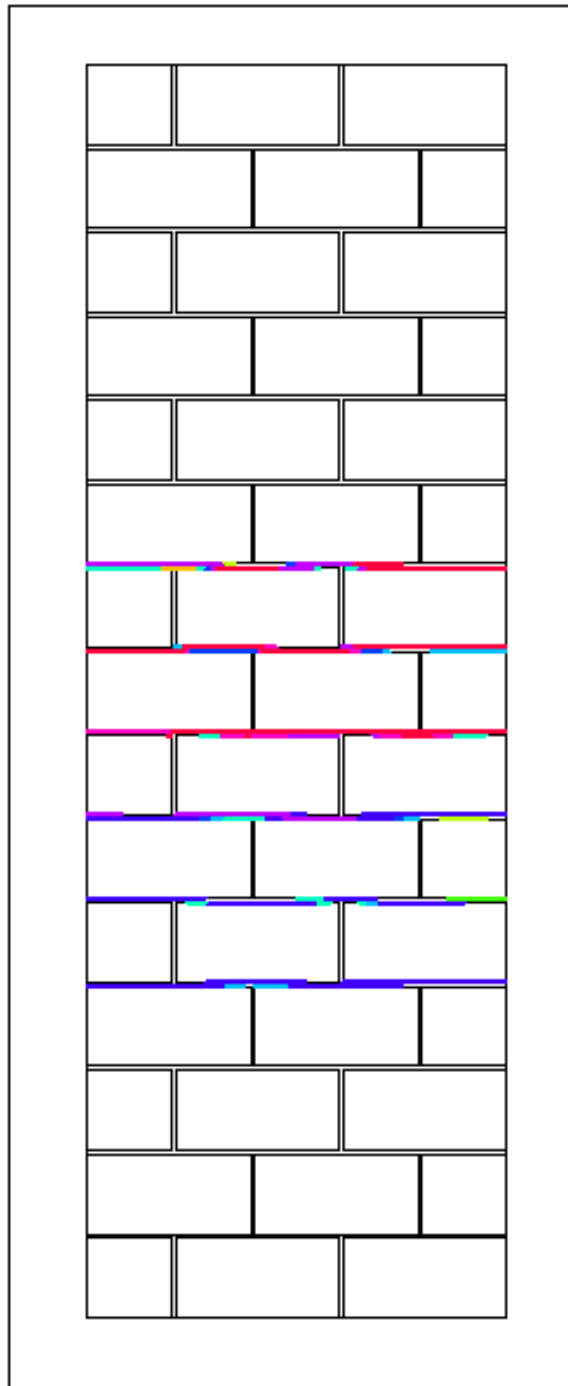


Figure B-0-32: Cracking Pattern of B-2 3m Wall with Rope in All Cells

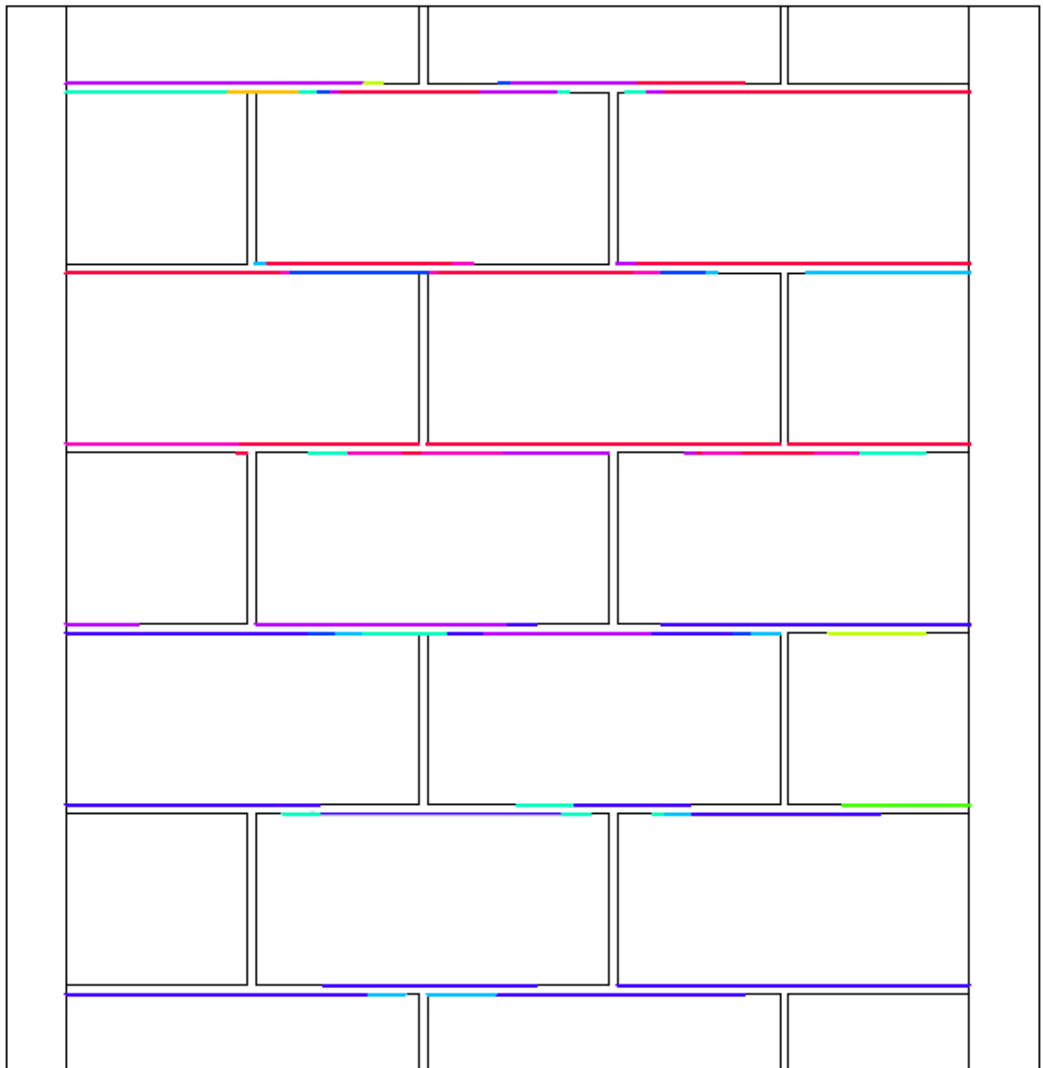


Figure B-0-33: Close-up of Crack Pattern of B-2 3m Wall with Rope in All Cells